How PAR Polarity is Established and Regulates Spindle Positioning in Early *C. elegans* Embryo

By

LAUREL ANNE KOCH
DISSERTATION

Submitted in partial satisfaction of the requirements for the degree of

DOCTOR OF PHILOSOPHY

in

Integrative Genetics and Genomics

in the

OFFICE OF GRADUATE STUDIES

of the

UNIVERSITY OF CALIFORNIA

DAVIS

Approved:

Lesilee Rose, Chair

JoAnne Engebrecht

Bruce Draper

Committee in Charge

2023

Dedicated to my family,

My parents Mark and Grace Koch,
My brother Daniel Koch, and dog Shiloh

For their love and support.

Table of Contents

Abstract

Asymmetric cell division is the process in which one cell divides to give rise to two daughter cells with different cell fates. This process is important throughout development and during stem cell maintenance. Defects in this process can lead to developmental defects and cancer. There are three important steps for a cell to divide asymmetrically. First the cell must generate a polarity axis, such as an anterior-posterior axis. Next the cell must distribute cell fate determinants, such as transcription factors, along this polarity axis. Finally, the cell must orient its spindle along this polarity axis so that when the cell divides each daughter cell receives the correct cell fate determinants. My dissertation work aimed to better understand this process. Specifically, I examined how a cell generates a polarity axis and how the spindle orients along this axis using the early *C. elegans* embryo as a model.

In the one-cell *C. elegans* embryo, polarity is established by the highly conserved PAR proteins which form two mutually exclusive domains on the membrane, in the anterior and posterior. These domains are maintained by the kinase activity of PKC-3 in the anterior and PAR-1 in the posterior. Polarity establishment and maintenance at the one-cell stage have been well studied, but the mechanisms of polarity establishment in the P_1 cell had not been examined. In my work, I found that there are two redundant pathways for polarity establishment. First I identified a novel early pathway in which PAR-1, and its downstream cytoplasmic factors MEX-5 and PLK-1 are required. Then through double mutant analysis, I identified a redundant pathway, similar to the P_0 cell pathway, in which AIR-1 and actomyosin flow are required.

The PAR polarity proteins also control cytoplasmic polarity and the orientation of the spindle to generate an asymmetric cell division. One of the downstream targets of the PAR proteins is LET-99, which localizes into a posterior-lateral band and acts as the link between cortical polarity and spindle positioning. LET-99 locally inhibits the force generating complex in its band causing asymmetric pulling forces which orient the spindle along the anterior-posterior axis. My work aimed to identify the mechanism by which LET-99 is localized to the membrane and how it is restricted from the anterior. Through a structure function analysis of LET-99, I found that the C-terminus of LET-99 is required for its cortical localization. I also found that PAR-3, PKC-3, and CDC-42 are all required for LET-99 localization. Our analysis of different LET-99 deletions is consistent with a role for PKC-3 in phosphorylating LET-99 to inhibit anterior localization. Overall, my studies contribute to our understanding of how cells generate a polarity axis and regulate spindle positioning.

Chapter I

Introduction

Asymmetric cell division is an important process needed to generate cellular diversity during animal development. (Sunchu & Cabernard, 2020; Venkei & Yamashita, 2018). Defects in this process can lead to developmental defects and cancer (Knoblich, 2010; Morrison & Kimble, 2006). For order for a cell to divide asymmetrically, it must successfully generate a polarity axis, distribute its cell fate determinants along this axis, and orient its spindle so that when it divides each daughter cell receives the correct cell fate determinants.

In many organisms, the PAR proteins coordinate asymmetric cell division. The PAR proteins are critical for orienting asymmetric cell division in early *C. elegans* embryo and *Drosophila* neuroblasts. They are also critical for forming polarity in *C. elegans, Drosophila,* and mammalian epithelial cells and *Drosophila* oocyte. The anterior PARs are made up of PAR-3 and PAR-6 which are PDZ-domain containing scaffolding proteins, aPKC (PKC-3 in *C. elegans)* which is atypical protein kinase-C, and CDC-42 which is a small GTPases. The posterior PARs are made of PAR-1 which is a serine/threonine kinase and PAR-2 which is a *C. elegans* specific RING-finger protein. (Goldstein & Macara, 2007; Pickett et al., 2019; Rose & Gonczy, 2014).

The PAR proteins also have a role in coordinating spindle positioning so that the cell divides along the same axis as the cell fate determinants. The PARs control spindle positioning by localizing downstream factors and the force generating complex. The force-generating complex is made up of the minus-end directed microtubule motor dynein and the ternary complex. In *C. elegans,* the ternary complex is made up of LIN-5 (Numa in humans and Mud in *Drosophila),* the G-protein regulators GPR-1/2 (LGN in humans and

Pins in *Drosophila)*, and are anchored to the membrane by Gα (Kotak, 2019). In *C. elegans,* the PARs coordinate the localization of LET-99, a DEP domain containing protein, and LIN-5 to orient the spindle. (Galli et al., 2011; Wu & Rose, 2007). By coordinating spindle positioning, the PARs ensure each daughter cell receives the correct cell fate determinants ensuring the asymmetric cell division is successful.

Polarity Establishment in the *C. elegans* early embryo

In the one-cell *C. elegans* embryo, polarity is established by the highly conserved PAR proteins which form two mutually exclusive domains in the anterior and posterior on the membrane (Goldstein & Macara, 2007; Pickett et al., 2019; Rose & Gonczy, 2014). These domains are maintained by the kinase activity of PKC-3 in the anterior and PAR-1 in the posterior (Benton & St Johnston, 2003; Hao et al., 2006; Hurov et al., 2004). These PAR kinases are required for regulating downstream targets which coordinate the movement of cell fate determinants and orient the spindle.

In *C. elegans*, polarity is originally established when the sperm fertilizes the oocyte and deposits centrioles (Cowan & Hyman, 2004). As the centrosome matures, Aurora-A kinase (AIR-1), a mitotic kinase, accumulates on the centrosomes and locally inhibits the Rho-GEF ECT-2 and thus the actomyosin cytoskeleton (Klinkert et al., 2019; Longhini & Glotzer, 2022; Munro et al., 2004; Schonegg et al., 2014; Zhao et al., 2019). The local relaxation of the actomyosin cytoskeleton, in the future posterior end, generates anterior directed flow. This flow moves the anterior PARs, which are originally uniform on the membrane, towards the future anterior end. Once this flow moves the anterior PARs

towards the anterior, the posterior PARs can move onto the posterior membrane (Boyd et al., 1996; Cheeks et al., 2004; Cowan & Hyman, 2004; Cuenca et al., 2003; Guo & Kemphues, 1995; Hao et al., 2006)(Figure 1)

There is also a second redundant pathway for establishing polarity in the P_0 cell, that can be observed in the absence of actomyosin flow. In mutants that inhibit actomyosin flow, polarity can still be formed but with a temporal delay. In this backup pathway, PAR-2 establishes polarity by binding to microtubules emanating from the sperm derived centrosomes. When PAR-2 is bound to microtubules it is sheltered from being phosphorylated by PKC-3 and thus can bind the membrane. This allows PAR-2 to form a domain where the sperm derived centrosomes are localized. Once PAR-2 is localized to the membrane it can help recruit PAR-1 and PAR-1's kinase activity can maintain the domain (Motegi et al., 2011; Zonies et al., 2010) (Figure 1).

These same polarity domains must be reestablished in every subsequent germline cell, such as P_1, but the mechanism of how polarity is reestablished at later cell stages and under different developmental conditions has not been studied in detail (Rose & Gonczy, 2014). After dividing, the P_0 cell gives rise to the larger AB cell which will divide symmetrically and the P_1 cell which will divide asymmetrically. In the P_1 cell, PAR-2 is inherited around the entire P_1 cell cortex. In response to an unknown polarity cue, the P_1 cell forms the same anterior and posterior PAR domains as the P_0 cell. At the four-cell stage, the P_2 cell also inherits PAR-2 uniformly. In the P_2 cell, reciprocal PAR domains form but they are oriented in a dorsal-ventral direction by MES-1/SRC-1 signaling at the EMS/P_2 cell contact (Arata et al., 2010; Bei et al., 2002). Unlike in the P_2 cell, the AB- P_1 cell contact is

not required for the spindle rotation or unequal division of the P_1 cell (Goldstein, 1993, 1995). However, previous work has shown that there is actomyosin flow in the P_1 cell towards the anterior and there is anterior directed flow of PAR-6 on the cortex (Munro et al., 2004). It has also been observed that the P_1 cell nucleus moves posteriorly after the end of P_0 cytokinesis, making it plausible that the centrosome and AIR-1 might be important for P_1 cell repolarization. However, the timing of these events and the exact mechanism by which PAR polarity is established in the P_1 cell is still unknown.

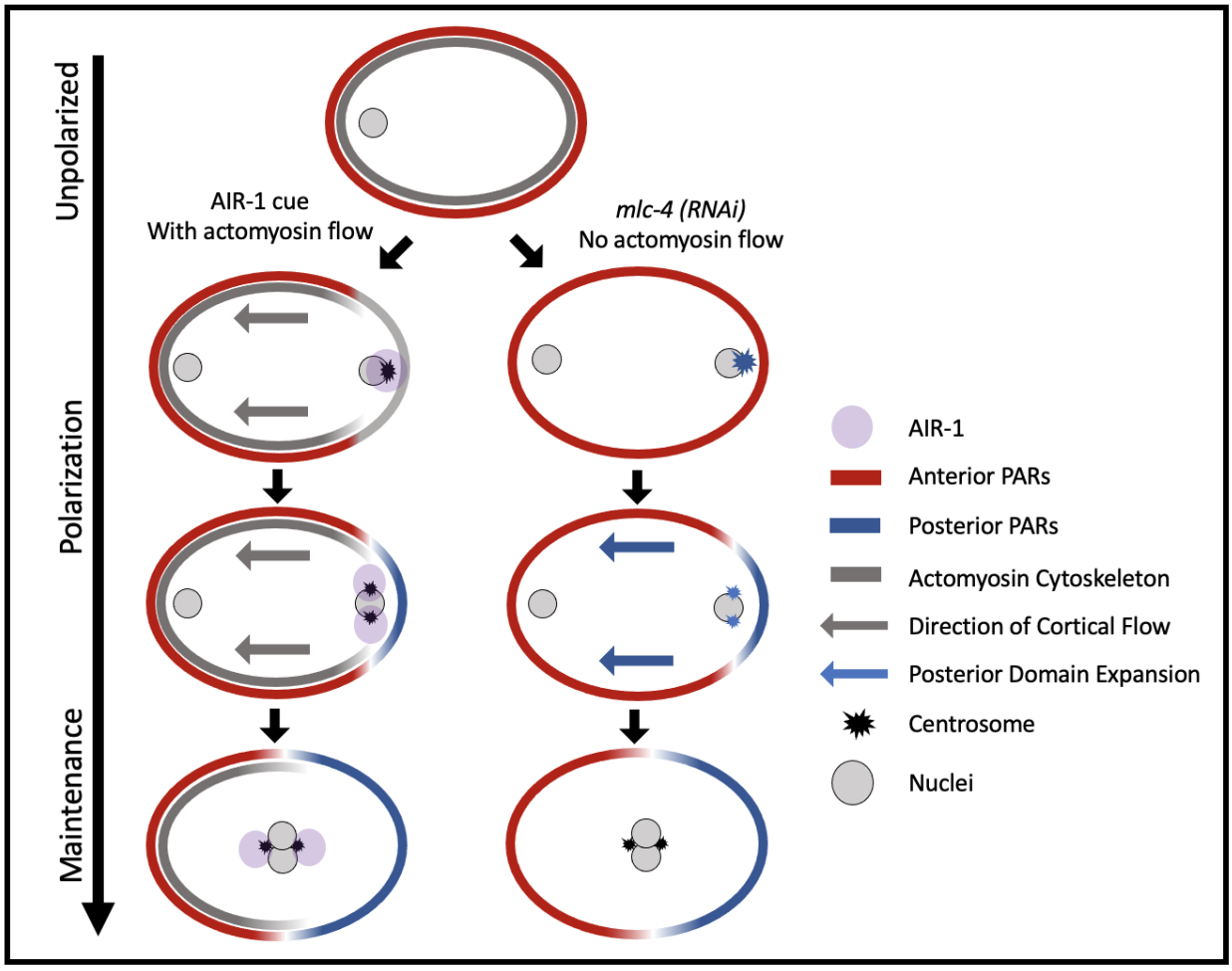

Figure 1 - Polarity Establishment in the P_0 cell. Illustration of the two pathways involved in P_0 cell polarization. Left shows the primary pathway in which AIR-1 locally inhibits the actomyosin cytoskeleton which causes anterior directed flow and moves the anterior PARs out of the posterior. Right shows the backup pathway, which is observed in the absence of actomyosin flow caused by RNAi of myosin light chain *mlc-4*. In this pathway PAR-2 is protected from phosphorylation by binding to microtubules emanating from the centrosome and can recruit PAR-1 to the posterior membrane. The two PAR domains are then maintained by the kinase activity of PKC-3 in the anterior and PAR-1 in the posterior.

PAR polarity and downstream targets

The PAR proteins form two mutually exclusive domains on the membrane and control downstream cytoplasmic polarity and spindle positioning. Previous research has identified how the PAR proteins interact with each other and work to maintain these domains (Goldstein & Macara, 2007; Rose & Gonczy, 2014). In the anterior, PAR-3 acts as the main scaffolding protein; without PAR-3 the other anterior PARs cannot localize to the membrane. The anterior PARs also cycle between two competing clusters. In one cluster PKC-3 and PAR-6 are bound to PAR-3 where they can respond to polarity cues and in this complex PKC-3 is localized properly to the anterior. In the other cluster, PKC-3 and PAR-6 bind to CDC-42; in this cluster PKC-3 is active and can phosphorylate downstream targets. (Rodriguez et al., 2017). It was shown in *Drosophila,* that PKC-3 can phosphorylate PAR-1 and in *C. elegans* they showed that PKC-3 can phosphorylate PAR-2 and PAR-1, keeping them from the anterior of the cell (Hao et al., 2006; Hurov et al., 2004; Motegi et al., 2011).

The posterior PARs are also important for regulating PAR polarity and downstream cytoplasmic polarity. PAR-1, the posterior kinase, has been shown to directly phosphorylate PAR-3 which keeps the anterior PARs out of the posterior (Benton & St Johnston, 2003; Motegi et al., 2011). PAR-1's role in regulating PAR-3 is conserved in *Drosophila* and mammalian epithelial cells, but is redundant in the *C. elegans* one-cell embryo (Goldstein & Macara, 2007). PAR-1 is also required for all cytoplasmic polarity. PAR-1's kinase activity is required for generating an anterior cytoplasmic gradient of MEX-5 and MEX-6. MEX-5 and MEX-6 are nearly identical cytoplasmic proteins that are redundantly required for controlling cytoplasmic polarity. PAR-1 phosphorylates MEX-5

and this releases it from slow diffusing RNA-containing complexes. Because MEX-5 is only phosphorylated and able to move in the posterior, this leads to more MEX-5 being trapped in the anterior of the cell (Griffin et al., 2011). MEX-5/6 then regulate other cytoplasmic factors such as PLK-1, PIE-1, and POS-1, which are essential for proper development (Kim & Griffin, 2020; Rose & Gonczy, 2014)(Figure 2).

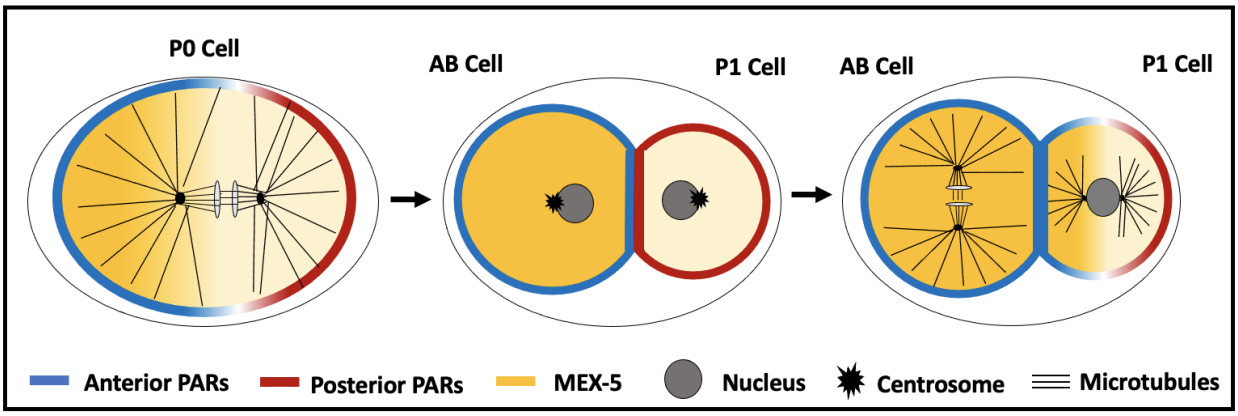

Figure 2 – PAR polarity in the early *C. elegans* embryo. Illustration of the division patterns of the P_0, AB, and P_1 cells. In the P_0 cell the PAR proteins form an anterior domain in blue and a posterior domain in red, cytoplasmic polarity protein MEX-5 forms an anterior domain, and the spindle lines up along this axis. When the P_0 cell divides it gives rise to the AB cell in the anterior and P_1 cell in the posterior. The AB cell divides symmetrically while the P_1 cell reestablishes the same PAR polarity and gradient of MEX-5 in the cytoplasm and also divides asymmetrically.

The PAR proteins regulate LET-99 localization to mediate spindle positioning

Another downstream target of the PAR proteins is LET-99. LET-99 is localized in a posterior lateral-band on the membrane between the two PAR domains and is required for orienting the spindle correctly for asymmetric cell division. Previous work has shown that LET-99's localization is dependent on PAR-3 in the anterior and PAR-1 in the posterior (Tsou et al., 2002; Wu & Rose, 2007)(Figure 3A). Further work showed that PAR-5, a 14-3-3 protein, acts with PAR-1 to restrict LET-99 from the posterior. 14-3-3 proteins bind phosphorylated targets and change their activity or localization. When two PAR-5 binding sites on LET-99 were mutated, this caused LET-99 to localize in a posterior cap rather than a band. These results are consistent with the model that PAR-1 phosphorylates LET-99 at the two predicted PAR-5 binding sites (Wu et al., 2016). These PAR-5 sites in LET-99, and PAR-5 itself, were not required for the anterior inhibition of LET-99. The mechanism by which LET-99 is restricted from the anterior has not yet been shown .

LET-99's unique localization pattern allows it to act as the link between cortical PAR polarity and spindle positioning. *let-99* mutants show defects in centration, rotation, and spindle displacement (Rose & Kemphues, 1998; Tsou et al., 2002). LET-99 locally inhibits the force generating complex to create asymmetric pulling forces on the nucleus and spindle. The force generating complex is made up of four important components in *C. elegans*: two partially redundant Gα subunits GOA-1 and GPA-16, two GoLoco containing proteins GPR-1 and GPR-2, the large coiled-coil protein LIN-5, and the minus end directed microtubule motor dynein (Figure 3B). The force generating complex exerts pulling force on astral microtubules, causing the nuclear-centrosome complex to move anteriorly and

rotate onto the anterior/posterior axis. It also generates asymmetric pulling forces on the spindle during cell division (Rose & Gonczy, 2014). Where LET-99 levels are highest GPR-1/2 are lowered, and in *let-99* mutants both GPR-1/2 and LIN-5 localization is uniform (Park & Rose, 2008) (Figure 3A).

LET-99 is 698 amino acids long and contains two predicted domains. At the N-terminus there is a DEP domain. The DEP domain is a globular domain named after the three proteins it was first identified in, Dishevelled, EGL-10, and Pleckstrin; it is found in several proteins involved in G-protein signaling (Consonni et al., 2014). LET-99 also has a Rho-GAP like domain which is a region of the protein that shares partial homology to Rho-GAPs (Figure 3C). The function of these domains in LET-99 has not been studied. How LET-99 is localized to the membrane, restricted from the anterior, and interacts with the force generating complex is still unknown.

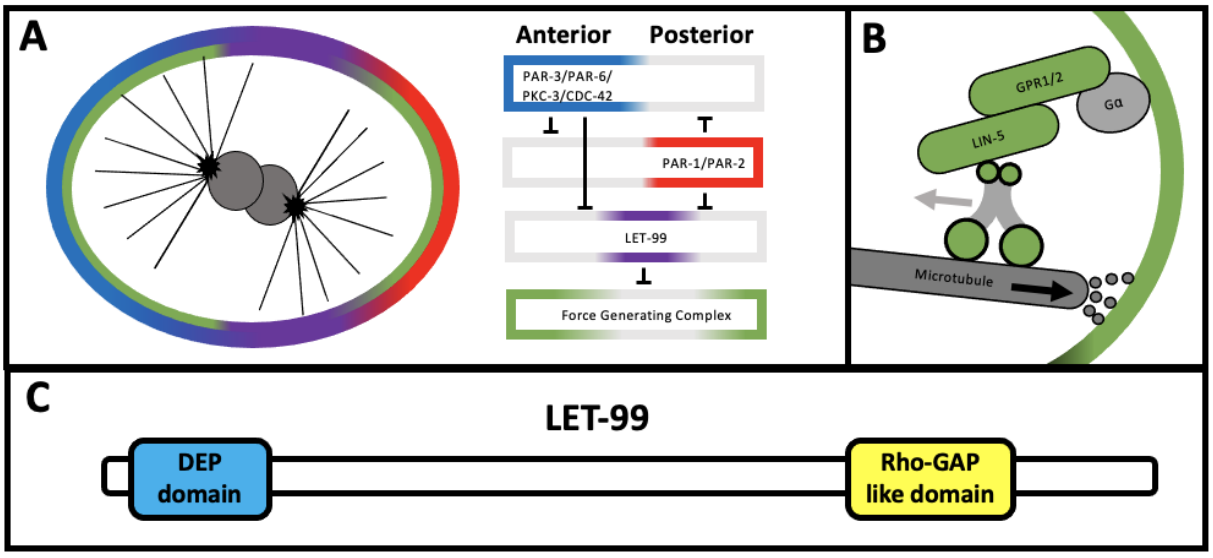

Figure 3 - LET-99 acts as the link between PAR polarity and spindle positioning. (A) Illustration of LET- 99 localization in a posterior lateral band between the anterior and posterior PAR domains. LET-99 inhibits the force generating complex in its band area forming caps of the force generation complex in the anterior and posterior. (B) Illustration of the force-generating complex which is made up of Ga, GPR1/2, and LIN-5 which anchor dynein to the membrane, as dynein walks along the microtubule it generates a pulling force on the spindle. (C) Structure of LET-99, which is 698 amino acids long and has two predicted domains: a DEP domain and a Rho-GAP like domain.

References

Arata, Y., Lee, J.-Y., Goldstein, B., & Sawa, H. (2010). Extracellular control of PAR protein localization during asymmetric cell division in the C. elegans embryo. *Development, 137*(19), 3337-3345. https://doi.org/10.1242/dev.054742

Bei, Y., Hogan, J., Berkowitz, L. A., Soto, M., Rocheleau, C. E., Pang, K. M., Collins, J., & Mello, C. C. (2002, Jul). SRC-1 and Wnt signaling act together to specify endoderm and to control cleavage orientation in early C. elegans embryos. *Dev Cell, 3*(1), 113-125. https://doi.org/10.1016/s1534-5807(02)00185-5

Benton, R., & St Johnston, D. (2003, Dec 12). Drosophila PAR-1 and 14-3-3 inhibit Bazooka/PAR-3 to establish complementary cortical domains in polarized cells. *Cell, 115*(6), 691-704. https://doi.org/10.1016/s0092-8674(03)00938-3

Boyd, L., Guo, S., Levitan, D., Stinchcomb, D. T., & Kemphues, K. J. (1996, Oct). PAR-2 is asymmetrically distributed and promotes association of P granules and PAR-1 with the cortex in C. elegans embryos. *Development, 122*(10), 3075-3084. https://doi.org/10.1242/dev.122.10.3075

Cheeks, R. J., Canman, J. C., Gabriel, W. N., Meyer, N., Strome, S., & Goldstein, B. (2004, May 25). C. elegans PAR proteins function by mobilizing and stabilizing asymmetrically localized protein complexes. *Curr Biol, 14*(10), 851-862. https://doi.org/10.1016/j.cub.2004.05.022

Consonni, S. V., Maurice, M. M., & Bos, J. L. (2014, May). DEP domains: structurally similar but functionally different. *Nat Rev Mol Cell Biol, 15*(5), 357-362. https://doi.org/10.1038/nrm3791

Cowan, C. R., & Hyman, A. A. (2004, Sep 2). Centrosomes direct cell polarity independently of microtubule assembly in C. elegans embryos. *Nature, 431*(7004), 92-96. https://doi.org/10.1038/nature02825

Cuenca, A. A., Schetter, A., Aceto, D., Kemphues, K., & Seydoux, G. (2003, Apr). Polarization of the C. elegans zygote proceeds via distinct establishment and maintenance phases. *Development, 130*(7), 1255-1265. https://doi.org/10.1242/dev.00284

Goldstein, B. (1993, Aug). Establishment of gut fate in the E lineage of C. elegans: the roles of lineage-dependent mechanisms and cell interactions. *Development, 118*(4), 1267-1277. https://doi.org/10.1242/dev.118.4.1267

Goldstein, B. (1995, May). Cell contacts orient some cell division axes in the Caenorhabditis elegans embryo. *J Cell Biol, 129*(4), 1071-1080. https://doi.org/10.1083/jcb.129.4.1071

Goldstein, B., & Macara, I. G. (2007, Nov). The PAR proteins: fundamental players in animal cell polarization. *Dev Cell, 13*(5), 609-622. https://doi.org/10.1016/j.devcel.2007.10.007

Griffin, E. E., Odde, D. J., & Seydoux, G. (2011, Sep 16). Regulation of the MEX-5 gradient by a spatially segregated kinase/phosphatase cycle. *Cell, 146*(6), 955-968. https://doi.org/10.1016/j.cell.2011.08.012

Guo, S., & Kemphues, K. J. (1995, May 19). par-1, a gene required for establishing polarity in C. elegans embryos, encodes a putative Ser/Thr kinase that is asymmetrically distributed. *Cell, 81*(4), 611-620. https://doi.org/10.1016/0092-8674(95)90082-9

Hao, Y., Boyd, L., & Seydoux, G. (2006, Feb). Stabilization of cell polarity by the C. elegans RING protein PAR-2. *Dev Cell, 10*(2), 199-208. https://doi.org/10.1016/j.devcel.2005.12.015

Hurov, J. B., Watkins, J. L., & Piwnica-Worms, H. (2004, Apr 20). Atypical PKC phosphorylates PAR-1 kinases to regulate localization and activity. *Curr Biol, 14*(8), 736-741. https://doi.org/10.1016/j.cub.2004.04.007

Kim, A. J., & Griffin, E. E. (2020). PLK-1 Regulation of Asymmetric Cell Division in the Early C. elegans Embryo. *Front Cell Dev Biol, 8*, 632253. https://doi.org/10.3389/fcell.2020.632253

Klinkert, K., Levernier, N., Gross, P., Gentili, C., von Tobel, L., Pierron, M., Busso, C., Herrman, S., Grill, S. W., Kruse, K., & Gönczy, P. (2019, Feb 26). Aurora A depletion reveals centrosome-independent polarization mechanism in Caenorhabditis elegans. *Elife, 8*. https://doi.org/10.7554/eLife.44552

Knoblich, J. A. (2010, 2010/12/01). Asymmetric cell division: recent developments and their implications for tumour biology. *Nature Reviews Molecular Cell Biology, 11*(12), 849-860. https://doi.org/10.1038/nrm3010

Longhini, K. M., & Glotzer, M. (2022, Dec 19). Aurora A and cortical flows promote polarization and cytokinesis by inducing asymmetric ECT-2 accumulation. *Elife, 11*. https://doi.org/10.7554/eLife.83992

Morrison, S. J., & Kimble, J. (2006, Jun 29). Asymmetric and symmetric stem-cell divisions in development and cancer. *Nature, 441*(7097), 1068-1074. https://doi.org/10.1038/nature04956

Motegi, F., Zonies, S., Hao, Y., Cuenca, A. A., Griffin, E., & Seydoux, G. (2011, Oct 9). Microtubules induce self-organization of polarized PAR domains in Caenorhabditis elegans zygotes. *Nat Cell Biol, 13*(11), 1361-1367. https://doi.org/10.1038/ncb2354

Munro, E., Nance, J., & Priess, J. R. (2004, Sep). Cortical flows powered by asymmetrical contraction transport PAR proteins to establish and maintain anterior-posterior polarity in the early C. elegans embryo. *Dev Cell, 7*(3), 413-424. https://doi.org/10.1016/j.devcel.2004.08.001

Park, D. H., & Rose, L. S. (2008, Mar 1). Dynamic localization of LIN-5 and GPR-1/2 to cortical force generation domains during spindle positioning. *Dev Biol, 315*(1), 42-54. https://doi.org/10.1016/j.ydbio.2007.11.037

Pickett, M. A., Naturale, V. F., & Feldman, J. L. (2019, Oct 6). A Polarizing Issue: Diversity in the Mechanisms Underlying Apico-Basolateral Polarization In Vivo. *Annu Rev Cell Dev Biol, 35*, 285-308. https://doi.org/10.1146/annurev-cellbio-100818-125134

Rodriguez, J., Peglion, F., Martin, J., Hubatsch, L., Reich, J., Hirani, N., Gubieda, A. G., Roffey, J., Fernandes, A. R., St Johnston, D., Ahringer, J., & Goehring, N. W. (2017, Aug 21). aPKC Cycles between Functionally Distinct PAR Protein Assemblies to Drive Cell Polarity. *Dev Cell, 42*(4), 400-415.e409. https://doi.org/10.1016/j.devcel.2017.07.007

Rose, L., & Gönczy, P. (2014, Dec 30). Polarity establishment, asymmetric division and segregation of fate determinants in early C. elegans embryos. *WormBook*, 1-43. https://doi.org/10.1895/wormbook.1.30.2

Rose, L. S., & Kemphues, K. (1998, Apr). The let-99 gene is required for proper spindle orientation during cleavage of the C. elegans embryo. *Development, 125*(7), 1337-1346. https://doi.org/10.1242/dev.125.7.1337

Schonegg, S., Hyman, A. A., & Wood, W. B. (2014, Jun). Timing and mechanism of the initial cue establishing handed left–right asymmetry in Caenorhabditis elegans embryos. *Genesis, 52*(6), 572-580. https://doi.org/10.1002/dvg.22749

Sunchu, B., & Cabernard, C. (2020, Jun 29). Principles and mechanisms of asymmetric cell division. *Development, 147*(13). https://doi.org/10.1242/dev.167650

Tsou, M. F., Hayashi, A., DeBella, L. R., McGrath, G., & Rose, L. S. (2002, Oct). LET-99 determines spindle position and is asymmetrically enriched in response to PAR polarity cues in C. elegans embryos. *Development, 129*(19), 4469-4481. https://doi.org/10.1242/dev.129.19.4469

Venkei, Z. G., & Yamashita, Y. M. (2018, Nov 5). Emerging mechanisms of asymmetric stem cell division. *J Cell Biol, 217*(11), 3785-3795. https://doi.org/10.1083/jcb.201807037

Wu, J. C., Espiritu, E. B., & Rose, L. S. (2016, Apr 15). The 14-3-3 protein PAR-5 regulates the asymmetric localization of the LET-99 spindle positioning protein. *Dev Biol, 412*(2), 288-297. https://doi.org/10.1016/j.ydbio.2016.02.020

Wu, J. C., & Rose, L. S. (2007, Nov). PAR-3 and PAR-1 inhibit LET-99 localization to generate a cortical band important for spindle positioning in Caenorhabditis elegans embryos. *Mol Biol Cell, 18*(11), 4470-4482. https://doi.org/10.1091/mbc.e07-02-0105

Zhao, P., Teng, X., Tantirimudalige, S. N., Nishikawa, M., Wohland, T., Toyama, Y., & Motegi, F. (2019, Mar 11). Aurora-A Breaks Symmetry in Contractile Actomyosin Networks Independently of Its Role in Centrosome Maturation. *Dev Cell, 48*(5), 631-645.e636. https://doi.org/10.1016/j.devcel.2019.02.012

Zonies, S., Motegi, F., Hao, Y., & Seydoux, G. (2010, May). Symmetry breaking and polarization of the C. elegans zygote by the polarity protein PAR-2. *Development, 137*(10), 1669-1677. https://doi.org/10.1242/dev.045823

Chapter 2

Multiple pathways for reestablishing PAR polarity in *C. elegans* early embryo

Laurel A. Koch and Lesilee S. Rose

Developmental Biology, Vol 500, 40-54 August 2023

Developmental Biology 500 (2023) 40–54

Contents lists available at ScienceDirect

Developmental Biology

journal homepage: www.elsevier.com/locate/developmentalbiology

Multiple pathways for reestablishing PAR polarity in *C. elegans* embryo

Laurel A. Koch, Lesilee S. Rose *

Department of Molecular and Cellular Biology and Integrative Genetics and Genomics Graduate Program, University of California, Davis, United States

ARTICLE INFO

Keywords:
Asymmetric division
Polarization
Asymmetry
Embryo
Polo kinase

ABSTRACT

Asymmetric cell divisions, where cells divide with respect to a polarized axis and give rise to daughter cells with different fates, are critically important for development. In many such divisions, the conserved PAR polarity proteins accumulate in distinct cortical domains in response to a symmetry breaking cue. The one-cell *C. elegans* embryo is a paradigm for understanding mechanisms of PAR polarization, but much less is known about polarity in subsequent divisions. Here, we investigate the polarization of the P_1 cell of the two-cell embryo. A posterior PAR-2 domain forms in the first 4 min, and polarization becomes stronger over time. Initial polarization depends on the PAR-1 and PKC-3 kinases, and the downstream polarity regulators MEX-5 and PLK-1. However, *par-1* and *plk-1* mutants exhibit delayed polarization. This late polarization correlates with the time of centrosome maturation and actomyosin flow, and loss of centrosome maturation or myosin in *par-1* mutant embryos causes an even stronger polarity phenotype. Based on these and other results, we propose that PAR polarity in the P_1 cell is generated by at least two redundant mechanisms: There is a novel early pathway dependent on PAR-1, PKC-3 and cytoplasmic polarity, and a late pathway that resembles symmetry breaking in the one-cell embryo and requires PKC-3, centrosome associated AIR-1 and myosin flow.

1. Introduction

Asymmetric cell division is the process in which one cell divides to give rise to two daughter cells with different cell fates. This process is important for generating cell diversity throughout development, as well as for maintaining stem cell populations in many organisms. One of the important steps in many asymmetric cell divisions is generating a polarity axis that will be bisected by cytokinesis, so that cell fate determinants are segregated differentially to the daughter cells (Sunchu and Cabernard, 2020; Venkei and Yamashita, 2018). In many organisms, the cortically localized partitioning-defective (PAR) proteins are required for generating this polarity axis. For example, the PAR proteins regulate asymmetric cell division in the *C. elegans* one-cell embryo and the Drosophila neuroblast. In these and other systems, groups of PAR proteins become localized to reciprocal, mutually exclusive cortical domains, for example anteriorly localized PARs (aPARs) and posteriorly localized PARs (pPARs)(Goldstein and Macara, 2007; Pickett et al., 2019; Rose and Gönczy, 2014).

The initial establishment of PAR polarity domains occurs in response to various symmetry breaking cues. In the one-cell *C. elegans* embryo (called P_0), symmetry is broken when the sperm fertilizes the oocyte (Cowan and Hyman, 2004). At the time of fertilization, the aPAR proteins, PAR-3 and PAR-6, which are PDZ domain containing scaffolding proteins, and PKC-3, which is an atypical kinase C, are uniform on the cortex (Cuenca et al., 2003; Kemphues et al., 1988; Tabuse et al., 1998; Watts et al., 1996). The sperm derived centrioles recruit centrosome components including Aurora A Kinase (AIR-1), which locally inhibits actomyosin contractility, generating actomyosin flow away from the location of the centrosome. This flow moves the aPARs towards the opposite end of the embryo, which will become the anterior pole (Klinkert et al., 2019; Munro et al., 2004; Schonegg et al., 2014; Zhao et al., 2019). As the aPARs clear from the posterior this allows PAR-1, a serine/threonine kinase, and PAR-2, a RING domain protein, to move onto the posterior cortex forming the pPAR domain. (Boyd et al., 1996; Cheeks et al., 2004; Cowan and Hyman, 2004; Cuenca et al., 2003; Guo and Kemphues, 1995; Hao et al., 2006). In this and other systems, the reciprocal PAR domains are then maintained by mutual exclusion. PKC-3 phosphorylates PAR-1 and PAR-2, restricting the pPARs from the anterior. Meanwhile, PAR-1 phosphorylates PAR-3 to inhibit PAR-3 association with the cortex, which with other mechanisms in *C. elegans* restricts aPARs from the posterior (Benton and St Johnston, 2003; Hao et al., 2006; Hurov et al., 2004).

There is also a redundant pathway that can establish PAR polarity in the P_0 cell when actomyosin flow is inhibited. In this backup pathway,

* Corresponding author.
E-mail address: lsrose@ucdavis.edu (L.S. Rose).

https://doi.org/10.1016/j.ydbio.2023.05.005
Received 19 December 2022; Received in revised form 12 May 2023; Accepted 22 May 2023
Available online 30 May 2023

PAR-2 appears to establish polarity by binding to microtubules emanating from the sperm-derived centrosomes. Microtubule association shelters PAR-2 from being phosphorylated by PKC-3, allowing PAR-2 to accumulate on the posterior cortex and then PAR-1 can load onto the cortex (Motegi et al., 2011; Zonies et al., 2010). This pathway thus generates the same reciprocal aPAR and pPAR domains, but with a temporal delay.

PAR domains are important for correctly segregating cytoplasmic polarity and orienting the spindle, so that the P_0 cell divides to give rise to a larger AB cell and smaller P_1 cell with different fates and division patterns. The PAR polarity axis is reestablished in P_1 and every subsequent germ-line P cell, which all divide asymmetrically (Rose and Gönczy, 2014). After P_0 cytokinesis, the P_1 cell has PAR-2 around the entire cortex. In response to an unknown polarity cue, an anterior-posterior PAR polarity axis forms again. At the four-cell stage, the P_2 cell also inherits PAR-2 uniformly; aPAR and pPAR domains form in this cell, oriented by MES-1/SRC-1 signalling at the EMS/P_2 cell contact (Arata et al., 2010; Bei et al., 2002). In contrast, contact between the AB and P_1 cell is not required for the spindle rotation or unequal division of the P_1 cell (Goldstein, 1993, 1995). However, previous work has shown that there is actomyosin flow in the P_1 cell towards the anterior and this correlates with the movement of PAR-6 on the cortex (Munro et al., 2004). The P_1 cell nucleus also moves posteriorly after the end of P_0 cytokinesis, making it plausible that the centrosome and AIR-1 might participate in the repolarization of P_1, in a mechanism similar to that used in the P_0 cell.

In this study, we sought to understand how PAR polarity is reestablished in the P_1 cell. Here we show that the PAR-2 domain starts to form in the P_1 cell within 2 min of the end of P_0 cytokinesis, before nuclear movement towards the posterior or actomyosin flow occurs. We also found that *par-1* and *plk-1* mutants exhibit late polarization, and defects in initial polarization correlate with incorrect cytoplasmic partitioning in the P_0 cell. Our findings support a model whereby the P_1 cell polarizes via at least two redundant pathways. The early pathway requires proper cytoplasmic polarity, PAR-1, and PKC-3, and clears PAR-2 from the anterior to form a PAR-2 domain. The late pathway requires centrosome maturation and actomyosin flow which resembles P_0 cell polarization. These results will further our understanding of how polarity can be established in response to different cues.

2. Results

2.1. Determining the timing of PAR polarization in the P_1 cell

To determine what components are present at the birth of the P_1 cell and the timing of P_1 cell polarization, we characterized the formation of PAR polarity using embryos co-labeled with endogenously tagged mCh::PAR-2 and PAR-6::GFP (Reich et al., 2019). Embryos were imaged from the end of P_0 cytokinesis (time 0:00) through the end of the P_1 cell cycle, and the cortical localization of PAR-2 and PAR-6 were quantified throughout the first 10 min of the cell cycle (Fig. 1A–C). During cytokinesis PAR-2 moved in with the furrow and only appeared to be present on the P_1 side of the furrow (Fig. 1D). Thus, at the birth of the P_1 cell, PAR-2 was localized around the entire cortex as previously described (Cuenca et al., 2003). Quantification showed that the cortical levels are uniform on average (time 0, Fig. 1C). In some embryos, the levels of PAR-2 at the AB-P_1 cell contact started to decrease as early as 1 min after P_0 cell cytokinesis, and in all embryos PAR-2 levels decreased at the AB-P_1 cell contact by 2 min. We refer to this decrease as "clearing of PAR-2" and note that clearing was also accompanied by a corresponding increase of PAR-2 at the posterior cortex of the P_1 cell. PAR-2 continued to clear from the anterior until 6 min and accumulated further in the posterior for the whole cell cycle (Fig. 1C, Fig. S1A). As a way to quantify the initial clearing of PAR-2 versus the formation of a stronger posterior domain over time in this and mutant backgrounds, we measured the posterior/anterior ratio of PAR-2 at 4 and 8 min after cytokinesis. At 4 min the posterior levels were three times higher than the anterior, and at 8 min the posterior levels were seven times higher (Fig. 1E and F). These data indicate that polarization of the P_1 cell with respect to PAR-2 begins by 2 min, a posterior domain of PAR-2 is present by as early as 4 min, and the PAR-2 domain becomes stronger as the cell cycle continues.

Similar to PAR-2, PAR-6 signal was present in the cytokinetic furrow but appeared to be move in predominantly from the AB side (Fig. 1D). At cytokinesis completion, PAR-6 signal appeared highest at the AB-P_1 cell contact and was at low levels throughout the cortex of the P_1 cell. For the first 4 min after cytokinesis, PAR-6 cortical levels increased globally. After 4 min, PAR-6 levels started to go down in the posterior and continued to accumulate in the anterior (Fig. 1A–C). We cannot distinguish whether the increase in signal at the cell contact is in the AB or P_1 cell. However, an increase in PAR-6 levels on the anterior cortex of P_1, just adjacent to the cell contact was detectable after 4 min. Thus, although we cannot address whether there is an inherited polarity of PAR-6 on the P_1 side of the cell contact initially, these data suggest that formation of the full anterior PAR-6 domain occurs after the initial polarization of PAR-2.

2.2. Early PAR-2 clearing does not correlate with AIR-1 localization and actomyosin flow

To test the hypothesis that AIR-1 on the centrosome is acting as the symmetry breaking cue in the P_1 cell, we first looked at where the nucleus and centrosome were located during polarization. If centrosomal AIR-1 is a localized cue as in the one-cell embryo, we predicted that the nucleus and centrosome would move close to the posterior before the clearing of PAR-2 from the AB-P_1 cell contact. We thus imaged embryos in DIC and measured the closest distance achieved between the posterior edge of the P_1 nucleus and the posterior cortex (Fig. 2A). On average, the nucleus was 24.5% of P_1 cell length from the posterior, and the P_1 nucleus reached its most posterior point at 5.15 min after P_0 cytokinesis. The timing of movement was highly variable (SD = 1.12 min) (Fig. 2B and C). Because PAR-2 polarization occurs before posterior nuclear movement, these data do not support the idea that proximity of the nuclear-centrosome complex to the cortex causes polarization.

To visualize the position of the centrosome specifically, we examined embryos expressing mCh::PAR-2 and GFP::AIR-1 (Fig. 2D) (Portier et al., 2007). At the end of P_0 cytokinesis, AIR-1 was localized on the posterior centrosome of the spindle, which at this stage has a disk shape in the center of the cell (Fig. S1A). AIR-1 was localized in a diffuse cloud around the disk aster during the first 2 min of the P_1 cell cycle and then dissociated from the centrosome by 3 min. Around 4 min, AIR-1 started to accumulate onto the new maturing centrosomes. We found that on average, AIR-1 on the centrosome was closest to the posterior (24.09% P_1 cell length) at 5.85 min after cytokinesis (Fig. 2E and F). These results do not support AIR-1 being the symmetry breaking cue in the P_1 cell, because it is not posteriorly localized until approximately 2 min after the time of PAR-2 clearing.

Previous studies also showed that there is anterior-directed actomyosin flow in the P_1 cell which correlates with the movement of PAR-6 to the anterior (Munro et al., 2004). To better understand the timing and role of this flow we imaged embryos expressing GFP::NMY-2 from a cortical view, and we also imaged GFP::NMY-2 in a mid-focal plane with mCh::PAR-2 (Fig. 3A, S1B–C). In some embryos (4/7), some anterior-directed flow of NMY-2 was visible for the first 1–2 min, but then ceased; this flow likely reflects the actomyosin movements at the end of cytokinesis. A strong flow of GFP::NMY-2, similar to what was previously reported (Munro et al., 2004) started 4–6 min after cytokinesis completion; flow continued through at least 10 min, and an anterior domain of GFP::NMY-2 became visible both cortically and in mid-plane (Fig. 3A). These data show that NMY-2 flow, which is known to correlate with PAR-6 movement, does not occur until after PAR-2 has already cleared substantially from the anterior of the P_1 cell at 4 min.

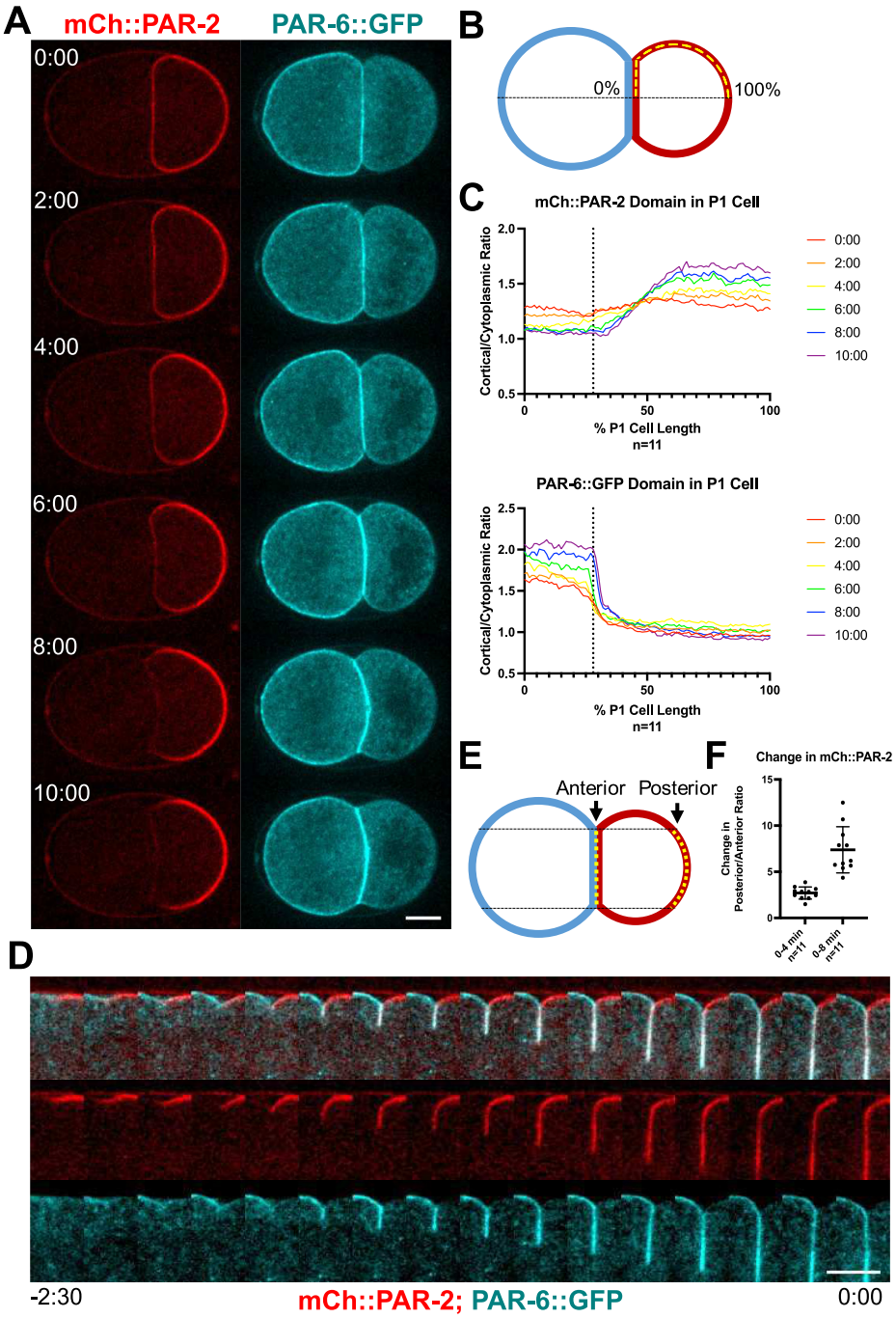

(caption on next page)

Fig. 1. P_1 cell polarization starts within 4 min of cytokinesis. (A) Confocal images of an embryo expressing mCh::PAR-2 and GFP::PAR-6. Anterior is to the left and posterior to the right in this and all figures. Time zero equals completion of cytokinesis. Scale bar is 10 μm. See also Supplemental Video 1. (B) Illustration of quantification of cortical fluorescence. Embryos were divided along the AP axis; the cortex was traced in Image J (yellow dotted line) from the cell contact (0%) to the posterior (100%) and then divided by cytoplasmic intensity. (C) Fluorescence intensity ratio plots every 2 min for the first 10 min of the P_1 cell cycle; each line is an average of multiple embryos. Dotted line highlights the end of the AB- P_1 cell contact. (D) Confocal images of the P_0 cell cytokinetic furrow with mCh::PAR-2 and PAR-6::GFP. Each frame represents a 10 s interval. Scale bar is 5 μm. (E) Illustration of how change in fluorescence measurements were taken for each time point. (F) Quantification of the change in posterior/anterior ratio from 0-4 min and 0–8 min after cytokinesis in control embryos. Means and statistics are reported in Supplemental Table 1.

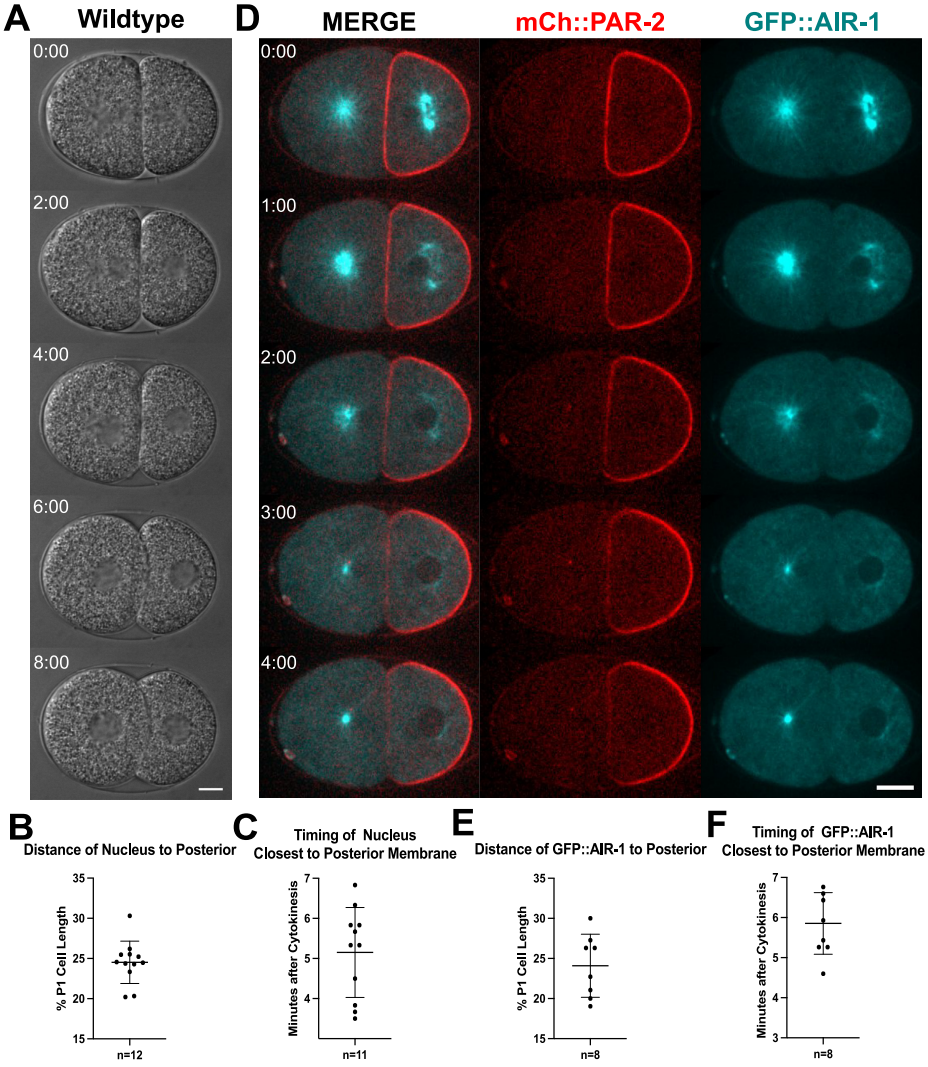

Fig. 2. Nuclear-centrosome movement in the P_1 cell does not correlate with early P_1 polarization. (A) DIC images of nuclear movement in the P_1 cell in a wild-type embryo. Scale bar is 10 μm. See also Supplemental Video 2. (B) Quantification of the closest distance measured between the P_1 nucleus and the posterior cortex (C) Quantification of the time after cytokinesis when the nucleus is closest to the P_1 cell posterior membrane. The total length of the P_1 cell cycle is 16.07 min (Fig. S2 and Supplemental Table 2). (D) Confocal images of embryos expressing mCh::PAR-2 and GFP::AIR-1 every minute from 0 to 4 min after the completion of cytokinesis. Scale bar is 10 μm. See also Supplemental Video 3. (E) Quantification of the closest distance of GFP::AIR-1 foci to the posterior membrane. (F) Quantification of the time after cytokinesis when GFP::AIR-1 foci are closest to the P_1 cell posterior membrane. Means are reported in Supplemental Table 1.

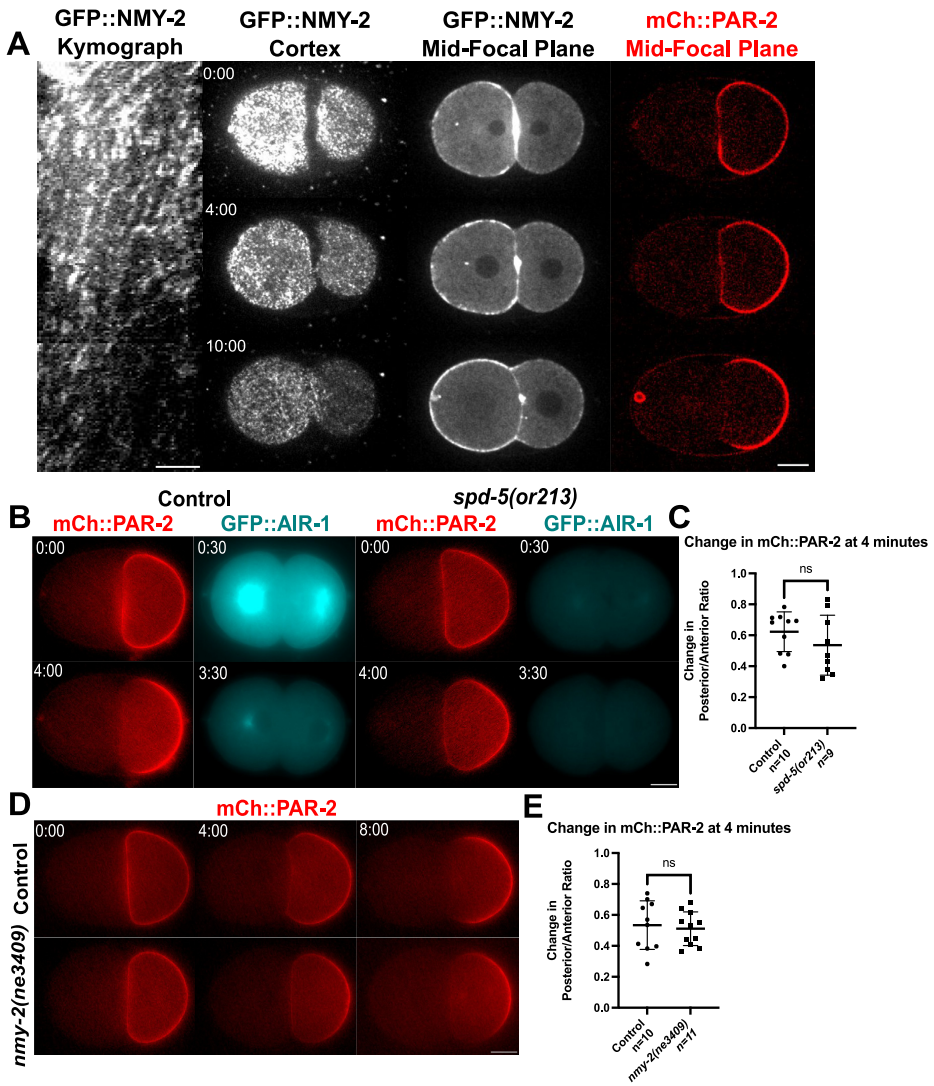

Fig. 3. Actomyosin flow does not correlate with early P_1 cell polarization. (A) Left: Kymograph of GFP::NMY-2 taken across the longest anterior-posterior axis of the P_1 cell in the embryo shown in next panel. Scale bar is 5 μm. Second panel: Confocal fluorescent images of embryo expressing GFP::NMY-2 (Myosin) from a surface view. See also Supplemental Video 4. Third and fourth panels: Confocal fluorescent images of an embryo expressing GFP::NMY-2 and mCh::PAR-2 from a mid-focal plane. Scale bar is 10 μm. (B) Epiflourescent images of embryos expressing mCh::PAR-2 and GFP::AIR-1 with or without *spd-5(or213);* embryos were shifted from 16 °C to 26 °C at P_0 cell NEB. Scale bar is 10 μm. (C) Quantification of the change in posterior/anterior ratio from 0 to 4 min after cytokinesis in control and *spd-5(or213)* embryos. (D) Epiflourescent images of embryos expressing mCh::PAR-2 with or without *nmy-2(ne3409);* embryos were shifted from 16 °C to 26 °C at the end of P_0 cytokinesis. Scale bar is 10 μm. (E) Quantification of the change in posterior/anterior ratio of PAR-2 from 0 to 4 min after cytokinesis in control and *nmy-2(ne3409)* embryos. Note that specific posterior/anterior ratio values differ from those in other figures where confocal images were measured (see Methods). ns = not significant ($p > 0.05$). See Supplemental Table 1 for means and specific P values.

Although AIR-1 does not seem to be localized near the posterior at the time of polarization, we were still interested in whether it could play a role in P_1 cell polarization. AIR-1 is required in the P_0 cell for normal polarization and cytokinesis, and conditional alleles are not available. Thus, to reduce AIR-1 levels on centrosomes before PAR-2 polarization, we used a fast-inactivating temperature sensitive mutant, *spd-5(or213)*. SPD-5 is a centrosome maturation factor required to recruit AIR-1 to the centrosome (Hamill et al., 2002). Embryos were shifted to the restrictive temperature (26 °C) during P_0 cell NEB, and mCh::PAR-2 and GFP::AIR-1 were examined. By the end of P_0 cytokinesis, AIR-1 levels were greatly reduced on the centrosome (Fig. 3B). The increase in the posterior/-anterior ratio of mCh::PAR-2 between the end of cytokinesis and 4 min

was similar for controls and *spd-5(or213)* embryos (Fig. 3C). This result, along with AIR-1's localization at the time of polarity establishment, leads us to believe that AIR-1 on centrosomes is not acting as the symmetry breaking cue in the P_1 cell.

To directly test the role of actomyosin flow in the P_1 cell, we used a fast-inactivating temperature sensitive mutant *nmy-2(ne3409)* and imaged mCh::PAR-2 (Fig. 3D) (Fievet et al., 2013; Liu et al., 2010). NMY-2 is required for cytokinesis and shifting embryos at the start of furrow ingression led to a failure of cytokinesis; such shifts indicated that NMY-2 function was affected within 2 min of the shift to restrictive temperature. To make sure cytokinesis completed and the P_1 cell inherited uniform PAR-2, *nmy-2(ne3409)* embryos were shifted to a restrictive temperature (26 °C) at the end of cytokinesis. We found that there was no significant difference in the timing of PAR-2 clearing compared to controls shifted in the same way at 4 min (Fig. 3D and E). These results are consistent with the view that NMY-2 flows do not stimulate early symmetry breaking in the P_1 cell.

2.3. PAR-1 is required for P_1 cell polarization

Since the mechanism of polarity establishment in the P_1 cell appears to be different than that of the P_0 cell, we examined whether other PAR proteins might be inherited asymmetrically and serve as a cue for P_1 repolarization. In particular we examined PAR-1 and PKC-3 (Fig. 4 and Fig. S2) because these kinases can function to mutually inhibit each other's cortical localization in several systems, and their localization early in the P_1 cell has not been examined in detail.

During furrowing, endogenously tagged PAR-1::meGFP appeared to

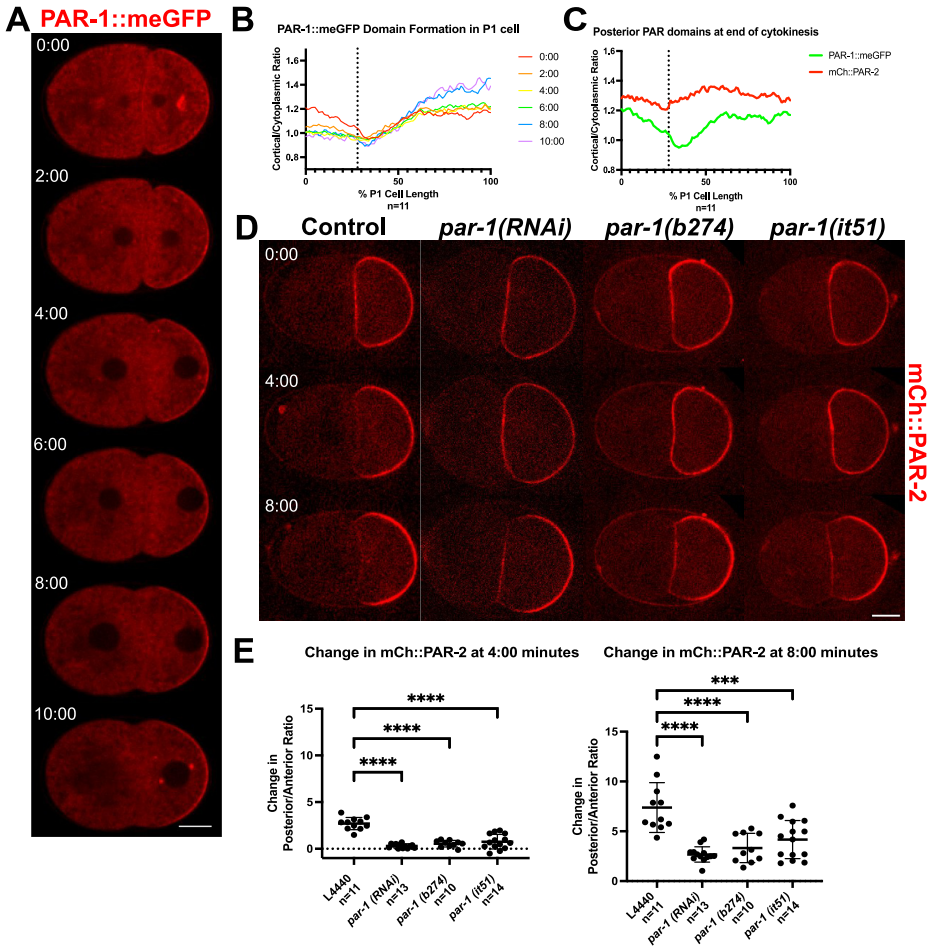

Fig. 4. PAR-1 is inherited asymmetrically in the P_1 cell and is required for early PAR-2 polarization. (A) Confocal images of embryos expressing PAR-1::meGFP. Time zero equals completion of cytokinesis. Scale bar is 10 μm. (B) Fluorescence intensity ratio plots measured as in Fig. 1, where each line represents a timepoint every 2 min for the first 10 min; each line is an average of multiple embryos. Dotted line highlights the end of the AB-P_1 cell contact. (C) Quantifications of fluorescence intensity at the end of cytokinesis. Dotted line highlights the end of the AB-P1 cell contact. (D) Confocal fluorescent images of mCh::PAR-2 in control (L4440, RNAi vector only) and genotypes indicated. Scale bar is 10 μm. See also Supplemental Videos 5 and 6. (E) Quantification of the change in posterior/anterior ratio of mCh::PAR-2 from 0 to 4 min and 0–8 min after cytokinesis. Asterisks (*) indicate statistical significance ($p \leq 0.05$). See Supplemental Table 1 for means and specific P values.

only move into the furrow from the posterior P_1 side (Fig. S2A) (Folkmann and Seydoux, 2019). At the end of cytokinesis, PAR-1::meGFP was present on part of the AB-P_1 cell contact. However, PAR-1 was absent from the anterior corners of the P_1 cell adjacent the contact, and cortical levels increased towards the posterior (Fig. 4A–C). Thus, unlike PAR-2, cortical PAR-1 was inherited in a posterior cortical gradient. PAR-1 cleared from the contact within 2 min and became more enriched in the posterior cortex during the cell cycle (Fig. 4A and B). Similar results were seen with embryos expressing a transgenic PAR-1::GFP (Figs. S2B and D). PKC-3 showed a similar distribution as described for PAR-6, with cortical levels of PKC-3 in the P_1 cell increasing globally in the first 4 min. After 4 min, cortical PKC-3 started to clear from the posterior and continued to accumulate in the anterior (Figs. S2B–C). As with PAR-6, we cannot distinguish whether early in the cell cycle there is any PKC-3 on the P_1 side of the cell contact. However, we did detect a weak gradient of cytoplasmic PKC-3 with more at the anterior side of P_1 at the end of cytokinesis. There was also a weak gradient of cytoplasmic PAR-1 with more in the posterior of the cell (Figs. S2E–F).

The presence of inherited gradients of both cortical and cytoplasmic PAR-1 in the P_1 cell prompted us to examine whether PAR-1 has a role in P_1 cell polarization. Previous work showed that PAR-1 is redundantly required for cortical polarization in the P_0 cell; in *par-1* mutant or RNAi embryos, aPAR and PAR-2 still form reciprocal domains, although the boundary is shifted towards the posterior. *par-1* mutants were reported to reform anterior and posterior PAR domains at the two-cell stage (Rose and Gönczy, 2014). However, the dynamics of domain formation were not examined, raising the possibility that a role for PAR-1 in early polarization was missed.

We first used RNAi to examine the effects of loss of PAR-1 on localization of mCh::PAR-2 throughout the P_1 cell cycle. PAR-2 was inherited all around the P_1 cell at cytokinesis completion, as in controls. However, in these embryos, clearing of PAR-2 from the anterior cell contact was substantially delayed and a PAR-2 domain was not apparent until 6 to 8 min after cytokinesis (Fig. 4D). Quantification of the posterior/anterior ratio of PAR-2 confirmed that there was almost no change in the posterior/anterior ratio of PAR-2 from cytokinesis to 4 min. By 8 min there was a posterior/anterior enrichment of PAR-2, but it was weaker than in controls (Fig. 4E). These results indicate that PAR-1 is required for the initial polarization of PAR-2.

Analysis of PAR-6::GFP and GFP::PKC-3 in *par-1(RNAi)* embryos showed that often cortical aPARs were already present on the P_1 cell adjacent to the cell contact after cytokinesis (Fig. S3A), consistent with the expanded aPAR domain seen in *par-1* one-cells. In addition, there were higher overall levels of PAR-6 and PKC-3 on the P_1 cell membrane than in controls, as predicted if PAR-1 inhibits cortical aPAR accumulation in this cell (Figs. S3B–C). The cytoplasmic gradient of PKC-3 was still present in *par-1(RNAi)* embryos (Fig. S3D).

The delayed polarization of PAR-2 in *par-1(RNAi)* in the P_1 cell was also exhibited by *par-1(b274)* null mutant embryos (Fig. 4D and E). To test if PAR-1's kinase activity is required for early clearing, we analyzed embryos with the kinase dead allele, *par-1(it51)* (Guo and Kemphues, 1995). These embryos also exhibited a polarity delay (Fig. 4D and E). Together these results show that there is an “early” polarization pathway for PAR-2 that depends on PAR-1 and its kinase activity and a “late” polarization pathway that doesn't require PAR-1.

2.4. Cytoplasmic polarity and PLK-1 are important for P_1 cell polarization

Although PAR-1 is redundant for cortical asymmetry maintenance at the one-cell stage, it is essential for the generation of downstream cytoplasmic asymmetries that specify cell fate (Rose and Gönczy, 2014). In wild-type one-cell embryos, PAR-1 is present in a cytoplasmic gradient with higher levels at the posterior, and this gradient is required to localize MEX-5 and MEX-6 in an opposite anterior gradient such that the AB cell inherits more MEX-5/6 (Griffin et al., 2011). MEX-5 and MEX-6 are highly similar RNA-binding proteins that are in turn required for generating the asymmetry of the majority of cell fate determinants downstream of PAR-1, including the mitotic kinase PLK-1(Kim and Griffin, 2020; Rose and Gönczy, 2014). Thus, the role of PAR-1 in polarizing the P_1 cell could stem from either the inherited cortical asymmetry of PAR-1 in the P_1 cell just described, or its role establishing cytoplasmic polarity.

We first verified that in our *par-1(RNAi)* conditions, MEX-5 and PLK-1 appeared uniform in the one-cell embryo and that the AB and P_1 cells received nearly equal amounts (Fig. S4). Next, to test whether the inherited cortical PAR-1 asymmetry is important for P_1 polarization, we utilized existing PAR-1 mutants that affect PAR-1 cortical localization: *par-1(T983A), par-1(KRSS),* and *par-1(ΔKA1)* (Folkmann and Seydoux, 2019). In *par-1(T983A)* mutants the PKC-3 phosphorylation site is mutated, resulting in uniform PAR-1 at the cortex. In contrast, in *par-1(KRSS)* and *par-1(ΔKA1)* mutants, PAR-1's autoinhibitory domain is mutated at two important sites or deleted, respectively, and the protein is also not detectable at the cortex. The effects of these mutants on overall cytoplasmic polarity at the two-cell stage, which is relevant to P_1 polarization, has not been examined and thus we characterized mCh::MEX-5 localization in the meGFP tagged *par-1* mutants. In *par-1(T983A)* embryos, PAR-1 was inherited uniformly on the cortex at reduced levels, and the levels of MEX-5::mCh were almost uniform between the AB and P_1 cell (Fig. 5A and B). In *par-1(KRSS)* and *par-1(ΔKA1)* embryos PAR-1 was not detectable at the membrane. The *par-1(KRSS)* mutant embryos had a normal enrichment of MEX-5 in the AB cell, while the *par-1(ΔKA1)* mutant had almost uniform levels of MEX-5 (Fig. 5A and B).

We then examined mCh::PAR-2 in the meGFP tagged *par-1* mutants. We found that *par-1(T983A)* mutant embryos formed a PAR-2 domain with a higher posterior/anterior enrichment than wildtype embryos at both 4 and 8 min (Fig. 5C and D). The *par-1(KRSS)* embryos cleared PAR-2 similarly to controls at 4 min and 8 min (Fig. 5C and D). Interestingly, the *par-1(ΔKA1)* mutant embryos showed a strong decrease in mCh::PAR-2 polarization at 4 min but formed a weak PAR-2 domain by 8 min (Fig. 5C and D), similar to what was observed for *par-1* null mutants. The opposite effects of the *par-1(T983A) and par-1(ΔKA1)* mutant effects on PAR-2 polarization, when neither mutant has cortical or cytoplasmic asymmetry at this stage, are surprising. Nonetheless, because the *par-1(KRSS)* mutant does not have PAR-1 on the membrane but clears normally, we conclude that PAR-1's cortical localization is not required for normal polarization. This prompted us to examine downstream polarity intermediates for a role in P_1 polarization.

2.5. plk-1 mutant embryos exhibit delayed P_1 polarization

Because MEX-5/6 generate cytoplasmic polarity downstream of PAR-1, we sought to test their role in P_1 polarization. In *mex-5(zu199); mex-6(pk440)* mutant embryos, the one-cell PAR-2 domain was smaller than in controls as previously reported (Cuenca et al., 2003) and the same was true for *mex-5(zu199)* mutant embryos. This resulted in strongly reduced levels of PAR-2 inherited at the AB-P_1 cell contact. Because PAR-2 was already inherited asymmetrically in the P_1 cell, we can't make conclusions about the role of MEX-5/6 in P_1 cell polarization from these data (Figs. S5A–C).

We next examined the role of PLK-1. PLK-1 regulates the cell cycle difference between AB and P_1 as well as the posterior enrichment of several cytoplasmic factors downstream of MEX-5/6 (Kim and Griffin, 2020; Nishi et al., 2008). At the same time, PLK-1 is known to inhibit cortical aPAR association in the oocyte and prevent premature symmetry breaking (Reich et al., 2019). We therefore hypothesized that the high levels of PLK-1 in the P_1 cell of *par-1* mutants might inhibit symmetry breaking and cause the late polarization in *par-1* embryos. To test this hypothesis, we examined a *plk-1(or683)* temperature sensitive mutant (O'Rourke et al., 2011) to determine if loss of PLK-1 could restore normal polarization kinetics in *par-1(RNAi)* embryos. Because PLK-1 also affects cell cycle timing, we quantified the change in polarization relative to P_1 cell cycle length, where 4 min in controls equals 25% of the cell cycle,

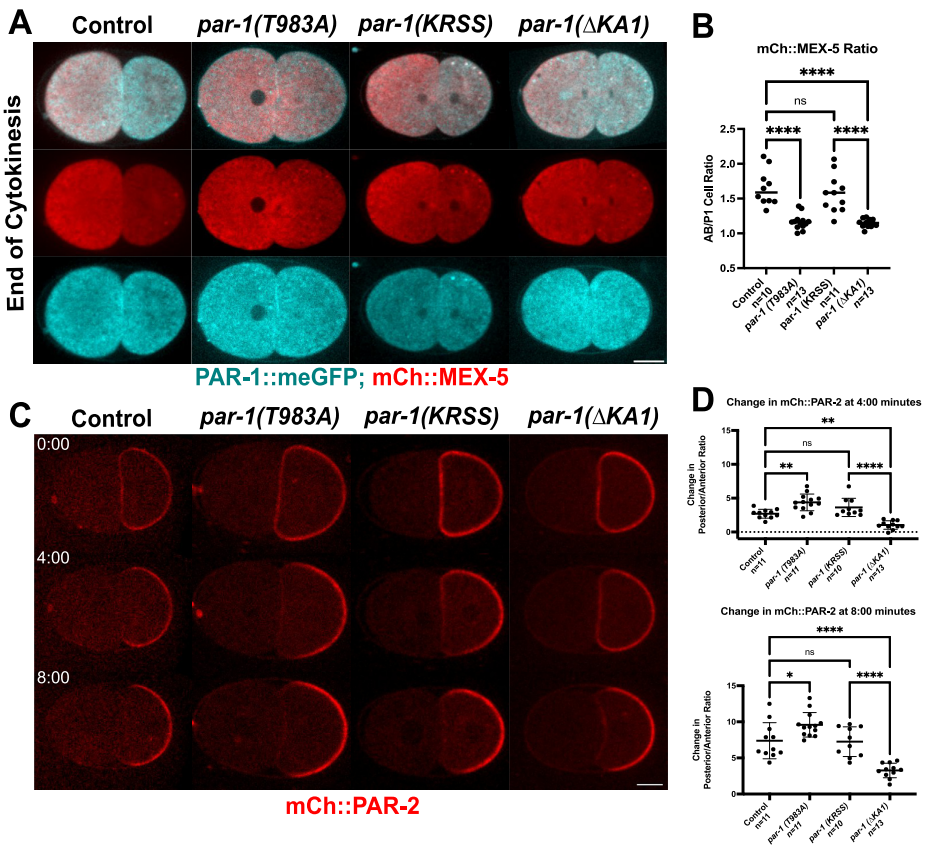

Fig. 5. Cortical PAR-1 is not required for P_1 cell polarization. (A) Confocal fluorescent images of mCh::MEX-5 and PAR-1::meGFP in control and genotypes indicated. Scale bar is 10 μm. (B) Quantification of MEX-5 cytoplasmic asymmetry at the end of P_0 cytokinesis, expressed as the ratio of the AB to P_1 cytoplasmic signals. (C) Confocal fluorescent images of mCh::PAR-2 in control and genotypes indicated. Scale bar is 10 μm. (D) Quantification of the change in posterior/anterior ratio of mCh::PAR-2 from 0 to 4 min and 0–8 min after cytokinesis. ns indicates not significant, asterisks (*) indicate statistical significance ($p \leq 0.05$). See Supplemental Table 1 for means and specific P values.

and 8 min equals 50% (Supplemental Table 2). We found that *plk-1(or683)* mutant embryos exhibited a PAR-2 polarization delay that was similar to that observed in *par-1(RNAi)* embryos (Fig. 6A and B). Further, the *plk-1(or683); par-1(RNAi)* embryos showed neither a rescued nor enhanced polarity defect compared to *par-1(RNAi)* embryos (Fig. 6A and B). These results suggest that excess PLK-1 does not cause the polarity delay in *par-1(RNAi)* embryos. Rather, the data suggest that PAR-1 and PLK-1 may act in the same pathway to regulate P_1 cell polarization.

To gain further evidence for a role for PLK-1 in P_1 polarization, we utilized the *mex-5(T186A)* mutant, which cannot bind to PLK-1 protein. The *mex-5(T186A)* mutant protein is localized normally in an anterior; however, PLK-1 is uniform in this background (Han et al., 2018; Nishi et al., 2008). In *mex-5(T186A)* mutant embryos, the P_1 cell inherited PAR-2 uniformly on the membrane at levels comparable to controls, but PAR-2 cleared to a lesser extent than in control embryos at 4 min (Fig. 6A–B, Fig. S5C). The same polarity delay was exhibited by *mex-5(T186A); mex-6(RNAi)* embryos (Figs. S5A–B). Together these data support a model in which PAR-1, MEX-5, and PLK-1 are required for P_1 cell polarization.

2.6. Centrosome maturation and actomyosin flow are required for late polarization

Although *par-1* mutant embryos exhibit a polarity delay, they do form a PAR-2 domain by 8 min after cytokinesis. Based on our analysis of the timing of nuclear movement and actomyosin flow, we hypothesized that late polarization could occur through a similar mechanism to that in the P_0 cell, where centrosome maturation and actomyosin flow are required.

To test if centrosome maturation is required for late PAR-2 clearing, we carried out *par-1(RNAi)* on the *spd-5(or213); mCh::PAR-2* strain and shifted the embryos to the restrictive temperature at NEB in the P_0 cell. *spd-5(or213); par-1(RNAi)* embryos exhibited a similar posterior/anterior ratio of PAR-2 as *par-1(RNAi)* embryos at 4 min after cytokinesis (Fig. 7A and B). However, at 8 min, more PAR-2 remained on the AB-P_1 cell contact in double mutants compared to *par-1(RNAi)* embryos (Fig. 7A and B). Similarly, *nmy-2(ne3409); par-1(RNAi)* embryos shifted to the restrictive temperature at the end of cytokinesis exhibited a lower posterior/anterior ratio of PAR-2 at 8 min than observed in *par-1(RNAi)* alone (Fig. 7A and B). Further, although initial PAR-2 clearing in *nmy-2(ne3409)* and *spd-5(or213)* single mutant embryos was normal as shown earlier, these singles mutants showed significantly less PAR-2 asymmetry

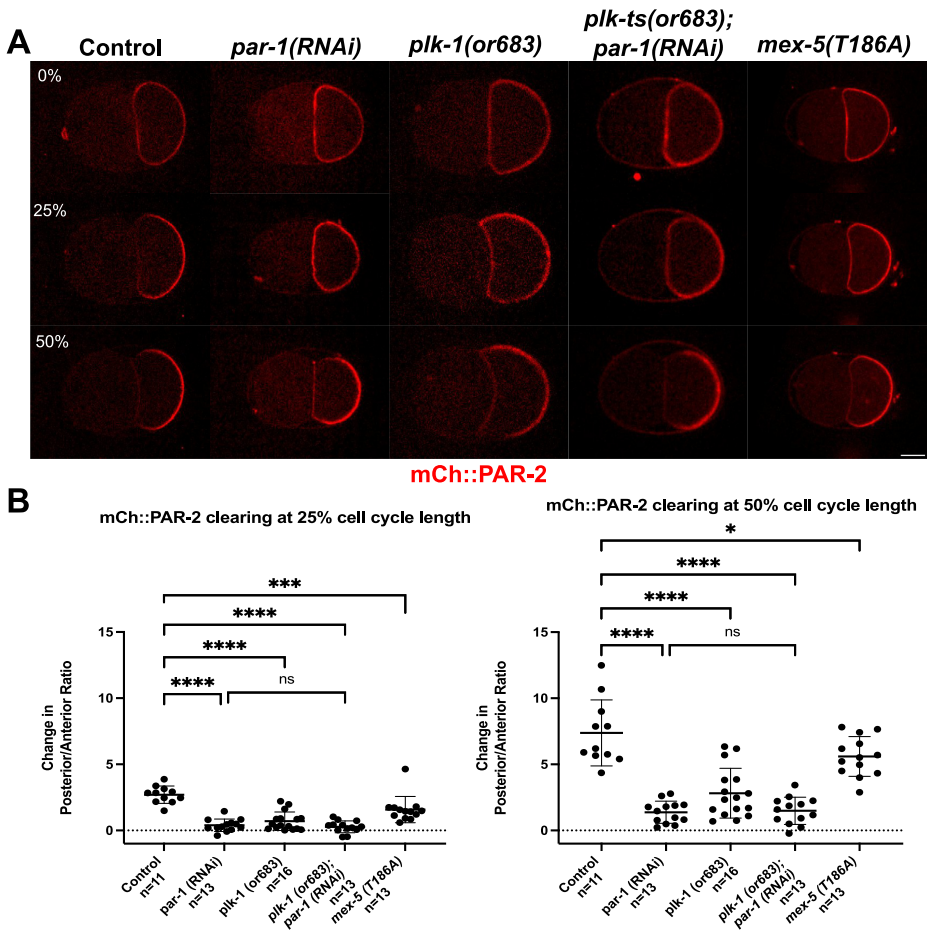

Fig. 6. *plk-1* mutants exhibit a delay in P_1 polarization. (A) Confocal fluorescent images of mCh::PAR-2 in control (L4440) and genotypes indicated. The data shown for control and *par-1* embryos is the same as shown in Fig. 4 for comparison. *plk-1(or683)* embryos were shifted to room temperature 30 min before filming. Scale bar is 10 μm. (B) Quantification of the change in posterior/anterior ratio of mCh::PAR-2 at 0 to 25%, and 0 to 50% P_1 cell cycle length relative to total cell cycle length in each treatment. See Supplemental Table 2 for cell cycle lengths for each genotype. ns indicates not significant, asterisks (*) indicate statistical significance $p \leq 0.05$). See Supplemental Table 1 for means and specific P values.

than controls at 8 min. These results, together with the timing of myosin flow and reaccumulation of AIR-1 on the centrosome (Fig. 3, Fig. 2) suggest that AIR-1 and NMY-2 have a role in P_1 cell polarization, but this pathway is not active until later in the cell cycle.

Interestingly, even though *spd-5(or213);par-1(RNAi)* and *nmy-2(ne3409);par-1(RNAi)* retained higher levels of PAR-2 at the anterior compared to *par-1* single mutants at 8 min, they nonetheless showed areas cleared of PAR-2 adjacent to the AB-P_1 cell contact. In 60% of *spd-5(or213);par-1(RNAi)* embryos and 78.5% of *nmy-2(ne3409);par-1(RNAi)* embryos PAR-2 clearing initiated from one side, rather than equally from the cell contract (Fig. S6). These data suggest that in addition to the early pathway and late pathways for P_1 polarization identified above, there are additional mechanisms for symmetry breaking present at the two-cell stage.

2.7. Loss of PKC-3 blocks P_1 cell polarization

To further probe the mechanism by which PAR-2 is cleared from the anterior of the P_1 cell, we tested whether PKC-3 plays a role, using a temperature sensitive mutant, *pkc-3(ne4250)* (Fievet et al., 2013), in the mCh::PAR-2 background. Even when grown and imaged at 16C, some *pkc-3(ne4250);* mCh::PAR-2 embryos exhibited *pkc-3* mutant phenotypes such as a symmetric first cell division and incorrect division patterns at the two-cell stage, suggesting that this allele is a hypomorph even at permissive temperature. Nevertheless, in such *pkc-3(ne4250)*, the one-cell embryo still formed a PAR-2 domain and the P_1 cell inherited uniform PAR-2. Surprisingly at the two-cell stage, a PAR-2 domain never formed in the P_1 cell (Fig. 8A and B), but in all embryos a PAR-2 domain formed in the AB cell by the time of AB cell cytokinesis (n = 7, Fig. S7).

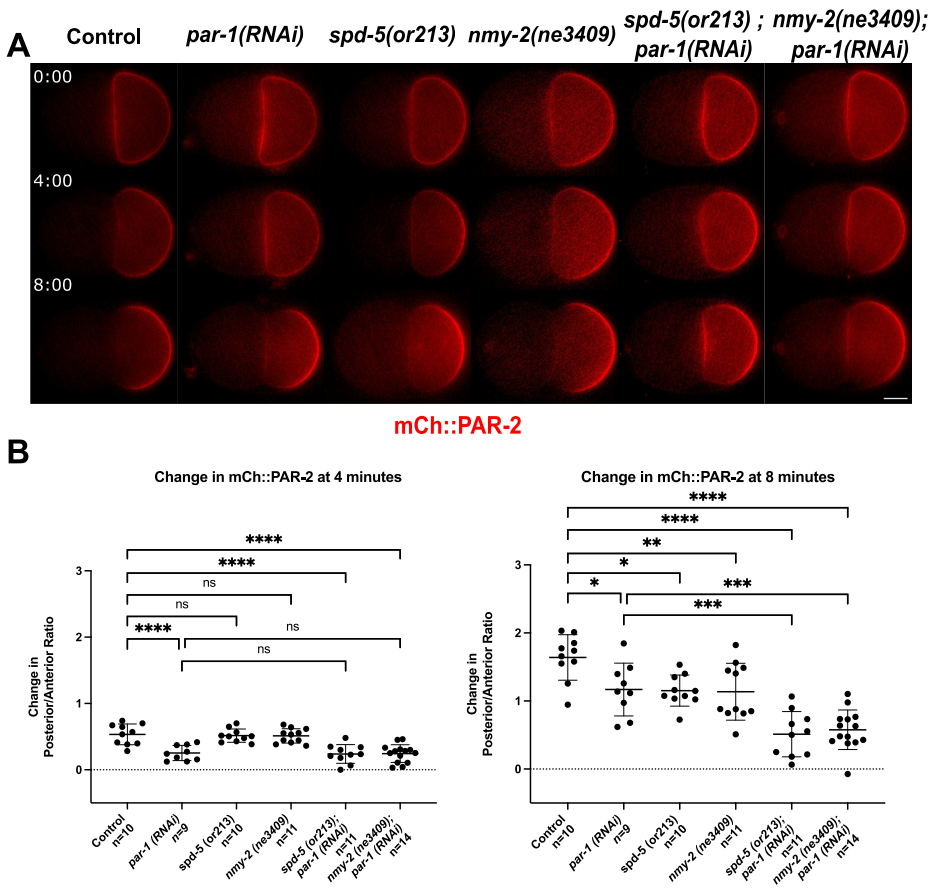

Fig. 7. Centrosome maturation and actomyosin flow are required for late polarization in the P_1 cell. (A) Epiflourescent images of mCh::PAR-2 in control(L4440) and genotypes indicated; all embryos were shifted from 16 °C to 26 °C at the end of P_0 cytokinesis or NEB (see Methods). The control and *nmy-2(ne3409)* single mutants are repeated from Fig. 3 for comparison. Scale bar is 10 μm. (B) Quantification of the change in posterior/anterior ratio of mCh::PAR-2 from 0 to 4 min and 0–8 min after cytokinesis. ns indicates not significant, asterisks (*) indicate statistical significance ($p \leq 0.05$). See Supplemental Table 1 for means and specific P values.

These results indicate that PKC-3 is required for early PAR-2 domain formation in the P_1 cell, but this data does not distinguish between a role for PKC-3 in one-cell polarity or acting more directly in the P_1 cell.

We also sought to test whether another anterior PAR, CDC-42, contributes to PAR-2 clearing in the P_1 cell. CDC-42 is a small GTPase that binds to PKC-3 and PAR-6 and is required for active PKC-3 in the one-cell embryo (Rodriguez et al., 2017; Seirin-Lee et al., 2020). To examine if CDC-42 is active at the two-cell stage, we used a GFP tagged version of the WSP-1 G-protein-Binding-Domain, which is a published reporter for CDC-42 activity (Kumfer et al., 2010). In control embryos, active CDC-42 started to accumulate at the AB-P_1 cell contact around 4 min after P_0 cytokinesis and continued to accumulate throughout the cell cycle (Fig. 8C and D).

Because CDC-42 is required for proper P_0 cell polarization we could not examine the P_1 cell in a *cdc-42* null mutant. Instead, we examined embryos mutant for CGEF-1, a guanine nucleotide exchange factor that is partially redundant for activating CDC-42 in the early embryo (Kumfer et al., 2010). We first imaged GFP::WSP-1(GBD) in *cgef-1(gk261)* null mutant embryos and found GFP::WSP-1(GBD) no longer accumulated on the AB-P_1 cell contact (Fig. 8C and D). This result indicates that CGEF-1 activates CDC-42 at the two-cell stage. We next examined mCh::PAR-2; *cgef-1(gk261)* embryos. These embryos exhibited partial *cdc-42* mutant phenotypes and were rounder than wild-type embryos (Kumfer et al., 2010), but the P_0 cell had a normal PAR-2 domain at the posterior cortex. We observed that in *cgef-1(gk261)* embryos, P_1 inherited PAR-2 uniform on the cortex, and polarization of the PAR-2 domain at 4 min was similar to controls. To test if CDC-42 has a role in the late pathway, we performed *par-1(RNAi)* on mCh::PAR-2; *cgef-1(gk261)*. In this double mutant, we did not see a significant difference, but we did see a lower mean at 8 min compared to *par-1(RNAi)* alone (Fig. 8E and F). These results suggest that CDC-42, and by implication PKC-3, is required for the late polarization pathway.

3. Discussion

The mechanisms by which polarity is established in the one-cell embryo (P_0) of *C. elegans* have been extensively studied, as has polarization in other cell types in other organisms. However, much remains to

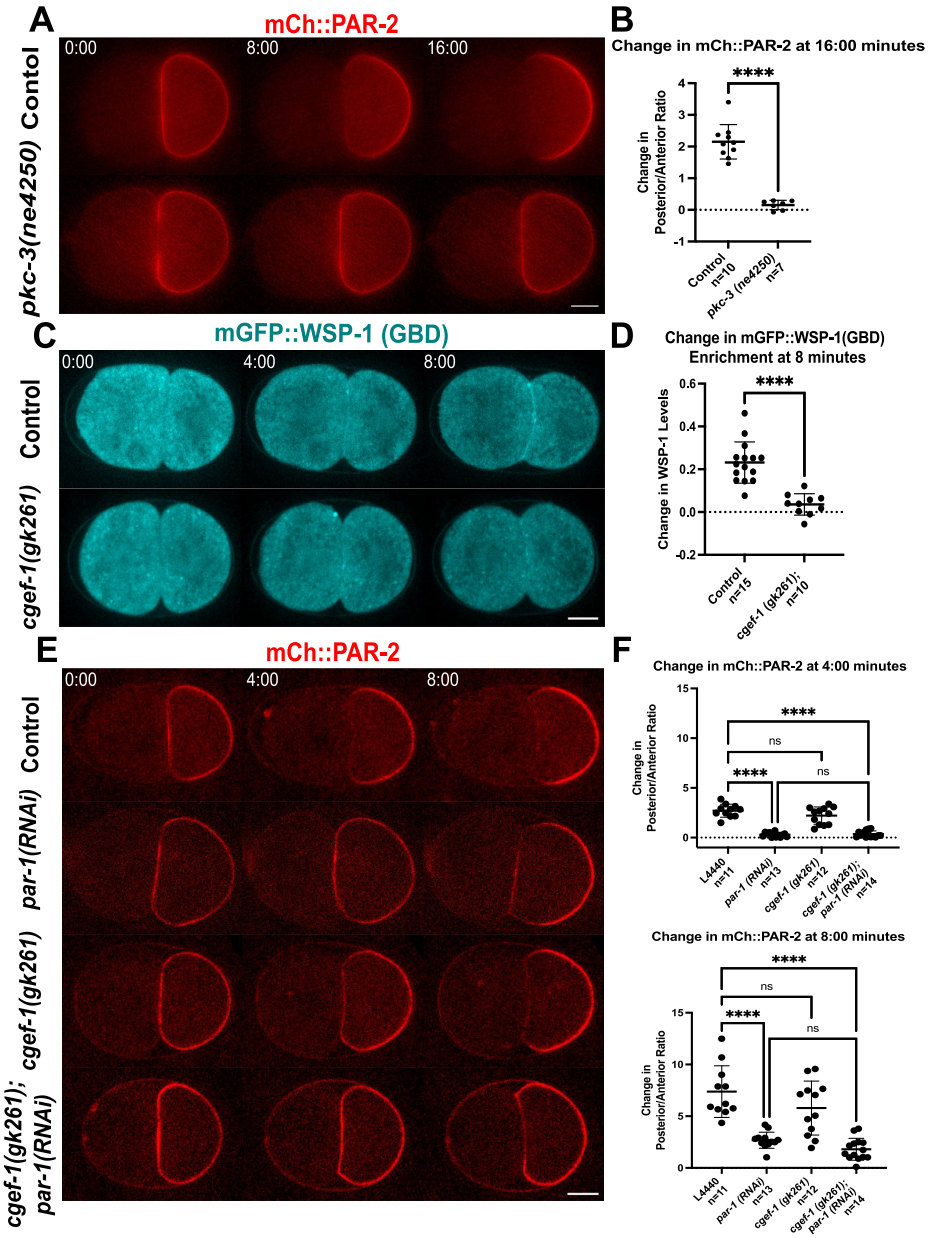

Fig. 8. PKC-3 is required for early and late polarization in the P_1 cell. (A) Epiflourescent images of mCh::PAR-2 in control and *pkc-3(ne4250)* embryo grown and imaged at 16 °C. Scale bar is 10 μm. (B) Quantification of the change in posterior/anterior ratio of mCh::PAR-2 from 0 to 16 min after cytokinesis. (C) Confocal fluorescent images of mGFP::WSP-1(GBD) in control and *cgef-1(gk261)* embryos. Scale bar is 10 μm. (D) Quantification of change in mGFP::WSP-1GBD at AB-P_1 cell contract from 0 to 8 min relative to cytoplasm. (E) Confocal images of mCh::PAR-2 in control (L4440) and genotypes indicated. The data shown for control and *par-1* embryos is the same as shown in Fig. 4 for comparison. Scale bar is 10 μm. (F) Quantification of the change in posterior/anterior ratio of mCh::PAR-2 from 0 to 4 min and 0–8 min after cytokinesis. ns indicates not significant, asterisks (*) indicate statistical significance ($p \leq 0.05$). See Supplemental Table 1 for means and specific P values.

be learned about how polarity is reestablished and maintained during successive asymmetric cell divisions and under different developmental conditions. Here, we characterized polarization of the P_1 cell at the second division of the *C. elegans* embryo. In the P_1 cell, reciprocal aPAR and pPAR domains form, but the cues for symmetry breaking and mechanism for polarization have not been investigated. We used mCh::PAR-2 as a marker for cortical polarity and confirmed that PAR-2 is inherited uniformly around the P_1 cell. The polarization of P_1 occurs very early in the P_1 cell cycle, with clearing of PAR-2 from the anterior AB-P_1 cell contact region beginning within 2 min after P_0 cytokinesis. Clearing continues and the levels of PAR-2 increase at the posterior so that a domain is visible at 4 min, but polarization of PAR-2 is stronger at 8 min.

In the P_0 cell, the presence of AIR-1 on the centrosome near the cortex appears to trigger symmetry breaking by inhibiting local myosin contractility; the resulting anterior directed myosin flow carries clusters of aPARs away from the centrosome and the presumptive posterior pole. PAR-1 and PAR-2 then associate with the posterior cortex (Klinkert et al., 2019; Munro et al., 2004; Schonegg et al., 2014; Zhao et al., 2019). Nuclear-centrosome movement towards the posterior and anterior-directed cortical myosin and PAR-6 flow have been observed in the P_1 cell (Munro et al., 2004). However, here we found that strong cortical myosin flows occur well after the PAR-2 domain has started to form. Similarly, by analyzing AIR-1's localization on the centrosome in P_1,we conclude that AIR-1 is not in the correct position at the right time to act as a localized cue for early P_1 polarization. Finally, using conditional mutants to inhibit AIR-1 recruitment to the centrosome or reduce myosin flow right after cytokinesis did not change the initial kinetics of PAR-2 clearing from the anterior cortex. These data together suggest that AIR-1 and actomyosin flow are not required for early polarization in the P_1 cell.

Interestingly, we identified several asymmetries inherited by the P_1 cell. Although PAR-2 is present uniformly around the P_1 cortex after one-cell cytokinesis, the P_1 cell is partially polarized for cortical PAR-1 and there are opposing cytoplasmic gradients of PAR-1 and PKC-3. It is also possible that low levels of PKC-3 or other aPARs are inherited in the P_1 cell on the anterior cortex. However, due to the resolution limits of light microscopy, we cannot determine whether the signal on the AB-P_1 contact is only in the AB cell or in both cells. Because PKC-3 and PAR-1 are known to inhibit each other's localization, these inherited cytoplasmic or cortical gradients, where levels of PKC-3 are higher near the anterior, could trigger initial clearing of PAR-2. Consistent with this view, we found that *pkc-3(ne4250)* mutants showed normal cortical PAR-2 polarity at the end of P_0 cytokinesis, but then never formed a normal PAR-2 domain. However, because the *pkc-3(ne4250)* allele has one-cell defects, these results are also consistent with a non-mutually exclusive model in which PKC-3 is needed for the proper asymmetry of other cytoplasmic components that play a role in P_1 polarization, as outlined below. Further, we found that in *par-1(RNAi)* embryos, the cytoplasmic gradient of PKC-3 is still present, and PKC-3 is visible on the anterior cortex of P_1, near the AB-P_1 cell contact. This suggests that at least in the background of loss of PAR-1, PKC-3 asymmetry is not sufficient for early polarization.

Because of PAR-1's initial asymmetry in the P_1 cell, we also tested whether PAR-1 has a functional role in P_1 cell polarization. We found however, that the lack of PAR-1 cortical asymmetry or cortical localization did not affect P_1 cell polarization. Rather, defects in PAR-2 polarization correlated with loss of overall cytoplasmic polarity when comparing the *par-1(KRSS)* and *par-1(ΔKA1)* mutants, neither of which is localized to the cortex. Further, we found that PLK-1, which is necessary for the asymmetric posterior localization of a number of cell fate determinants downstream of PAR-1 and MEX-5, is required for P_1 polarization. *plk-1(or683)* embryos and the *plk-1(or683); par-1(RNAi)* double mutants showed the same polarity delay as *par-1* mutant embryos. These observations suggest that PLK-1 and PAR-1 are acting in the same pathway to regulate a downstream cytoplasmic factor that is required for early polarization. We can envision two explanations for the polarity delay in *par-1* and *plk-1* mutants. One hypothesis is that a downstream cytoplasmic target of PAR-1 and PLK-1 is enriched in the P_1 cell, and that cytoplasmic factor either acts as an inherited cue or activates a yet to be identified cue. The lower levels of this factor present in *par-1*and *plk-1* mutant embryos would result in a failure of early polarization. Alternatively, there may be a cytoplasmic component that normally suppresses symmetry breaking in the AB cells, and this factor is enriched in the AB cell by PLK-1. This component would be more uniformly distributed in the *par-1* and *plk-1* mutants, such that higher levels now suppress polarization of P_1 as well. Further experiments are required to identify such potential activators or inhibitors of polarity. However, it seems unlikely that PLK-1 is itself the inhibitor since loss of PLK-1 activity did not rescue the polarization defect in *par-1(RNAi)* embryos.

Even though *par-1* mutant embryos do not polarize at the same time as wild-type embryos, they do eventually form a weak posterior PAR-2 domain. The time of AIR-1's re-recruitment to centrosomes at the posterior and of NMY-2 flow in wild-type embryos correlates with the timing of late polarization observed in *par-1* mutants. Further, we found that simultaneous loss of PAR-1 and NMY-2 or SPD-5 resulted in more severe polarization defects. In addition, *nmy-2* and *spd-5* single mutants have a less robust PAR-2 domain at 8 min. These data lead us to propose that AIR-1 and NMY-2 have a role in the P_1 cell, but they act in the late pathway, after the initial symmetry breaking event described above occurs. It was previously shown that actomyosin flow corresponds with the movement of PAR-6, and our data is consistent with flow being a major driver of aPAR clearing in the posterior and accumulation in the anterior observed after 4 min in the wild-type embryo. In addition, the decrease in polarization of PAR-2 observed in *cgef-1* mutants, and the absence of late polarization in *pkc-3* mutants described, is consistent with PKC-3 playing a role in late polarization through exclusion of PAR-2. Cortical PAR-1 may similarly help reinforce reciprocal domains at this stage by inhibiting aPARs at the posterior, based on our finding that although a PAR-2 domain forms late in *par-1* mutants, it is not as strong as in controls.

All the data in this study supports a model in which there are two major pathways for timely polarization in the P_1 cell (Fig. 9). There is a novel early pathway that initiates P_1 polarization within 2 min after cytokinesis, which requires PAR-1, PKC-3, MEX-5, PLK-1 and the inheritance of normal cytoplasmic polarity. There is a second late pathway, which involves centrosome maturation and actomyosin flow-dependent accumulation of aPARs in the anterior. This second pathway enhances posterior PAR-1 and PAR-2 asymmetry in wild-type embryos as the cell cycle progresses and can function to polarize PAR-2 when early polarization is blocked. We also propose there are other pathways that can break symmetry in the P_1 cell, because even the double mutants in this study are able to clear PAR-2. One possible mechanism for this clearing is that PAR-2 binding to microtubules emanating from the posterior centrosome at this time could protect it from phosphorylation by PKC-3; this pathway is redundant in P_0 polarity (Motegi et al., 2011). However, in many *par-1* mutants with *spd-5 or nmy-2,* PAR-2 did not clear from the anterior AB-P_1 cell contact as in controls, but instead cleared laterally, in one or both of the anterior corners of the P_1 cell. It has been previously reported that in the absence of the normal cue in the one-cell *C. elegans embryos*, there are other mechanisms that can spontaneously break symmetry that are influenced by cell shape (Klinkert et al., 2019); this phenomenon might be yet another way to break symmetry in the P_1 cell.

In summary, our results identify a novel PAR-1 and PLK-1 dependent mechanism for polarization in the *C. elegans* embryo, which gives new insight into how cells in different developmental contexts can establish PAR polarity. The results also build on previous work in the *C. elegans* one-cell and *Drosophila* neuroblasts showing that cells employ multiple partially redundant pathways to promote robust polarization during asymmetric division.

4. Materials and methods

4.1. C. elegans strains

C. elegans strains were maintained on MYOB plates with *E. coli* OP50 as a food source (Brenner, 1974; Church et al., 1995). The following strains were used in this study, listed in the order they appear in the paper:

Strain #	Genotype	Source
N2	*Wild type, Bristol Strain*	CGC
KK1264	*par-6(it310[par-6::gfp]) I; par-2(it315 [mCherry::par-2]) III*	Ken Kemphues, (Reich et al., 2019)
RL439	*par-2(it315[mCherry::par-2]) III; ltIs78[(pKO5) pie-1::GFP::TEV::Stag::air-1 spliced coding + unc-119(+)]*	This study
JH2759	*unc-119(ed3) III; axIs1929[nmy-2::GFP + mCherry::par-2]*	Zonies et al. (2010)
RL530	*axIs1929[nmy-2::GFP + mCherry::par-2]; par-2(it315[mCH::PAR-2]) III*	This study
RL450	*spd-5(or213) I; par-2(it315[mCherry::par-2]) III; ltIs78[(pKO5) pie-1::GFP::TEV::Stag::air-1 spliced coding]*	This study
KK1254	*par-2(it315[mCherry::par-2]) III*	Ken Kemphues
RL497	*nmy-2(ne3409) I; par-2(it315[mCherry::par-2]) III*	This study
JH3616	*par-1(ax4206[PAR-1::meGFP]) V*	Folkmann and Seydoux (2019)
RL520	*par-2(it315[mCherry::par-2]) III; par-1(it51) rol-4/nTl V*	This study
RL521	*par-2(it315[mCherry::par-2]) III; par-1(b274) rol-4/nTl V*	This study
JH3679	*mex-5(ax3050[mCherry::mex-5]); par-1(ax4206 [PAR-1::meGFP]) V*	Folkmann and Seydoux (2019)
JH3678	*mex-5(ax3050[mCherry::mex-5]); par-1(ax4209 [PAR-1(T983A)::meGFP])/nT1 [qIs51(pha::GFP)] V*	Folkmann and Seydoux (2019)
RL563	*mex-5(ax3050[mCherry::mex-5]); par-1(ax4207 [PAR-1(K1170S R1171S)::meGFP])*	This study
RL564	*mex-5(ax3050[mCherry::mex-5]); par-1(ax4208 [PAR-1(ΔKA1)::meGFP])/nT1[qIs51(pha::GFP)] V*	This study
RL444	*par-2(it315[mCherry::par-2]) III; par-1(ax4206 [PAR-1::meGFP]) V*	This study
RL544	*par-2(it315[mCherry::par-2]) III; par-1(ax4209 [PAR-1(T983A)::meGFP])/nT1 [qIs51(pha::GFP)] V*	This study
RL542	*par-2(it315[mCherry::par-2]) III; par-1(ax4207 [PAR-1(K1170S R1171S)::meGFP])*	This study
RL543	*par-2(it315[mCherry::par-2]) III; par-1(ax4208 [PAR-1(ΔKA1)::meGFP])/nT1[qIs51(pha::GFP)] V*	This study
RL545	*par-2(it315[mCherry::par-2]) III; plk-1(or683) III*	This study
RL565	*par-2(it315[mCherry::par-2]) III; mex-5(egx2 [T186A]) IV.*	This study
RL557	*spd-5(or213) I; par-2(it315[mCherry::par-2]) III*	This study
RL473	*pkc-3(ne4250) II; par-2(it315[mCherry::par-2]) III*	This study
WH517	*ojIs40 [wsp-1(GBD)::GFP + unc-119(+)]*	Kumfer et al. (2010)
WH527	*cgef-1(gk261) X; ojIs40 [wsp-1(GBD)::GFP + unc-119(+)]*	Kumfer et al. (2010)
RL533	*par-2(it315par-2(it315[mCherry::par-2]) III; cgef-1(gk261) X*	This study
RL396	*par-2(it315par-2(it315[mCherry::par-2]))III; ltIs37 [pie-1p::mCherry::his-58 + unc-119(+)] him-8(e1489) IV; ruls57[pie-1::GFP::tubulin + unc-119(+)]*	This study
KK1228	*pkc-3(it309[GFP::PKC-3]) II*	Ken Kemphues
JH1734	*axIs1245 [PAR-1::GFP]*	Griffin et al. (2011)
OD2425	*plk-1(lt18[plk-1::sGFP]::loxp) III.*	(Martino L. et al., 2017)
RL298	*axEx73[GFP::PIE-1 rol-6]; axIs1731[pie-1p::mCherry::mex-5::pie-1 3′UTR + unc-199(+)]*	This study
RL566	*par-2(it315par-2(it315[mCherry::par-2])) III; unc-30(e191) mex-5(zu199) IV/nT1 (IV;V)*	This study
RL522	*par-2(it315par-2(it315[mCherry::par-2])) III; mex-6(pk440) II; unc-30(e191) mex-5(zu199) IV/nT1 (IV;V)*	This study

4.2. Live imaging

Because all of the proteins under study are maternally provided, embryos were derived from homozygous mutant hermaphrodites, or hermaphrodites treated for RNAi, in all cases. Embryos were removed from gravid hermaphrodites, dissected into egg buffer (25 mM HEPES, pH 7.4, 120 mM NaCl, 48 mM KCl, 2 mM CaCl2, MgCl2), mounted on 2% agar pads, and covered with coverslip.

Epifluorescent microscopy was carried out on an Olympus BX60 microscope equipped with PlanApo N 60X, 1.42 NA oil immersion objective lens, a CoolLED light source, a Hammatasu Orca 12-bit digital camera, and MicroManager software. All time-lapse videos were taken at 10 s intervals, except for temperature sensitive mutants and their controls which were taken every 30 s.

Confocal microscopy was carried out using the spinning disc module of an Intelligent Imaging Innovations (3i) Marianas SDC Real-Time 3D Confocal-TIRF microscope fit with a Yokogawa spinning disc head, a 60 × 1.4 numerical aperture oil-immersion objective, EMCCD camera, and Slidebook 6 software. Images were taken in a mid-focal plane at 10 s intervals, except for cortical images of NMY-2 for which 3 Z-planes were imaged with 0.5-μm steps every 3 s.

4.3. RNAi and temperature sensitive mutants

RNAi was performed by feeding (Timmons and Fire, 1998). The *par-1(RNAi)* construct used was obtained from the Ahringer RNAi library (Kamath et al., 2003). RNAi was conducted for 48hrs at 20 °C to obtained published strong loss of function phenotypes, such as synchronous two-cell divisions and symmetric P_0 cell division.

Fast-inactivating temperature sensitive mutants were grown and mounted on slides at 16 °C and then transferred to a stage controlled by a Linkam PE95/T95 System Controller with an Eheim Water Circulation Pump to maintain the temperature of the slide. The stage was set to 12 °C for 16 °C and 26 °C for 26 °C; true temperatures were determined by inserting the wire probe of an Omega HH81 digital thermometer between the cover slip and an agar pad with oil on the 60X objective. The shift from 16 °C to 26 °C occurred in 1 min. The strength of each temperature sensitive mutant was compared to published mutant or loss of function phenotypes.

4.4. Quantification

Some images in figures were contrast adjusted for better visualization, but all measurements were made on the raw data from original TIFF files using Fiji as outlined below. Measurements were exported into Excel for determination of means and ratios, then analyzed for statistical significance using Graphpad Prism version 9.0 with the following symbols used in the figures: ns $p > 0.05$, *$p \leq 0.05$, **$p \leq 0.01$, ***$p \leq 0.001$, ****$p \leq 0.0001$. Statistical tests used and p values are presented in Supplemental Table 1.

Analysis of cortical mCh::PAR-2, PAR-6::GFP, PAR-1::meGFP, and GFP::PKC-3 domains in the P_1 cell were done by dividing the embryo along its longest anterior-posterior axis. Then both the top and bottom cortices were traced using the segmented line tool (width = 2 pixels) in Fiji (as in Fig. 1B). Cytoplasmic mean was measured by drawing a small circle in they cytoplasm, avoiding the cortex and nucleus. Cortical intensity was divided by cytoplasmic mean and adjusted to percent P_1 cell length. This was done for each embryo and then averaged to get a plot for each time point. The overall cortical levels of PAR-6::GFP and PKC-3::GFP in the P_1 cell were measured by tracing the single membranes of the P_1 cell and dividing by the cytoplasmic mean for each embryo (as in Fig. S3B).

Analysis of cytoplasmic polarity in N2, PAR-1::meGFP and GFP::PKC-3 was measured at the end of cytokinesis. As above, embryos were divided along their longest anterior-posterior axis, but then traces were made in the cytoplasm approximately 5 pixels below the cortex, using the

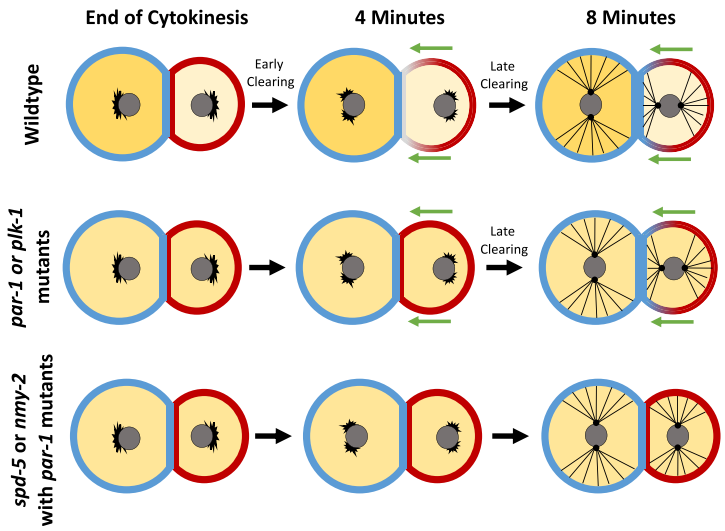

Fig. 9. Model for Polarity Establishment in the P_1 cell. Illustration of two pathways for establishing polarity at the 2-cell stage. Stages of polarization are shown at three timepoints in wildtype, *par-1* or *plk-1* mutants, and *spd-5;par-1* or *nmy-2;par-1 mutants*. PAR-2 is in red, PAR-6 is in blue, and cytoplasmic factors are in yellow; the grey circles are nuclei, the black line shows microtubules emanating from the centrosome and the green arrows illustrate actomyosin flow.

segment line tool (width = 2 pixels) in Fiji (as in Fig S2E). Cytoplasmic intensity was divided by the background outside of the cell and adjusted to percent P_1 cell length.

To analyze how close the centrosome moves towards the posterior cortex, the frame where cytokinesis ended and then the frame in which the nucleus or GFP::AIR-1 foci were closest to the membrane were scored. At this timepoint the Fiji line tool was used to measure the distance from the edge of the P_1 nucleus or the GFP::AIR-1 foci to the posterior membrane. The distance of the nucleus or GFP::AIR-1 foci was normalized to P_1 cell length (longest anterior-posterior axis) to account for differences in embryo size.

Analysis of the change in mCh::PAR-2 domain over time was quantified using the Fiji line segment tool (width = 2 pixels) to trace the AB-P_1 cell contract and the same length of the posterior cortex at zero, four and 8 min after cytokinesis. For embryos filmed on the 3i confocal microscope, cortical traces were normalized to cytoplasmic mean. Because of the large amount of out of focus fluorescence within the cell, for embryos filmed with epifluorescence the cortical traces were normalized to the background outside of the cell. The normalized posterior value was divided by the normalized anterior value to give a posterior/anterior ratio for each time point. The difference between time points was found (example: P/A ratio at 4:00 – P/A ratio at 0:00) to calculate the change over time.

The mCh::MEX-5 and PLK-1::GFP cytoplasmic ratios were determined by drawing a small circle in the AB cell and P_1 cell, avoiding membranes and the nucleus. The average mean of the AB cytoplasm was divided by the P_1 cell to find the AB-P_1 ratio.

Change in GFP::WSP-1(GBD) was measured by tracing the AB-P_1 cell contact using Fiji line segment tool (width = 2 pixels). This was normalized to cytoplasmic mean to get a normalized intensity for each time point. Then the normalized intensity at 8 min was subtracted by the normalized intensity at 0 min to find the changed in GFP::WSP-1(GBD).

Data availability

Data will be made available on request.

Acknowledgements

We thank Christy Kok for help with filming N2 embryos and data analysis, Aidan van Cleef and Kathie Urrutia-Paniagua for media preparation, Katherine Plance and Mike Van Gompel for strain generation, and members of the Rose and McNally labs for helpful discussions. We are grateful to Ken Kemphues, Geraldine Seydoux for providing strains. Other strains were provided by *Caenorhabditis* Genetics Center, which is funded by the National Institutes of Health Office of Research Infrastructure Programs (P40 OD010440). The 3i Marianas spinning disk confocal used in this study was purchased using a National Institutes of Health Shared Instrumentation Grant [1S10RR024543-01]. We thank the MCB Light Microscopy Imaging Facility, which is a UC-Davis Campus Core Research Facility, for maintaining this microscope. This research was funded by awards to LR from the National Institutes of Health Grant [R01GM68744] and the National Institute of Food and Agriculture [CA-D*-MCB-6239-H].

Appendix A. Supplementary data

Supplementary data to this article can be found online at https://doi.org/10.1016/j.ydbio.2023.05.005.

References

Arata, Y., Lee, J.-Y., Goldstein, B., Sawa, H., 2010. Extracellular control of PAR protein localization during asymmetric cell division in the C. elegans embryo. Development 137 (19), 3337–3345. https://doi.org/10.1242/dev.054742.

Bei, Y., Hogan, J., Berkowitz, L.A., Soto, M., Rocheleau, C.E., Pang, K.M., Collins, J., Mello, C.C., 2002. SRC-1 and Wnt signaling act together to specify endoderm and to control cleavage orientation in early C. elegans embryos. Dev. Cell 3 (1), 113–125. https://doi.org/10.1016/s1534-5807(02)00185-5.

Benton, R., St Johnston, D., 2003. Drosophila PAR-1 and 14-3-3 inhibit Bazooka/PAR-3 to establish complementary cortical domains in polarized cells. Cell 115 (6), 691–704. https://doi.org/10.1016/s0092-8674(03)00938-3.

Boyd, L., Guo, S., Levitan, D., Stinchcomb, D.T., Kemphues, K.J., 1996. PAR-2 is asymmetrically distributed and promotes association of P granules and PAR-1 with the cortex in C. elegans embryos. Development 122 (10), 3075–3084. https://doi.org/10.1242/dev.122.10.3075.

Brenner, S., 1974. The genetics of Caenorhabditis elegans. Genetics 77 (1), 71–94. https://www.ncbi.nlm.nih.gov/pubmed/4366476.

Cheeks, R.J., Canman, J.C., Gabriel, W.N., Meyer, N., Strome, S., Goldstein, B., 2004. May 25). C. elegans PAR proteins function by mobilizing and stabilizing asymmetrically localized protein complexes. Curr. Biol. 14 (10), 851–862. https://doi.org/10.1016/j.cub.2004.05.022.

Church, D.L., Guan, K.L., Lambie, E.J., 1995. Three genes of the MAP kinase cascade, mek-2, mpk-1/sur-1 and let-60 ras, are required for meiotic cell cycle progression in Caenorhabditis elegans. Development 121 (8), 2525–2535. https://doi.org/10.1242/dev.121.8.2525.

Cowan, C.R., Hyman, A.A., 2004. Sep 2). Centrosomes direct cell polarity independently of microtubule assembly in C. elegans embryos. Nature 431 (7004), 92–96. https://doi.org/10.1038/nature02825.

Cuenca, A.A., Schetter, A., Aceto, D., Kemphues, K., Seydoux, G., 2003. Polarization of the C. elegans zygote proceeds via distinct establishment and maintenance phases. Development 130 (7), 1255–1265. https://doi.org/10.1242/dev.00284.

Fievet, B.T., Rodriguez, J., Naganathan, S., Lee, C., Zeiser, E., Ishidate, T., Shirayama, M., Grill, S., Ahringer, J., 2013. Systematic genetic interaction screens uncover cell polarity regulators and functional redundancy. Nat. Cell Biol. 15 (1), 103–112. https://doi.org/10.1038/ncb2639.

Folkmann, A.W., Seydoux, G., 2019. Mar 25). Spatial regulation of the polarity kinase PAR-1 by parallel inhibitory mechanisms. Development 146 (6). https://doi.org/10.1242/dev.171116.

Goldstein, B., 1993. Establishment of gut fate in the E lineage of C. elegans: the roles of lineage-dependent mechanisms and cell interactions. Development 118 (4), 1267–1277. https://doi.org/10.1242/dev.118.4.1267.

Goldstein, B., 1995. Cell contacts orient some cell division axes in the Caenorhabditis elegans embryo. J. Cell Biol. 129 (4), 1071–1080. https://doi.org/10.1083/jcb.129.4.1071.

Goldstein, B., Macara, I.G., 2007. The PAR proteins: fundamental players in animal cell polarization. Dev. Cell 13 (5), 609–622. https://doi.org/10.1016/j.devcel.2007.10.007.

Griffin, E.E., Odde, D.J., Seydoux, G., 2011. Regulation of the MEX-5 gradient by a spatially segregated kinase/phosphatase cycle. Cell 146 (6), 955–968. https://doi.org/10.1016/j.cell.2011.08.012.

Guo, S., Kemphues, K.J., 1995. par-1, a gene required for establishing polarity in C. elegans embryos, encodes a putative Ser/Thr kinase that is asymmetrically distributed. Cell 81 (4), 611–620. https://doi.org/10.1016/0092-8674(95)90082-9.

Hamill, D.R., Severson, A.F., Carter, J.C., Bowerman, B., 2002. Centrosome maturation and mitotic spindle assembly in C. elegans require SPD-5, a protein with multiple coiled-coil domains. Dev. Cell 3 (5), 673–684. https://doi.org/10.1016/s1534-5807(02)00327-1.

Han, B., Antkowiak, K.R., Fan, X., Rutigliano, M., Ryder, S.P., Griffin, E.E., 2018. Polo-like kinase couples cytoplasmic protein gradients in the C. elegans zygote, 2018/01/08/ Curr. Biol. 28 (1), 60–69.e68. https://doi.org/10.1016/j.cub.2017.11.048.

Hao, Y., Boyd, L., Seydoux, G., 2006. Stabilization of cell polarity by the C. elegans RING protein PAR-2. Dev. Cell 10 (2), 199–208. https://doi.org/10.1016/j.devcel.2005.12.015.

Hurov, J.B., Watkins, J.L., Piwnica-Worms, H., 2004. Atypical PKC phosphorylates PAR-1 kinases to regulate localization and activity. Curr. Biol. 14 (8), 736–741. https://doi.org/10.1016/j.cub.2004.04.007.

Kamath, R.S., Fraser, A.G., Dong, Y., Poulin, G., Durbin, R., Gotta, M., Kanapin, A., Le Bot, N., Moreno, S., Sohrmann, M., Welchman, D.P., Zipperlen, P., Ahringer, J., 2003. Systematic functional analysis of the Caenorhabditis elegans genome using RNAi. Nature 421 (6920), 231–237. https://doi.org/10.1038/nature01278.

Kemphues, K.J., Priess, J.R., Morton, D.G., Cheng, N.S., 1988. Feb 12). Identification of genes required for cytoplasmic localization in early C. elegans embryos. Cell 52 (3), 311–320. https://doi.org/10.1016/s0092-8674(88)80024-2.

Kim, A.J., Griffin, E.E., 2020. PLK-1 regulation of asymmetric cell division in the early C. elegans embryo. Front. Cell Dev. Biol. 8, 632253. https://doi.org/10.3389/fcell.2020.632253.

Klinkert, K., Levernier, N., Gross, P., Gentili, C., von Tobel, L., Pierron, M., Busso, C., Herrman, S., Grill, S.W., Kruse, K., Gönczy, P., 2019. Aurora A depletion reveals centrosome-independent polarization mechanism in Caenorhabditis elegans. Elife 8. https://doi.org/10.7554/eLife.44552.

Kumfer, K.T., Cook, S.J., Squirrell, J.M., Eliceiri, K.W., Peel, N., O'Connell, K.F., White, J.G., 2010. CGEF-1 and CHIN-1 regulate CDC-42 activity during asymmetric division in the Caenorhabditis elegans embryo. Mol. Biol. Cell 21 (2), 266–277. https://doi.org/10.1091/mbc.e09-01-0060.

Liu, J., Maduzia, L.L., Shirayama, M., Mello, C.C., 2010. NMY-2 maintains cellular asymmetry and cell boundaries, and promotes a SRC-dependent asymmetric cell division. Dev. Biol. 339 (2), 366–373. https://doi.org/10.1016/j.ydbio.2009.12.041.

Motegi, F., Zonies, S., Hao, Y., Cuenca, A.A., Griffin, E., Seydoux, G., 2011. Microtubules induce self-organization of polarized PAR domains in Caenorhabditis elegans zygotes. Nat. Cell Biol. 13 (11), 1361–1367. https://doi.org/10.1038/ncb2354.

Munro, E., Nance, J., Priess, J.R., 2004. Cortical flows powered by asymmetrical contraction transport PAR proteins to establish and maintain anterior-posterior polarity in the early C. elegans embryo. Dev. Cell 7 (3), 413–424. https://doi.org/10.1016/j.devcel.2004.08.001.

Nishi, Y., Rogers, E., Robertson, S.M., Lin, R., 2008. Polo kinases regulate C. elegans embryonic polarity via binding to DYRK2-primed MEX-5 and MEX-6. Development 135 (4), 687–697. https://doi.org/10.1242/dev.013425.

O'Rourke, S.M., Carter, C., Carter, L., Christensen, S.N., Jones, M.P., Nash, B., Price, M.H., Turnbull, D.W., Garner, A.R., Hamill, D.R., Osterberg, V.R., Lyczak, R., Madison, E.E., Nguyen, M.H., Sandberg, N.A., Sedghi, N., Willis, J.H., Yochem, J., Johnson, E.A., Bowerman, B., 2011. A survey of new temperature-sensitive, embryonic-lethal mutations in C. elegans: 24 alleles of thirteen genes. PLoS One 6 (3), e16644. https://doi.org/10.1371/journal.pone.0016644.

Pickett, M.A., Naturale, V.F., Feldman, J.L., 2019. A polarizing issue: diversity in the mechanisms underlying apico-basolateral polarization in vivo. Annu. Rev. Cell Dev. Biol. 35, 285–308. https://doi.org/10.1146/annurev-cellbio-100818-125134.

Portier, N., Audhya, A., Maddox, P.S., Green, R.A., Dammermann, A., Desai, A., Oegema, K., 2007. A microtubule-independent role for centrosomes and aurora a in nuclear envelope breakdown. Dev. Cell 12 (4), 515–529. https://doi.org/10.1016/j.devcel.2007.01.019.

Reich, J.D., Hubatsch, L., Illukkumbura, R., Peglion, F., Bland, T., Hirani, N., Goehring, N.W., 2019. Regulated activation of the PAR polarity network ensures a timely and specific response to spatial cues. Curr. Biol. 29 (12), 1911–1923.e1915. https://doi.org/10.1016/j.cub.2019.04.058.

Rodriguez, J., Peglion, F., Martin, J., Hubatsch, L., Reich, J., Hirani, N., Gubieda, A.G., Roffey, J., Fernandes, A.R., St Johnston, D., Ahringer, J., Goehring, N.W., 2017. aPKC cycles between functionally distinct PAR protein assemblies to drive cell polarity. Dev. Cell 42 (4), 400–415.e409. https://doi.org/10.1016/j.devcel.2017.07.007.

Rose, L., Gönczy, P., 2014. Polarity establishment, asymmetric division and segregation of fate determinants in early C. elegans embryos. WormBook 1–43. https://doi.org/10.1895/wormbook.1.30.2.

Schonegg, S., Hyman, A.A., Wood, W.B., 2014. Timing and mechanism of the initial cue establishing handed left–right asymmetry in Caenorhabditis elegans embryos. Genesis 52 (6), 572–580. https://doi.org/10.1002/dvg.22749.

Seirin-Lee, S., Gaffney, E.A., Dawes, A.T., 2020. CDC-42 interactions with par proteins are critical for proper patterning in polarization. Cells 9 (9). https://doi.org/10.3390/cells9092036.

Sunchu, B., Cabernard, C., 2020. Principles and mechanisms of asymmetric cell division. Development 147 (13). https://doi.org/10.1242/dev.167650.

Tabuse, Y., Izumi, Y., Piano, F., Kemphues, K.J., Miwa, J., Ohno, S., 1998. Atypical protein kinase C cooperates with PAR-3 to establish embryonic polarity in Caenorhabditis elegans. Development 125 (18), 3607–3614. https://doi.org/10.1242/dev.125.18.3607.

Timmons, L., Fire, A., 1998. Specific interference by ingested dsRNA. Nature 395 (6705), 854. https://doi.org/10.1038/27579.

Venkei, Z.G., Yamashita, Y.M., 2018. Emerging mechanisms of asymmetric stem cell division. J. Cell Biol. 217 (11), 3785–3795. https://doi.org/10.1083/jcb.201807037.

Watts, J.L., Etemad-Moghadam, B., Guo, S., Boyd, L., Draper, B.W., Mello, C.C., Priess, J.R., Kemphues, K.J., 1996. par-6, a gene involved in the establishment of asymmetry in early C. elegans embryos, mediates the asymmetric localization of PAR-3. Development 122 (10), 3133–3140. https://doi.org/10.1242/dev.122.10.3133.

Zhao, P., Teng, X., Tantirimudalige, S.N., Nishikawa, M., Wohland, T., Toyama, Y., Motegi, F., 2019. Aurora-A breaks symmetry in contractile actomyosin networks independently of its role in centrosome maturation. Dev. Cell 48 (5), 631–645.e636. https://doi.org/10.1016/j.devcel.2019.02.012.

Zonies, S., Motegi, F., Hao, Y., Seydoux, G., 2010. Symmetry breaking and polarization of the C. elegans zygote by the polarity protein PAR-2. Development 137 (10), 1669–1677. https://doi.org/10.1242/dev.045823.

Chapter III

Structure function analysis of LET-99's posterior lateral band localization

Introduction

Asymmetric cell division is the process in which a cell divides to give rise to two daughter cells with different cell fates. During intrinsically asymmetric cell divisions, such as in the *C. elegans* P_0 cell, the cell must first establish a polarity axis. Next, it must segregate its cell fate determinants along this axis, and lastly it will orient its spindle along this polarity axis so that when the cell divides each daughter cell receives the correct cell fate determinants. Asymmetric cell division is conserved in all animals and is important throughout development and during stem cell maintenance (Sunchu & Cabernard, 2020; Venkei & Yamashita, 2018).

In *C. elegans,* this polarity axis is set up by the conserved PAR proteins. The PAR proteins are required for other asymmetrically dividing cells such as *Drosophila* neuroblasts or mammalian epithelial cells (Goldstein & Macara, 2007; Pickett et al., 2019; Rose & Gonczy, 2014). In the one-cell *C. elegans* embryo, the PAR proteins form two mutually exclusive domains on the cortex in the anterior and posterior of the cell. The anterior PARs (aPARs) are PAR-3 and PAR-6, which are PDZ domain containing scaffolding proteins, PKC-3 which is an atypical protein kinase C, and CDC-42 which is a small GTPase (Cuenca et al., 2003; Kemphues et al., 1988; Tabuse et al., 1998; Watts et al., 1996). Previous work has shown that the aPARs exist in two clusters. One cluster where PKC-3 and PAR-6 cycle between being bound to PAR-3 where they can respond to polarity cues and localize properly to the anterior. In the other cluster, PKC-3 and PAR-6 binds to CDC-42 and in this cluster PKC-3 is active and can phosphorylate downstream targets (Rodriguez et al., 2017).

The posterior PARs (pPARs) include PAR-2 which is a RING finger protein and PAR-1 which is a serine/threonine kinase (Boyd et al., 1996; Cowan & Hyman, 2004; Guo & Kemphues, 1995; Hao et al., 2006). PAR-1 is also present in a posterior cytoplasmic gradient. PAR-1 restricts the localization of the cytoplasmic polarity proteins MEX-5/6, which form an anterior domain and regulate cell fate determinants leading to daughter cells with different cell fates (Griffin et al., 2011; Kim & Griffin, 2020; Rose & Gonczy, 2014).

PAR proteins also signal through downstream targets to orient the mitotic spindle with the polarity axis so that each daughter cell receives the correct cell fate determinants. In the *C. elegans* P_0 cell, the nuclear-centrosome complex centers and rotates along the anterior-posterior axis. Then during anaphase, the spindle displaces posteriorly leading to an unequal cell division with a larger AB cell and smaller P_1 cell.

For the nuclear-centrosomal complex to center and rotate there must be asymmetric pulling forces on the spindle. PKC-3 and LET-99 regulate these asymmetric pulling forces on the spindle by regulating the force-generating complex. The force-generating complex is made up of two partially redundant Gα subunits GOA-1 and GPA-16, two completely redundant GoLoco containing proteins GPR-1 and GPR-2, the large coiled-coil protein LIN-5, and the minus end directed microtubule motor dynein (Rose & Gonczy, 2014). PKC-3 regulates the force generating complex by phosphorylating LIN-5, decreasing pulling forces in the anterior (Galli et al., 2011).

Another mechanism of regulating pulling forces is through LET-99. *let-99* mutants show defects in centration, rotation, and spindle displacement (Rose & Kemphues, 1998; Tsou et al., 2002). LET-99 localizes to a posterior lateral band on the cortex with highest

levels where the aPAR and pPAR protein levels are lowest. The presence of LET-99 results in lower GPR-1/2 levels in the band region, generating asymmetric pulling forces. In *let-99* mutants both GPR-1/2 and LIN-5 localization is uniform on the cortex causing uniform pulling forces on the spindle (Bouvrais et al., 2018; Krueger et al., 2010; Park & Rose, 2008).

Previous work has shown that PAR-3 is required to restrict LET-99 from the anterior and PAR-1 and PAR-5 are required for inhibiting LET-99 from the posterior, but the cytoplasmic polarity mediator MEX-5 is not required for LET-99 localization (Wu et al., 2016; Wu & Rose, 2007). PAR-5 is a 14-3-3 protein, which binds to phosphorylated targets to alter their activity or localization. LET-99 binds both PAR-1 and PAR-5. These and other results suggest that spindle positioning and cytoplasmic polarity are controlled by the PAR proteins by two sperate mechanisms, and that LET-99 is a direct target of the PAR-1 kinase. (Wu & Rose, 2007). However, the mechanism by which LET-99 localizes to the membrane and how the aPARs inhibit LET-99 from the anterior have not been identified.

Results

PAR-3, PKC-3, and CDC-42 are all required for proper LET-99 localization.

Previous work showed that PAR-3 is required for proper LET-99 localization, but the role of the other aPAR proteins was not tested. To further investigate the mechanism by which LET-99 is restricted from the anterior we looked at YFP::LET-99 localization (Bringmann et al., 2007), after RNAi knockdowns of *par-3, pkc-3,* and *cdc-42*. We did this RNAi in a mCh::PAR-2 background, because PAR-2 should be uniform on the membrane in

these mutant backgrounds. We examined the YFP::LET-99 pattern at NEB, when a band has formed in control embryos (Figure 1A). To quantify LET-99 localization, we traced the cortex from the anterior to posterior pole and normalized it to the cytoplasmic mean and plotted it as percent embryo length (Figure 1B). As was previously described, in *par-3(RNAi)* LET-99 is uniform on the cortex but at lower levels (Tsou et al., 2002). We also found that in *pkc-3(RNAi)* and *cdc-42(RNAi)* embryos, LET-99 was present at uniform levels. This data supports the hypothesis that LET-99 could be a direct target of PKC-3.

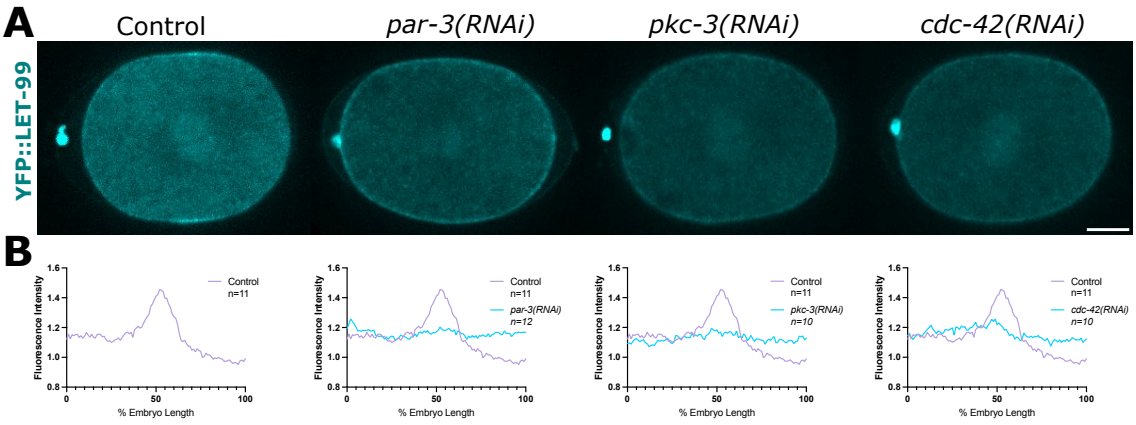

Figure 1. PAR-3, PKC-3, and CDC-42 are required for proper LET-99 localization. (A) Fluorescent images of YFP::LET-99 in *par-3, pkc-3, and cdc-42* at NEB. Scale bar is 10µm. (B) Plots showing the average cortical intensities of YFP::LET-99 localization at NEB.

The C-terminus of LET-99 is required for membrane localization

LET-99 is a DEP domain-containing protein and based on BLAST searches using *C. elegans* and other nematode LET-99 proteins, it is most related to the DEP domain-containing-1 (DEPDC1) family of proteins. This family has the DEP domain near the N-terminus of the protein (from 23-107aa in LET-99, Fig. 2). DEP domain was named for the proteins in which it was first identified in Dishevelled, EGL-10, and Pleckstrin, but has since been found in several proteins involved in G-protein signaling (Consonni et al., 2014). The DEP domain is also negatively charged and in proteins such as in Dishevelled, the DEP domain was shown to associate with positively charged lipids and to be required for membrane localization. LET-99 also has a region that shares partial homology to a Rho-GAP domain found in the DEPDC1 family of proteins when run through the NCBI-CDD motif search. We also identified six potential PKC-3 phosphorylation sites by using an atypical protein kinase C consensus sequence and motif search tool(Fig. 2A)(Wang et al., 2012).

To understand how LET-99 is localized to the membrane and restricted from the anterior we used a structure function approach. The YFP::LET-99 transgene rescues LET-99 lethality, but this randomly integrated transgene is prone to silencing. Thus, we first tested two different fluorescent tags at the N-terminus and C-terminus. We made four new LET-99 fluorescently tagged strains with either mKate2 or GFP at the N-terminus or C-terminus using MOS-1 mediated single copy insertion. We tested the ability of the transgenes to rescue normal LET-99 localization in the *let-99(dd17)* background. GFP::LET-99 and LET-99::GFP had very low signal in the one-cell stage. Both mKate versions had

visible LET-99 on the cortex but only LET-99::mKate localized normally into a band by NEB (Fig. S1).

Previous work in the lab showed that the DEP domain of LET-99 is sufficient for binding lipids in vitro, which led to the hypothesis that the DEP domain is required for LET-99 localization to the membrane (E. Espiritu Dissertation 2015). To test this, constructs of GFP::LET-99 with deletions of the N-terminal region or C-terminal regions were expressed in Xenopus cells. LET-99 was able to localize to the membrane in Xenopus cells but the DEP domain was neither required nor sufficient for membrane localization. Surprisingly, any deletion of the C-terminal region of LET-99 did affect localization to the membrane (E. Espiritu, K. Plance, and L. Rose, personal communication). Based on these preliminary results, we hypothesize that in *C. elegans*, the C-terminus of LET-99 is required for membrane localization rather than the DEP domain.

To test this hypothesis in *C. elegans* and gain further insight into the potential role of the DEP domain, we designed deletions of the N-terminus (Δ1-300aa and Δ130-330) and C-terminus (Δ608-698aa) of LET-99. We then crossed these deletion transgenes into the *let-99(dd17)* background. To test what region is required for membrane localization, we examined the mKate signal using epifluorescence microscopy. The LET-99(Δ1-300)::mKate and LET-99(Δ130-330)::mKate deletions both localized to the membrane. While the LET-99(Δ608-698)::mKate deletion did not localize to the membrane, whole cell intensity measurements showed that it was expressed at levels similar to full length LET-99::mKate (Fig. 2B-C). These data support the hypothesis that the C-terminal region is required for

localizing LET-99 to the membrane and that the DEP domain is not required for LET-99 to localize to the membrane.

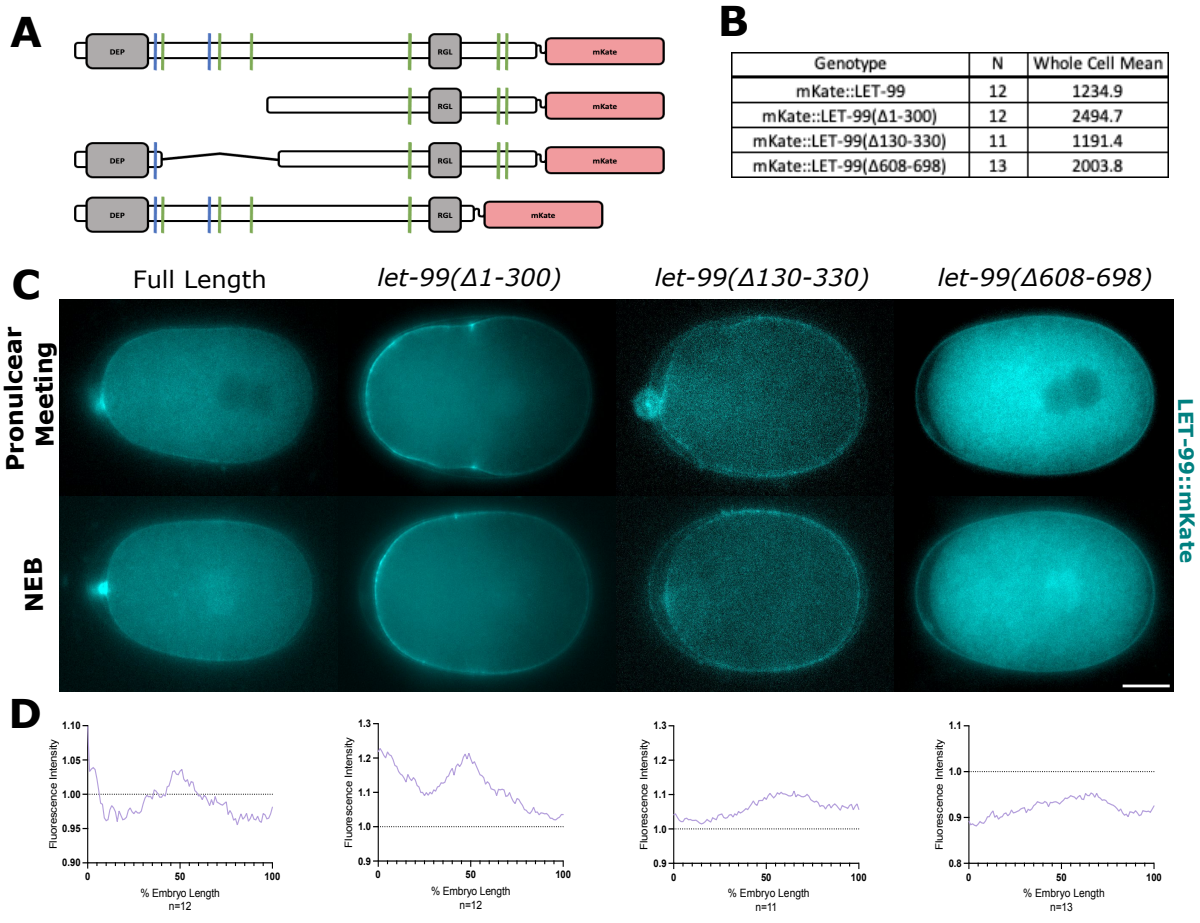

Genotype	N	Whole Cell Mean
mKate::LET-99	12	1234.9
mKate::LET-99(Δ1-300)	12	2494.7
mKate::LET-99(Δ130-330)	11	1191.4
mKate::LET-99(Δ608-698)	13	2003.8

Figure 2. LET-99::mKate deletion constructs and fluorescent localization. (A) Schematic diagram of LET-99 constructs: full length LET-99, LET-99(Δ1-300), LET-99(Δ130-330), and LET-99(Δ608-698). (B) Whole cell means and number of embryos for each genotype shown. (C) Fluorescent images of each genotype shown at NEB. Scale bar is 10μm. (D) Plots showing the average cortical intensities of LET-99::mKate localization at NEB normalized to the cytoplasm.

Analysis of LET-99::mKate cortical asymmetry

To better understand how LET-99 is restricted from the anterior, we further analyzed our deletion constructs for cortical asymmetry by quantifying cortical intensity from the anterior to the posterior and measured whole cell intensity. The LET-99(Δ1-300)::mKate deletion removes the DEP domain and three potential PKC-3 phosphorylation sites. It also deletes two previously identified PAR-5 binding sites, which are predicted to be PAR-1 phosphorylation sites and are required for restricting LET-99 from the posterior. The LET-99(Δ130-330)::mKate deletion deletes these three sites as well as one of the PAR-5 binding sites.

We found that the LET-99(Δ1-300)::mKate deletion was over two times brighter than the control embryos and its cortical trace was above cytoplasmic levels at all points along the cortex. (Fig. 2B-D). Compared to control, the LET-99(Δ1-300)::mKate deletion is present at higher levels in the anterior from the time of pronuclear meeting and remains high in the anterior throughout the cell cycle. At the time of NEB, although levels at the very anterior are still high, there is a banded pattern in the center of the cell (Fig. 2C-D). We hypothesize that LET-99 is being pulled to the anterior during polarity establishment and remains high because of the deleted PKC-3 phosphorylation sites. The higher cortical levels in the posterior compared to controls is consistent with the deletion of the PAR-5 sites.

The LET-99(Δ130-330)::mKate deletion had the lowest whole cell mean but was still close to the control (Fig. 2B). The LET-99(Δ130-330)::mKate deletion appeared in a posterior domain that extended further anteriorly than controls, although levels were still slightly higher in the normal band region (Fig. 2C-D). These results are consistent with deleting one of the PAR-5 sites. The anterior expansion may be the result of deleting three

of the potential PKC-3 sites and without them PKC-3 is less efficient at inhibiting LET-99 from the anterior. Together these results support the hypothesis that these three potential PKC-3 sites are important for LET-99 localization, but because the LET-99(Δ608-698)::mKate deletion was not on the cortex we could not test the other two potential PKC-3 sites at the C-terminus.

LET-99(Δ130-330)::mKate rescues the spindle positioning phenotypes of the null mutation

To test how well these different deletions rescued *let-99(dd17)* null phenotypes, we filmed them in Differential Interference Contrast (DIC) microscopy. *let-99* mutants have defects in nuclear centration, rotation, and spindle displacement (Fig. 3A). In wildtype embryos, the nuclear-centrosomal complex centers before NEB and rotates onto the anterior-posterior axis, then during anaphase the spindle is displaced towards the posterior end leading to a larger AB cell and smaller P_1 cell. *let-99* mutants fail to center and rotate properly and exhibit a nuclear rocking phenotype which is not seen in controls. The full-length LET-99::mKate control was viable in the *let-99(dd17)* background and did not show any nuclear rocking phenotypes. When compared to N2 wildtype controls, LET-99::mKate rescued nuclear rotation, but did not fully rescue centration and spindle displacement. We used our full-length LET-99::mKate as a control for our deletions because they were generated in the same way.

To test if the deletions rescued centration we measured the position of the nuclear-centrosomal complex at NEB. We found that LET-99(Δ130-330)::mKate rescued centration

to a similar degree as LET-99::mKate, while LET-99(Δ1-300)::mKate and LET-99(Δ608-698)::mKate deletions were significantly different than full-length (Fig. 3B and F). We then looked at rotation angle at NEB. We found that LET-99(Δ130-330)::mKate rescued rotation to the same extent as full length, while LET-99(Δ1-300)::mKate and LET-99(Δ608-698)::mKate deletions did not rotate properly by NEB (Fig 3C and F). We also looked at spindle displacement at anaphase by measuring the change in the center of the spindle from NEB to anaphase. We found that full length and LET-99(Δ130-330)::mKate deletion showed a similar amount of spindle displacement, while LET-99(Δ1-300)::mKate and LET-99(Δ608-698)::mKate deletions did not rescue displacement (Fig 3D and F). We also looked at the size of the AB and P_1 cell by measuring the position of the AB- P_1 cell contract and found that it was similar in all deletions (Fig 3E-F). These results support the hypothesis that both the DEP domain and the C-terminus are required for proper LET-99 function and although LET-99(Δ1-300)::mKate localizes to the membrane it is not sufficient to rescue *let-99(dd17).* This also showed that although the LET-99(Δ130-330)::mKate deletion does not localize normally at NEB it is able to rescue *let-99(dd17).*

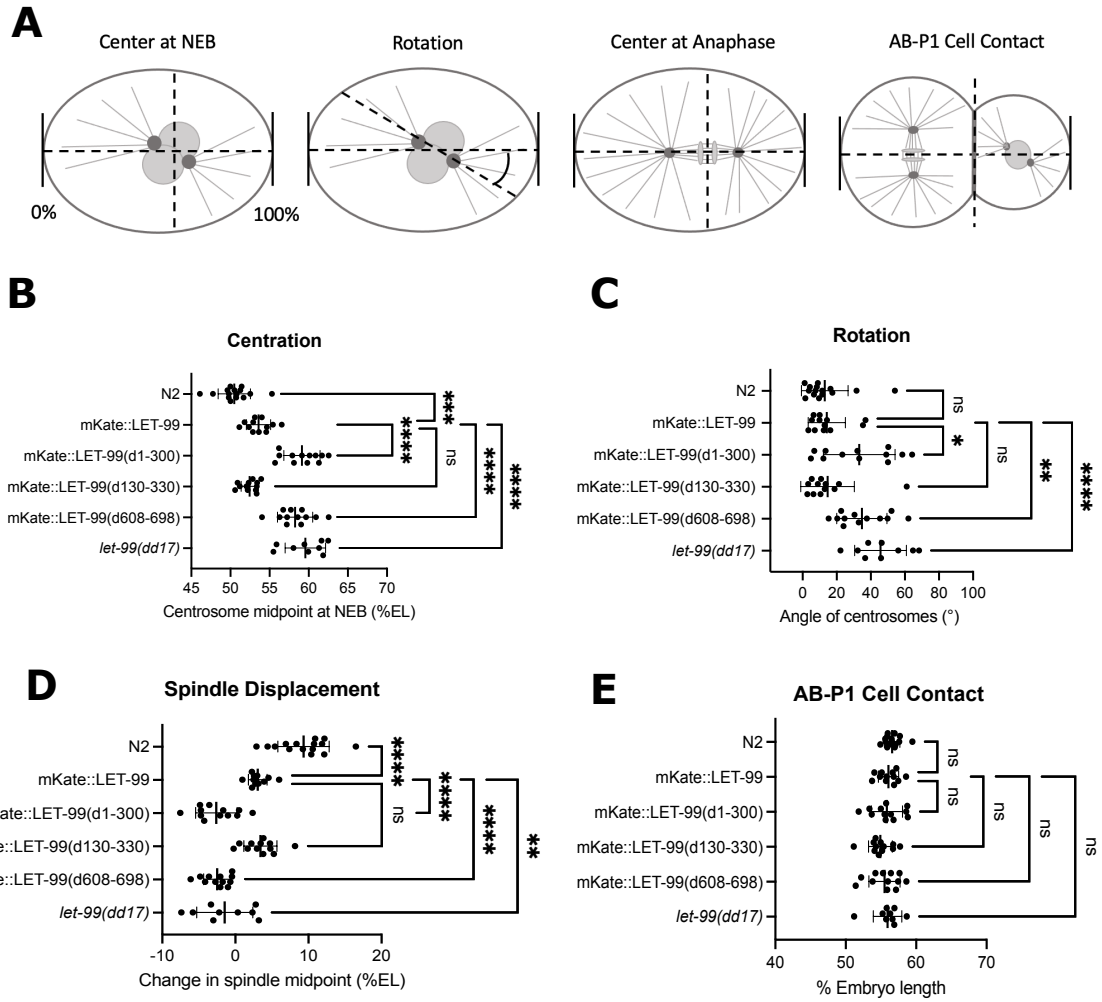

F

Genotype	N	Centration (%EL)	Rotation (°)	Spindle Displacement (%EL)	AB-P1 Cell Contact (%EL)
N2	15	50.49±2.0	12.95±13.7	9.33±3.5	56.6±1.1
mKate::LET-99	12	53.59±1.5	20.03±20.2	3.06±1.2	56.07±1.4
mKate::LET-99(Δ1-300)	12	59.14±2.3	33.18±21.0	-2.6±2.8	55.84±2.2
mKate::LET-99(Δ130-330)	12	52.45±1.1	14.62±15.7	3.43±2.3	54.92±1.7
mKate::LET-99(Δ608-698)	12	58.26±2.2	30.6±17.3	-2.49±1.8	55.5±2.2
let-99(dd17)	13	59.57±2.6	45.7±15.2	-1.45±±3.8	55.94±2.0

Figure 3. Spindle positioning in LET-99 deletion constructs. (A) Schematic diagram of how centration, rotation, spindle displacement, and AB- P_1 cell contact were measured (B) Midpoint of the nuclear–centrosome complex at NEB, expressed as percent embryo length (%EL) (C) Rotation angle of nuclear–centrosome complex at NEB. (D) Displacement of the spindle, measured as the change in midpoint between the two centrosomes from NEB to anaphase, expressed as percent embryo length (%EL). (E) Position of AB- P_1 cell contact at the end of cytokinesis, expressed as percent embryo length (%EL) (F) Means, standard deviations, and number of embryos for each genotype and measurement shown.

Discussion

In the process of asymmetric cell division, properly orienting the spindle is an important step in making sure the daughter cells inherit the correct cell fate determinants. In the P_0 cell, LET-99 is critical for nuclear-centrosomal complex centering and rotation onto the polarity axis. LET-99 is also important for making sure there are asymmetric pulling forces on the spindle during metaphase and anaphase so that division gives rise to a larger AB cell and smaller P_1 cell. Here, we investigated the mechanism by which LET-99 is localized to the cortex, how it is restricted from the anterior of the cell, and whether deleting different regions of the protein affected its function.

By analyzing YFP::LET-99 localization in *par-3(RNAi), pkc-3(RNAi), and cdc-42(RNAi),* we found that they are all require for restricting LET-99 from the anterior of the cell.. As was previously show, CDC-42 is required for binding to and activating PKC-3. Our data is thus consistent with LET-99 being a direct target of PKC-3 (Rodriguez et al., 2017). Consistent with this model we identified six 6 potential PKC-3 phosphorylation sites in LET-99.

We made deletions across LET-99 to test if removing any of the potential PKC-3 phosphorylation sites would affect the banding pattern of LET-99. We found that the LET-99(Δ1-300)::mKate deletion which deletes three of these sites was still on the membrane at higher levels than the full-length construct, but it appeared in an anterior cap and did not rescue the mutant phenotype. We also found that the LET-99(Δ130-330)::mKate deletion which also deletes three potential PKC-3 phosphorylation sites and one PAR-5 binding site, formed a posterior domain which was extended further into the anterior than controls. The

posterior cap is likely because we deleted one of the PAR-5 binding sites required for its restriction from the posterior. It has been shown that PKC-3 is in an anterior gradient (Wu & Rose, 2007). The anterior extension of LET-99 in LET-99(Δ130-330)::mKate may be the result of PKC-3 being less efficient at restricting LET-99, where it is at lowest levels. LET-99 might still be restricted in the very anterior because of the other potential PKC-3 sites that are still present. Because the LET-99(Δ608-698)::mKate deletion was not on the membrane, we could not differentiate whether the two potential PKC-3 sites at the C-terminus are required for anterior restriction of LET-99.

By deleting different regions, we also found that the DEP domain is not required for membrane localization. This shows that even though DEP domains are required for membrane localization in other proteins and LET-99's DEP domain can bind lipids in vitro, it is not required for membrane localization in *C. elegans*. We also found that LET-99(Δ1-300)::mKate did not rescue centration and rotation, and we hypothesize that the DEP domain might be required for LET-99's role in interacting with other downstream targets involved in spindle positioning. Instead, we found that the C-terminus is required for membrane localization.

In summary our data supports a model in which LET-99 is localized to the membrane by sequences at the C-terminus and it is downstream of PKC-3. But the exact mechanism by which LET-99 is restricted from the anterior is still unknown. Further analysis by mutating these six PKC-3 sites is needed to test whether they are the specific sequences required to restrict LET-99 from the anterior. These results build on our

knowledge of how the PARs control downstream targets, coordinate asymmetric cell division, and how LET-99 functions to regulate spindle positioning.

Materials and Methods

C. elegans strains

C. elegans strains were maintained on MYOB plates with *E. coli* OP50 as a food source (Brenner, 1974; Church et al., 1995). The following strains were used in this study.

Strain #	*Genotype*
N2	*Wild type, Bristol Strain*
RL398	*par-2(it315[mCherry::par-2]) III; unc-22(e66) let-99(dd17) IV; ddIs64[pie-1p::YFP::let-99(genomic); unc-119(+)]*
RL474	*daSi59[pLAK03(mex-5p::LET-99:: mKate-GLO::PIE-1 3'UTR) unc-119+] II; unc-22(e66) let-99(dd17) IV*
RL456	*daSi52[pAR767(mex-5p::mKate-GLO::LET-99::pie-1 3'UTR) unc-119+] II; unc-119(ed3)III; unc-22(e66) let-99(dd17)/nT1 IV; +/nT1*
RL511	*daSi63[pAR774-18(mex-5p::GFP-GLO::LET-99::pie-1 3'UTR) unc-119+] II; unc-119(ed3)III; unc-22(e66) let-99(dd17)/nt1 IV*
RL512	*daSi64[pAR775-7(mex-5p::LET-99::GFP-GLO::pie-1 3'UTR) unc-119+] II; unc-119(ed3)III; unc-22(e66) let-99(dd17)/ nT1 IV; +/nT1*
RL578	*daSi86[pLAK15-7(mex-5p::LET-99(Δ1-300)::mKate2::pie-1 3'UTR) unc-119+] II; unc-22(e66) let-99(dd17)/ nT1 IV; +/nT1*

RL536	*daSi79[pLAK07-02(mex-5p::LET-99(Δ130-330)::mKate2::pie-1 3'UTR) unc-119+] II; unc-22(e66) let-99(dd17)/ nT1 IV; +/nT1*
RL578	*daSi79[pLAK14-11(mex-5p::LET-99(Δ608-698)::mKate2::pie-1 3'UTR) unc-119+] II; unc-22(e66) let-99(dd17)/ nT1 IV; +/nT1*
RL469	*daSi56[pAR770.22(mex-5p::mKate2::pie-1 3'UTR) unc-119+] II; unc-22(e66) let-99(dd17)/ nT1 IV; +/nT1*
RL276	*unc-119(ed3) III; unc-22(e66) let-99(dd17)/ nT1 IV; +/nT1*

RNA interference

RNAi was performed by feeding (Timmons & Fire, 1998). The *par-3, pkc-3, and cdc-42* RNAi construct used was obtained from the Ahringer RNAi library (Kamath et al., 2003). L4 stage worms were places on RNAi plates and incubated for 48hrs at 20°C to obtained published strong loss of function phenotypes, such as defects in division pattern and cell cycle timing. The strength of the RNAi was verified by looking at the localization of mCh::PAR-2 which was uniform on the membrane after anterior PAR knockdown.

Generation of LET-99 constructs and transgenic strains

The following plasmids were used to generate *let-99* constructs, using standard restriction enzyme cloning and Gibson assembly: *let-99* genomic DNA was obtained from pAR762 and pAR763, which have modifications to allow cloning of the fluorescent tag at the N-terminus or C-terminus respectively (courtesy of Alan Rose). mKate2-GLO and GFP-GLO tags were subcloned from pDD376 and pDD373 (Addgene) (Heppert et al., 2016). The *mex-5* promoter was subcloned from pXF121, the *pie-1* 3'UTR was subcloned from pXF85, and pXF87 was used as the MosSCi vector backbone (Fan et al., 2020). Q5 Site-Directed Mutagenesis Kit from New England BioLabs was used to make deletions in *let-99* genomic sequence from pAR762 and pAR763. Final plasmids were checked by restriction enzyme digest and gel electrophoresis for size, followed by Sanger sequencing of the entire insertion from *mex-5* promoter to *pie-1* 3'UTR.

Transgenic strains were generated through the MosSCI single copy insertion method (Frøkjaer-Jensen et al., 2008). Plasmid constructs were injected into a strain carrying the Chromosome II Mos insertion ttTi5605 by InVivo Biosystems. Worms containing integrations were isolated and bred to homozygosity. These were then crossed to RL276 to generate strains homozygous for the transgene in the *let-99(dd17)/nT1* background. PCR was used to confirm the identity of the transgene in balanced strains, and in cases where the transgene rescued the *let-99(dd17)* mutation to viability, PCR was used to confirm the presence of the *let-99(dd17)* deletion. Multiple independent lines were isolated for each transgene to ensure they showed consistent phenotypes.

Live Imaging

Because all of the proteins under study are maternally provided, embryos were derived from homozygous mutant hermaphrodites, or hermaphrodites treated for RNAi, in all cases. Embryos were removed from gravid hermaphrodites, dissected into egg buffer (25 mM HEPES, pH 7.4, 120 mM NaCl, 48 mM KCl, 2 mM CaCl2, MgCl2), mounted on 2% agar pads, and covered with coverslip.

Confocal microscopy was carried out using the spinning disc module of an Intelligent Imaging Innovations (3i) Marianas SDC Real-Time 3D Confocal-TIRF microscope fit with a Yokogawa spinning disc head, a 60x 1.4 numerical aperture oil-immersion objective, EMCCD camera, and Slidebook 6 software. Images were taken in 488nm for 150ms and 561nm for 300ms at 50% laser power in a mid-focal plane at 10 seconds intervals.

Epifluorescent microscopy was carried out on Olympus BX53 microscope outfitted with a Hamamatsu Orca Fusion BT camera, a SpectraX light engine, and motorized turret, all run by Olympus Cellsens software. Fluorescent images were taken at 10 second intervals with 300ms exposure, and 50% laser power. Parallel samples were imaged using DIC optics only on the same microscope, with images taken every 5 seconds.

Quantification

Some images in figures were contrast adjusted for better visualization, but all measurements were made on the raw data from original TIFF files using Fiji as outlined

below. Measurements were exported into Excel for determination of means and ratios, then analyzed for statistical significance using Graphpad Prism version 9.0.

Analysis of cortical YFP::LET-99 and LET-99::mKate2 was performed at NEB by dividing the embryo along its longest anterior-posterior axis, then tracing both the top and bottom cortices using the segmented line tool (width = 3 pixels) in Fiji. For confocal images, cytoplasmic mean was measured by drawing a small circle in the cytoplasm, avoiding the cortex and nucleus. Cortical traces were then normalized to the cytoplasmic mean and all embryos of each condition were averaged and plotted along 100% embryo length. For epifluorescent images the cortical trace was normalized to a cytoplasmic trace approximately 5um under the cortex, to correct for out of focus light. Individual embryo measurements were then averaged to get one plot for each condition. The overall fluorescent levels were measured by tracing the whole cell at NEB.

Spindle positioning was quantified as shown in Figure 3A. For centration, the midpoint of the nuclear-centrosome complex at NEB was measured and expressed as percent embryo length. Nuclear rotation was measured as the angle of the centrosome in relation to the anterior-posterior axis. Spindle displacement was quantified by finding the difference between the center of the spindle at NEB and anaphase (160s after NEB). The position of the AB- P_1 cell contact was measured by finding the position of the contact at the end of cytokinesis and expressing it ass percent embryo length.

Acknowledgements

We thank Minjae Yoo for help verifying transgene lines, Rowena Mendieta for help doing crosses, Aidan van Cleef and Kathie Urrutia-Paniagua for media preparation, and members of the Rose and McNally labs for helpful discussions. We are grateful to Alan Rose help in plasmid and strain generation. We are grateful to Erik Griffin for providing plasmids. Other strains were provided by *Caenorhabditis* Genetics Center, which is funded by the National Institutes of Health Office of Research Infrastructure Programs (P40 OD010440). The 3i Marianas spinning disk confocal used in this study was purchased using a National Institutes of Health Shared Instrumentation Grant [1S10RR024543-01]. We thank the MCB Light Microscopy Imaging Facility, which is a UC-Davis Campus Core Research Facility, for maintaining this microscope. This research was funded by awards to LR from the National Institutes of Health Grant [R01GM68744] and the National Institute of Food and Agriculture [CA-D*-MCB-6239-H].

Supplemental Figures

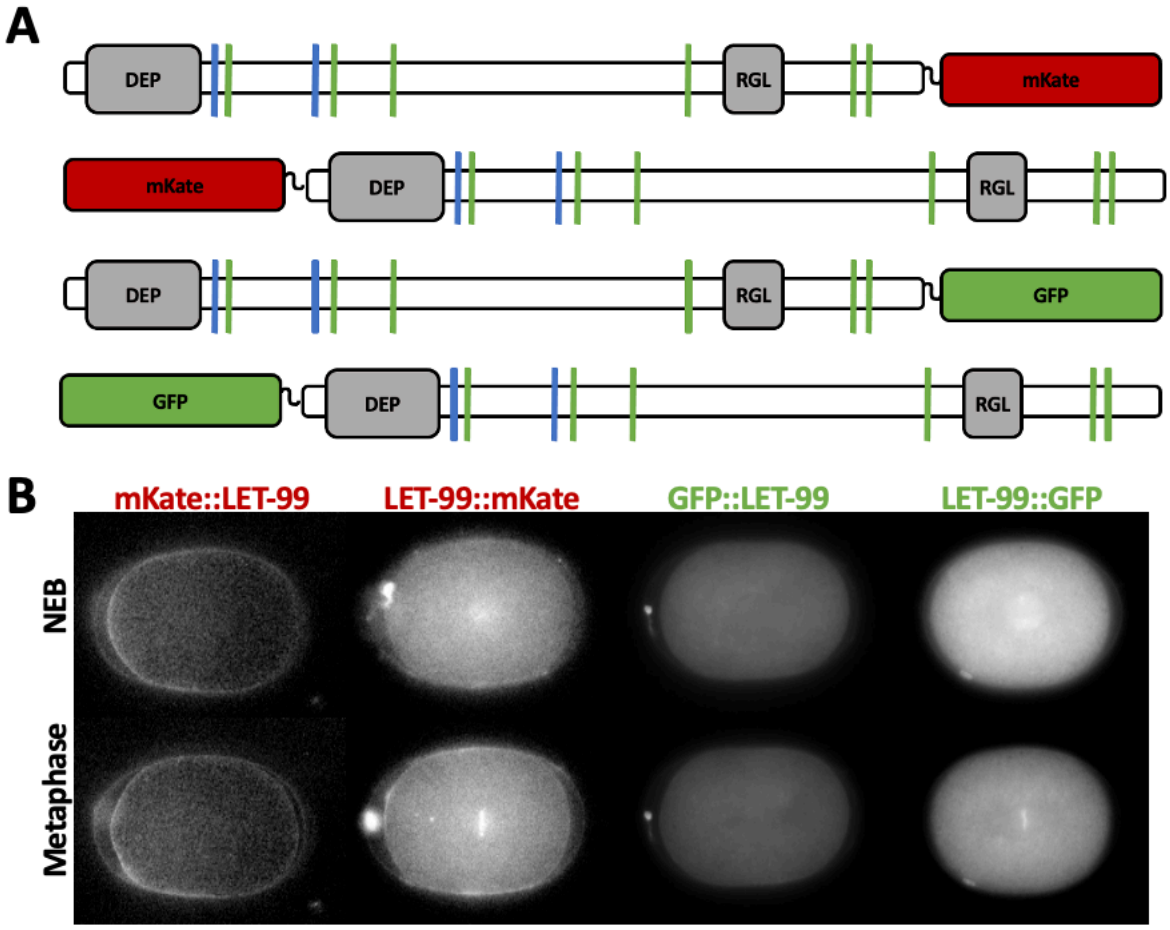

Supplemental Figure 1. Testing LET-99 fluorescent tags and positions. (A) Schematic diagram of LET-99 constructs: LET-99::mKate, mKate::LET-99, LET-99::GFP, and GFP::LET-99. (B) Fluorescent images of each genotype construct shown at NEB and metaphase.

References

Bouvrais, H., Chesneau, L., Pastezeur, S., Fairbrass, D., Delattre, M., & Pécréaux, J. (2018, Dec 4). Microtubule Feedback and LET-99-Dependent Control of Pulling Forces Ensure Robust Spindle Position. *Biophys J, 115*(11), 2189-2205. https://doi.org/10.1016/j.bpj.2018.10.010

Boyd, L., Guo, S., Levitan, D., Stinchcomb, D. T., & Kemphues, K. J. (1996, Oct). PAR-2 is asymmetrically distributed and promotes association of P granules and PAR-1 with the cortex in C. elegans embryos. *Development, 122*(10), 3075-3084. https://doi.org/10.1242/dev.122.10.3075

Brenner, S. (1974, May). The genetics of Caenorhabditis elegans. *Genetics, 77*(1), 71-94. http://www.ncbi.nlm.nih.gov/pubmed/4366476

Bringmann, H., Cowan, C. R., Kong, J., & Hyman, A. A. (2007, Jan 23). LET-99, GOA-1/GPA-16, and GPR-1/2 are required for aster-positioned cytokinesis. *Curr Biol, 17*(2), 185-191. https://doi.org/10.1016/j.cub.2006.11.070

Church, D. L., Guan, K. L., & Lambie, E. J. (1995, Aug). Three genes of the MAP kinase cascade, mek-2, mpk-1/sur-1 and let-60 ras, are required for meiotic cell cycle progression in Caenorhabditis elegans. *Development, 121*(8), 2525-2535. https://doi.org/10.1242/dev.121.8.2525

Consonni, S. V., Maurice, M. M., & Bos, J. L. (2014, May). DEP domains: structurally similar but functionally different. *Nat Rev Mol Cell Biol, 15*(5), 357-362. https://doi.org/10.1038/nrm3791

Cowan, C. R., & Hyman, A. A. (2004, Sep 2). Centrosomes direct cell polarity independently of microtubule assembly in C. elegans embryos. *Nature, 431*(7004), 92-96. https://doi.org/10.1038/nature02825

Cuenca, A. A., Schetter, A., Aceto, D., Kemphues, K., & Seydoux, G. (2003, Apr). Polarization of the C. elegans zygote proceeds via distinct establishment and maintenance phases. *Development, 130*(7), 1255-1265. https://doi.org/10.1242/dev.00284

Fan, X., De Henau, S., Feinstein, J., Miller, S. I., Han, B., Frøkjær-Jensen, C., & Griffin, E. E. (2020, Feb 6). SapTrap Assembly of Caenorhabditis elegans MosSCI Transgene Vectors. *G3 (Bethesda), 10*(2), 635-644. https://doi.org/10.1534/g3.119.400822

Frøkjaer-Jensen, C., Davis, M. W., Hopkins, C. E., Newman, B. J., Thummel, J. M., Olesen, S. P., Grunnet, M., & Jorgensen, E. M. (2008, Nov). Single-copy insertion of transgenes in Caenorhabditis elegans. *Nat Genet, 40*(11), 1375-1383. https://doi.org/10.1038/ng.248

Galli, M., Muñoz, J., Portegijs, V., Boxem, M., Grill, S. W., Heck, A. J., & van den Heuvel, S. (2011, Aug 21). aPKC phosphorylates NuMA-related LIN-5 to position the mitotic spindle during asymmetric division. *Nat Cell Biol, 13*(9), 1132-1138. https://doi.org/10.1038/ncb2315

Goldstein, B., & Macara, I. G. (2007, Nov). The PAR proteins: fundamental players in animal cell polarization. *Dev Cell, 13*(5), 609-622. https://doi.org/10.1016/j.devcel.2007.10.007

Griffin, E. E., Odde, D. J., & Seydoux, G. (2011, Sep 16). Regulation of the MEX-5 gradient by a spatially segregated kinase/phosphatase cycle. *Cell, 146*(6), 955-968. https://doi.org/10.1016/j.cell.2011.08.012

Guo, S., & Kemphues, K. J. (1995, May 19). par-1, a gene required for establishing polarity in C. elegans embryos, encodes a putative Ser/Thr kinase that is asymmetrically distributed. *Cell, 81*(4), 611-620. https://doi.org/10.1016/0092-8674(95)90082-9

Hao, Y., Boyd, L., & Seydoux, G. (2006, Feb). Stabilization of cell polarity by the C. elegans RING protein PAR-2. *Dev Cell, 10*(2), 199-208. https://doi.org/10.1016/j.devcel.2005.12.015

Heppert, J. K., Dickinson, D. J., Pani, A. M., Higgins, C. D., Steward, A., Ahringer, J., Kuhn, J. R., & Goldstein, B. (2016, Nov 7). Comparative assessment of fluorescent proteins for in vivo imaging in an animal model system. *Mol Biol Cell, 27*(22), 3385-3394. https://doi.org/10.1091/mbc.E16-01-0063

Kamath, R. S., Fraser, A. G., Dong, Y., Poulin, G., Durbin, R., Gotta, M., Kanapin, A., Le Bot, N., Moreno, S., Sohrmann, M., Welchman, D. P., Zipperlen, P., & Ahringer, J. (2003, Jan 16). Systematic functional analysis of the Caenorhabditis elegans genome using RNAi. *Nature, 421*(6920), 231-237. https://doi.org/10.1038/nature01278

Kemphues, K. J., Priess, J. R., Morton, D. G., & Cheng, N. S. (1988, Feb 12). Identification of genes required for cytoplasmic localization in early *C. elegans* embryos. *Cell, 52*(3), 311-320. http://www.ncbi.nlm.nih.gov/entrez/query.fcgi?cmd=Retrieve&db=PubMed&dopt=Citation&list_uids=3345562

Kim, A. J., & Griffin, E. E. (2020). PLK-1 Regulation of Asymmetric Cell Division in the Early C. elegans Embryo. *Front Cell Dev Biol, 8*, 632253. https://doi.org/10.3389/fcell.2020.632253

Krueger, L. E., Wu, J. C., Tsou, M. F., & Rose, L. S. (2010, May 3). LET-99 inhibits lateral posterior pulling forces during asymmetric spindle elongation in C. elegans embryos. *J Cell Biol, 189*(3), 481-495. https://doi.org/10.1083/jcb.201001115

Park, D. H., & Rose, L. S. (2008, Mar 1). Dynamic localization of LIN-5 and GPR-1/2 to cortical force generation domains during spindle positioning. *Dev Biol, 315*(1), 42-54. http://www.ncbi.nlm.nih.gov/entrez/query.fcgi?cmd=Retrieve&db=PubMed&dopt=Citation&list_uids=18234174

Pickett, M. A., Naturale, V. F., & Feldman, J. L. (2019, Oct 6). A Polarizing Issue: Diversity in the Mechanisms Underlying Apico-Basolateral Polarization In Vivo. *Annu Rev Cell Dev Biol, 35*, 285-308. https://doi.org/10.1146/annurev-cellbio-100818-125134

Price, K. L., & Rose, L. S. (2017, Sep 1). LET-99 functions in the astral furrowing pathway, where it is required for myosin enrichment in the contractile ring. *Mol Biol Cell, 28*(18), 2360-2373. https://doi.org/10.1091/mbc.E16-12-0874

Rodriguez, J., Peglion, F., Martin, J., Hubatsch, L., Reich, J., Hirani, N., Gubieda, A. G., Roffey, J., Fernandes, A. R., St Johnston, D., Ahringer, J., & Goehring, N. W. (2017, Aug 21). aPKC Cycles between Functionally Distinct PAR Protein Assemblies to Drive Cell Polarity. *Dev Cell, 42*(4), 400-415.e409. https://doi.org/10.1016/j.devcel.2017.07.007

Rose, L., & Gönczy, P. (2014, Dec 30). Polarity establishment, asymmetric division and segregation of fate determinants in early C. elegans embryos. *WormBook*, 1-43. https://doi.org/10.1895/wormbook.1.30.2

Rose, L. S., & Kemphues, K. (1998, Apr). The let-99 gene is required for proper spindle orientation during cleavage of the C. elegans embryo. *Development, 125*(7), 1337-1346. http://www.ncbi.nlm.nih.gov/entrez/query.fcgi?cmd=Retrieve&db=PubMed&dopt=Citation&list_uids=9477332

Sunchu, B., & Cabernard, C. (2020, Jun 29). Principles and mechanisms of asymmetric cell division. *Development, 147*(13). https://doi.org/10.1242/dev.167650

Tabuse, Y., Izumi, Y., Piano, F., Kemphues, K. J., Miwa, J., & Ohno, S. (1998, Sep). Atypical protein kinase C cooperates with PAR-3 to establish embryonic polarity in Caenorhabditis elegans. *Development, 125*(18), 3607-3614. https://doi.org/10.1242/dev.125.18.3607

Timmons, L., & Fire, A. (1998, Oct 29). Specific interference by ingested dsRNA. *Nature, 395*(6705), 854. https://doi.org/10.1038/27579

Tsou, M. F., Hayashi, A., DeBella, L. R., McGrath, G., & Rose, L. S. (2002, Oct). LET-99 determines spindle position and is asymmetrically enriched in response to PAR polarity cues in C. elegans embryos. *Development, 129*(19), 4469-4481. http://www.ncbi.nlm.nih.gov/entrez/query.fcgi?cmd=Retrieve&db=PubMed&dopt=Citation&list_uids=12223405

Venkei, Z. G., & Yamashita, Y. M. (2018, Nov 5). Emerging mechanisms of asymmetric stem cell division. *J Cell Biol, 217*(11), 3785-3795. https://doi.org/10.1083/jcb.201807037

Wang, C., Shang, Y., Yu, J., & Zhang, M. (2012, May 9). Substrate recognition mechanism of atypical protein kinase Cs revealed by the structure of PKCι in complex with a substrate peptide from Par-3. *Structure, 20*(5), 791-801. https://doi.org/10.1016/j.str.2012.02.022

Watts, J. L., Etemad-Moghadam, B., Guo, S., Boyd, L., Draper, B. W., Mello, C. C., Priess, J. R., & Kemphues, K. J. (1996, Oct). par-6, a gene involved in the establishment of asymmetry in early C. elegans embryos, mediates the asymmetric localization of PAR-3. *Development, 122*(10), 3133-3140. https://doi.org/10.1242/dev.122.10.3133

Wu, J. C., Espiritu, E. B., & Rose, L. S. (2016, Apr 15). The 14-3-3 protein PAR-5 regulates the asymmetric localization of the LET-99 spindle positioning protein. *Dev Biol, 412*(2), 288-297. https://doi.org/10.1016/j.ydbio.2016.02.020

Wu, J. C., & Rose, L. S. (2007, Nov). PAR-3 and PAR-1 inhibit LET-99 localization to generate a cortical band important for spindle positioning in Caenorhabditis elegans embryos. *Mol Biol Cell, 18*(11), 4470-4482. https://doi.org/10.1091/mbc.e07-02-0105

Chapter IV

Conclusions and Future Directions:

The role of cytoplasmic polarity and spindle positioning in P_1 cell polarity.

Our work in Chapter II, supported a model in which there are two major pathways for polarity reestablishment in the P_1 cell. An early pathway requires PAR-1, PKC-3, MEX-5, PLK-1 and the inheritance of normal cytoplasmic polarity from the P_0 cell. In the absence of early polarization there is a secondary late pathway, which involves centrosome maturation and actomyosin flow-dependent accumulation of anterior PARs. To further analyze the mechanism of the early pathway, downstream targets of PAR-1, MEX-5, and PLK-1 could be tested to see if they share the same polarity defect. Possible candidates would include POS-1, MEX-1, and PIE-1 which are inherited at high levels in the P_1 cell (Rose & Gonczy, 2014). It would also be interesting to test whether LGL-1 has a role in polarity establishment in the P_1 cell, because although it is required for polarization in *Drosophila* it is only redundantly required in the P_0 cell in *C. elegans* (Hoege et al., 2010).

Previous work has also shown that OOC-3, OOC-5, and NPP-1 affect PAR polarity and spindle positioning in the P_1 cell (Basham & Rose, 1999, 2001; Pichler et al., 2000; Schetter et al., 2006). To test these proteins' role in the P_1 cell, one could cross the null mutants to mCh::PAR-2 and GFP::PAR-6. By watching the PAR proteins dynamically in these mutants, you could differentiate if these proteins are required for establishing polarity or if they are needed to maintain polarity and orient the spindle properly in the P_1 cell. It would also be interesting to check whether LET-99 still forms its posterior lateral band in these mutants and whether LIN-5 and GPR-1/2 localization is affected.

To test the two redundant pathways for polarity establishment in the P_1 cell, we performed double mutant analysis of *par-1(RNAi)* with *spd-5 or nmy-2* temperature

sensitive mutants. In these double mutants, PAR-2 cleared later than in controls and single mutants. Also, in the double mutants, PAR-2 did not clear from the anterior AB-P_1 cell contact as in controls, but instead PAR-2 cleared from the corners of the P_1 cell. It has been previously reported that in the absence of the normal polarity cues in the *C. elegans* P_0 cell, there are other mechanisms that can spontaneously break symmetry that are influenced by cell shape (Klinkert et al., 2019); this phenomenon might be yet another way to break symmetry in the P_1 cell. To test if this mechanism is causing PAR-2 clearing in our double mutants, one could perform this same double mutant experiment while dissolving the eggshell with a chitinase digestion. This would test if P_1 cell shape affects the clearing in the double mutants.

Another mechanism of polarity establishment that has already been described in *C. elegans* is the backup pathway in the P_0 cell. In the backup pathway, PAR-2 establishes polarity by binding to microtubules emanating from centrosome, which protects it from phosphorylation by PKC-3. This allows PAR-2 to accumulate on the posterior cortex in the P_0 cell even when there is no actomyosin flow to remove the aPARs (Motegi et al., 2011; Zonies et al., 2010). This mechanism might also be present in the P_1 cell protecting PAR-2 from PKC-3 phosphorylation in the posterior. The clearing from the corners might be because this is where PAR-2 is not sheltered from phosphorylation. To test this hypothesis, one could utilize a previously generated PAR-2 microtubule binding mutant (Zonies et al., 2010), in combination with our double mutant, and test for loss of corner clearing. This work would further our understanding of the different ways polarization can occur under different cellular conditions.

Investigating how the aPAR's regulate symmetric cell division in the AB cell.

In the process of investigating how polarity is established in the P_1 cell, I observed polarity forming in the AB cell in *pkc-3(ne4250ts)* mutants. This phenotype is interesting because it implies that PKC-3's role in the AB cell is to suppress PAR-2 from moving onto the cortex and forming polarity in the P_1 cell.

In these *pkc-3(ne4250ts)* mutant embryos, the PAR-2 domain formed in the anterior of the cell opposite of where it forms in the P_1 cell. This position correlates with where the centrosome is located in the AB cell at the end of cytokinesis. To further investigate this spontaneous symmetry breaking one could inhibit centrosome maturation or actomyosin flow in this *pkc-3* mutant and see if this prevents the PAR-2 domain formation. In wild-type AB cells, the centrioles migrate perpendicular to the anterior-posterior axis, and the spindle forms on this axis. However, in aPAR mutant embryos, the spindle then rotates onto the AP axis, suggesting that the aPARs are required to prevent rotation in the AB cell (Bondaz et al., 2019; Cheng et al., 1995). Prior work has also shown that PKC-3 can phosphorylate LIN-5 to inhibit pulling forces in the P_0 cell (Galli et al., 2011). I hypothesize that PKC-3 directly inhibits LIN-5's localization to the anterior of the AB cell and prevents the spindle from rotating onto the AP axis. Analyzing LIN-5's localization in *pkc-3(ne4250ts)* would show whether PKC-3 affects LIN-5's localization in the AB cell. To further test if spindle positioning in the AB cell is controlled by PKC-3 and LIN-5, one could perform double mutant analysis with of PKC-3 and LIN-5 to see if the rotation in these mutants is LIN-5 dependent. This work would further our understanding of how polarization is suppressed as well as how spindle positioning is controlled.

Further analysis of how LET-99 is restricted from the anterior of the P_0 cell.

As discussed in chapter III, we have initiated a structure function analysis of LET-99. Our results showed that the C-terminal region (Δ608-698aa) is required for membrane localization. I have made a number of other constructs that will facilitate the continuation of this approach to identify the role of the other domains in LET-99. Figure 1 illustrates the constructs that have already been designed and whether the construct has already been made as a plasmid and introduced into *C. elegans*. Constructs that delete just the DEP domain or RGL domain will be especially useful in furthering our understanding of how LET-99 interacts with the force-generating complex. Motif programs also identified a hydrophobic region (H) at the C-terminus (Kyte & Doolittle, 1982). I have designed a construct that just deletes this region that could be used to test if it is required for LET-99's membrane localization.

In Chapter III, we also showed that PKC-3 is required for proper LET-99 localization. There are six potential PKC-3 phosphorylation sites in LET-99 and deleting regions that contain some of these sites affects LET-99's localization pattern. To test whether these sites are functional, I generated a phospho-mutant in which all six sites were mutated to alanine. This transgene has already been isolated in *C. elegans,* but we are still in the process of crossing it to *let-99(dd17)* and analyzing it. Preliminary imaging of this strain supports our hypothesis that these sites are required for anterior restriction of LET-99. The next step would be to make constructs that mutate a subset of these sites to determine which sites are required for anterior restriction. After identifying which sites are required, one could generate a phosphomimetic version of LET-99 by mutating these sites to glutamic acid (Fig. 1). These experiments would further our understanding of how LET-99 is localized by the

PAR proteins and how it functions in spindle positioning.

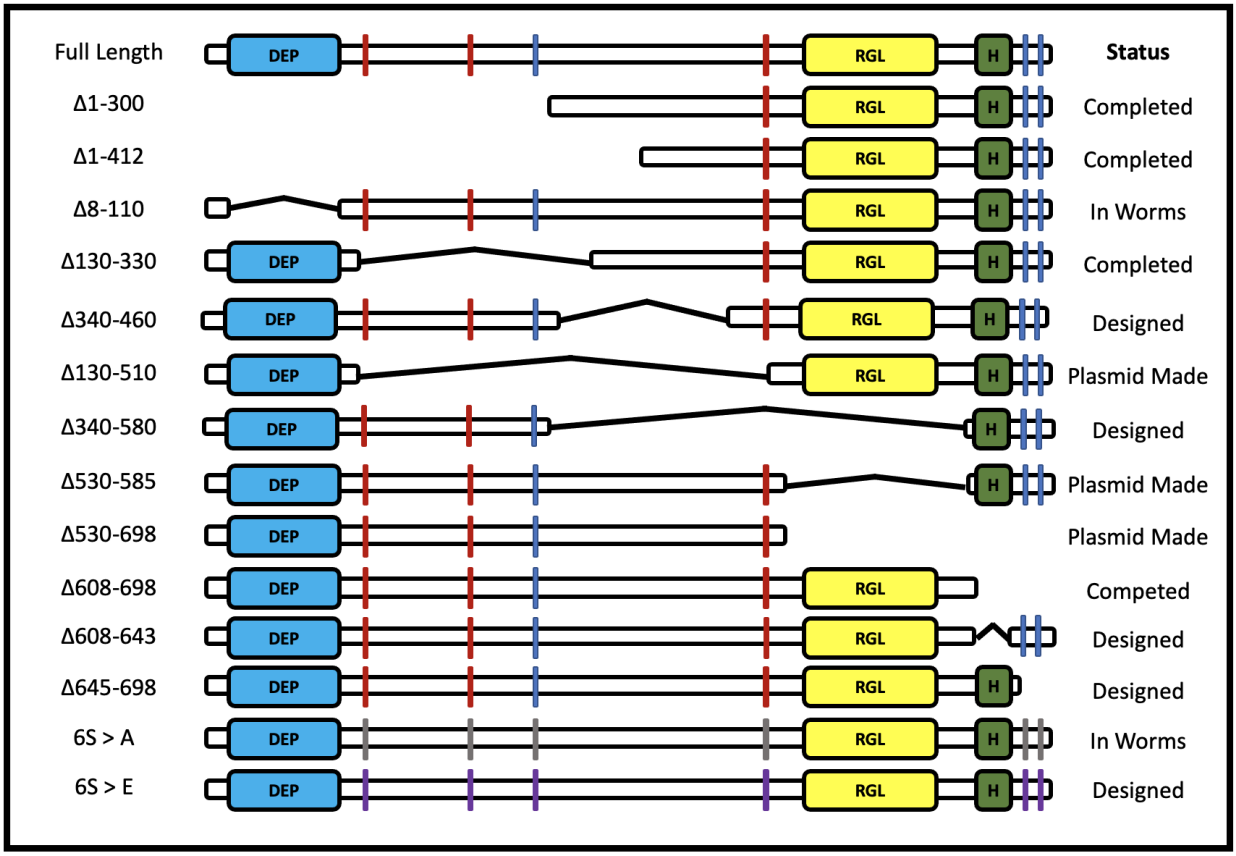

Figure 1. LET-99 structure function analysis. Illustration of LET-99 deletion constructs to generate in *C. elegans* to test localization and function. Each construct is followed with its status in being generated in worms: "Completed" means the line has been generated in worms, crossed to *let-99(dd17),* and analyzed, "In Worms" means the transgene has been generated in worms, "Plasmid Made" means a plasmid with the construct has been generated and is ready to inject into worms, "Designed" means the plasmid is not complete but is in progress.

Reconstitute LET-99 localization in *S. cerevisiae*

As I showed in Chapter III, PKC-3 is required for proper LET-99 localization and previous work in the lab showed that PAR-1 is required for restricting LET-99 from the posterior (Wu & Rose, 2007). To test whether PKC-3 and PAR-1 are sufficient to localize LET-99 into a band, one could reconstitute these three proteins in *S. cerevisiae* budding yeast. The only component of the PAR system that is conserved in *S. cerevisiae* is CDC-42. In *S. cerevisiae*, CDC-42 localizes to the bud membrane. A previous study generated *S. cerevisiae* strains expressing GFP::PAR-1 and a Gic2::PKC-3::Cer. The Gic2 domain recruits PKC-3 to CDC-42 in the bud. When these two proteins were expressed in the same cell, the presence of PKC-3 in the bud was sufficient to restrict PAR-1 localization to the mother cell (Ramanujam et al., 2018). I would generate a mKate::LET-99 *S. cerevisiae* strain and express it with GFP::PAR-1 and Gic2::PKC-3::Cer. If PKC-3 and PAR-1 are sufficient for LET-99 localization into a band, LET-99 will either be completely excluded from the cortex or localize at the bud neck as shown in Figure 2. This experiment would test if PKC-3 and PAR-1 are sufficient to regulate LET-99, furthering our understanding of how PAR proteins interact with downstream targets.

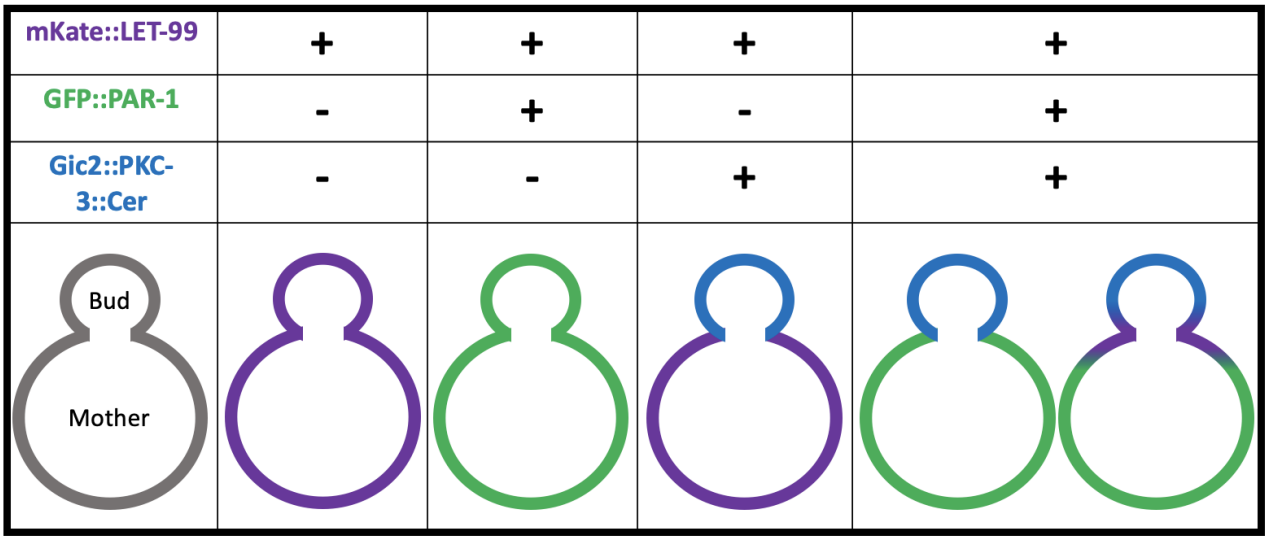

Figure 2. Reconstitution of LET-99 localization in *S. cerevisiae*. Model of where PAR-1, PKC-3, and LET-99 should localize in reconstitution of PAR polarity and LET-99 in *S. cerevisiae.*

References

Arata, Y., Lee, J.-Y., Goldstein, B., & Sawa, H. (2010). Extracellular control of PAR protein localization during asymmetric cell division in the C. elegans embryo. *Development, 137*(19), 3337-3345. https://doi.org/10.1242/dev.054742

Basham, S. E., & Rose, L. S. (1999, Nov 15). Mutations in *ooc-5* and *ooc-3* disrupt oocyte formation and the reestablishment of asymmetric PAR protein localization in two-cell *Caenorhabditis elegans* embryos. *Dev Biol, 215*(2), 253-263. http://www.ncbi.nlm.nih.gov/entrez/query.fcgi?cmd=Retrieve&db=PubMed&dopt=Citation&list_uids=10545235

Basham, S. E., & Rose, L. S. (2001, Nov). The *Caenorhabditis elegans* polarity gene *ooc-5* encodes a Torsin-related protein of the AAA ATPase superfamily. *Development, 128*(22), 4645-4656. http://www.ncbi.nlm.nih.gov/entrez/query.fcgi?cmd=Retrieve&db=PubMed&dopt=Citation&list_uids=11714689

Bei, Y., Hogan, J., Berkowitz, L. A., Soto, M., Rocheleau, C. E., Pang, K. M., Collins, J., & Mello, C. C. (2002, Jul). SRC-1 and Wnt signaling act together to specify endoderm and to control cleavage orientation in early *C. elegans* embryos. *Dev Cell, 3*(1), 113-125. http://www.ncbi.nlm.nih.gov/entrez/query.fcgi?cmd=Retrieve&db=PubMed&dopt=Citation&list_uids=12110172

Benton, R., & St Johnston, D. (2003, Dec 12). Drosophila PAR-1 and 14-3-3 inhibit Bazooka/PAR-3 to establish complementary cortical domains in polarized cells. *Cell, 115*(6), 691-704. http://www.ncbi.nlm.nih.gov/entrez/query.fcgi?cmd=Retrieve&db=PubMed&dopt=Citation&list_uids=14675534

Bondaz, A., Cirillo, L., Meraldi, P., & Gotta, M. (2019, Dec 2). Cell polarity-dependent centrosome separation in the C. elegans embryo. *J Cell Biol, 218*(12), 4112-4126. https://doi.org/10.1083/jcb.201902109

Bouvrais, H., Chesneau, L., Pastezeur, S., Fairbrass, D., Delattre, M., & Pécréaux, J. (2018, Dec 4). Microtubule Feedback and LET-99-Dependent Control of Pulling Forces Ensure Robust Spindle Position. *Biophys J, 115*(11), 2189-2205. https://doi.org/10.1016/j.bpj.2018.10.010

Boyd, L., Guo, S., Levitan, D., Stinchcomb, D. T., & Kemphues, K. J. (1996, Oct). PAR-2 is asymmetrically distributed and promotes association of P granules and PAR-1 with the cortex in *C. elegans* embryos. *Development, 122*(10), 3075-3084. http://www.ncbi.nlm.nih.gov/entrez/query.fcgi?cmd=Retrieve&db=PubMed&dopt=Citation&list_uids=8898221

Brenner, S. (1974, May). The genetics of Caenorhabditis elegans. *Genetics, 77*(1), 71-94. http://www.ncbi.nlm.nih.gov/entrez/query.fcgi?cmd=Retrieve&db=PubMed&dopt=Citation&list_uids=4366476

Bringmann, H., Cowan, C. R., Kong, J., & Hyman, A. A. (2007, Jan 23). LET-99, GOA-1/GPA-16, and GPR-1/2 are required for aster-positioned cytokinesis. *Curr Biol, 17*(2), 185-191. http://www.ncbi.nlm.nih.gov/entrez/query.fcgi?cmd=Retrieve&db=PubMed&dopt=Citation&list_uids=17189697

Cheeks, R. J., Canman, J. C., Gabriel, W. N., Meyer, N., Strome, S., & Goldstein, B. (2004, May 25). *C. elegans* PAR proteins function by mobilizing and stabilizing asymmetrically localized protein complexes. *Curr Biol, 14*(10), 851-862. http://www.ncbi.nlm.nih.gov/entrez/query.fcgi?cmd=Retrieve&db=PubMed&dopt=Citation&list_uids=15186741

Cheng, N. N., Kirby, C. M., & Kemphues, K. J. (1995, Feb). Control of cleavage spindle orientation in *Caenorhabditis elegans*: the role of the genes *par-2* and *par-3*. *Genetics, 139*(2), 549-559. http://www.ncbi.nlm.nih.gov/entrez/query.fcgi?cmd=Retrieve&db=PubMed&dopt=Citation&list_uids=7713417

Church, D. L., Guan, K. L., & Lambie, E. J. (1995, Aug). Three genes of the MAP kinase cascade, mek-2, mpk-1/sur-1 and let-60 ras, are required for meiotic cell cycle progression in Caenorhabditis elegans. *Development, 121*(8), 2525-2535. http://www.ncbi.nlm.nih.gov/entrez/query.fcgi?cmd=Retrieve&db=PubMed&dopt=Citation&list_uids=7671816

Consonni, S. V., Maurice, M. M., & Bos, J. L. (2014, May). DEP domains: structurally similar but functionally different. *Nat Rev Mol Cell Biol, 15*(5), 357-362. https://doi.org/10.1038/nrm3791

Cowan, C. R., & Hyman, A. A. (2004, Sep 2). Centrosomes direct cell polarity independently of microtubule assembly in *C. elegans* embryos. *Nature, 431*(7004), 92-96. http://www.ncbi.nlm.nih.gov/entrez/query.fcgi?cmd=Retrieve&db=PubMed&dopt=Citation&list_uids=15343338

Cuenca, A. A., Schetter, A., Aceto, D., Kemphues, K., & Seydoux, G. (2003, Apr). Polarization of the *C. elegans* zygote proceeds via distinct establishment and maintenance phases. *Development, 130*(7), 1255-1265. http://www.ncbi.nlm.nih.gov/entrez/query.fcgi?cmd=Retrieve&db=PubMed&dopt=Citation&list_uids=12588843

Fan, X., De Henau, S., Feinstein, J., Miller, S. I., Han, B., Frøkjær-Jensen, C., & Griffin, E. E. (2020, Feb 6). SapTrap Assembly of Caenorhabditis elegans MosSCI Transgene Vectors. *G3 (Bethesda), 10*(2), 635-644. https://doi.org/10.1534/g3.119.400822

Frøkjaer-Jensen, C., Davis, M. W., Hopkins, C. E., Newman, B. J., Thummel, J. M., Olesen, S. P., Grunnet, M., & Jorgensen, E. M. (2008, Nov). Single-copy insertion of transgenes in Caenorhabditis elegans. *Nat Genet, 40*(11), 1375-1383. https://doi.org/10.1038/ng.248

Galli, M., Muñoz, J., Portegijs, V., Boxem, M., Grill, S. W., Heck, A. J., & van den Heuvel, S. (2011, Aug 21). aPKC phosphorylates NuMA-related LIN-5 to position the mitotic spindle during asymmetric division. *Nat Cell Biol, 13*(9), 1132-1138. https://doi.org/10.1038/ncb2315

Goldstein, B. (1993, Aug). Establishment of gut fate in the E lineage of *C. elegans*: the roles of lineage-dependent mechanisms and cell interactions. *Development, 118*(4), 1267-1277. http://www.ncbi.nlm.nih.gov/entrez/query.fcgi?cmd=Retrieve&db=PubMed&dopt=Citation&list_uids=8269853

Goldstein, B. (1995, May). Cell contacts orient some cell division axes in the *Caenorhabditis elegans* embryo. *J Cell Biol, 129*(4), 1071-1080. http://www.ncbi.nlm.nih.gov/entrez/query.fcgi?cmd=Retrieve&db=PubMed&dopt=Citation&list_uids=7744956

Goldstein, B., & Macara, I. G. (2007, Nov). The PAR proteins: fundamental players in animal cell polarization. *Dev Cell, 13*(5), 609-622. https://doi.org/10.1016/j.devcel.2007.10.007

Griffin, E. E., Odde, D. J., & Seydoux, G. (2011, Sep 16). Regulation of the MEX-5 gradient by a spatially segregated kinase/phosphatase cycle [Research Support, N.I.H., Extramural Research Support, Non-U.S. Gov't]. *Cell, 146*(6), 955-968. https://doi.org/10.1016/j.cell.2011.08.012

Guo, S., & Kemphues, K. J. (1995, May 19). *par-1*, a gene required for establishing polarity in *C. elegans* embryos, encodes a putative Ser/Thr kinase that is asymmetrically distributed. *Cell, 81*(4), 611-620. http://www.ncbi.nlm.nih.gov/entrez/query.fcgi?cmd=Retrieve&db=PubMed&dopt=Citation&list_uids=7758115

Hao, Y., Boyd, L., & Seydoux, G. (2006, Feb). Stabilization of cell polarity by the C. elegans RING protein PAR-2. *Dev Cell, 10*(2), 199-208. http://www.ncbi.nlm.nih.gov/entrez/query.fcgi?cmd=Retrieve&db=PubMed&dopt=Citation&list_uids=16459299

Heppert, J. K., Dickinson, D. J., Pani, A. M., Higgins, C. D., Steward, A., Ahringer, J., Kuhn, J. R., & Goldstein, B. (2016, Nov 7). Comparative assessment of fluorescent proteins for in vivo imaging in an animal model system. *Mol Biol Cell, 27*(22), 3385-3394. https://doi.org/10.1091/mbc.E16-01-0063

Hoege, C., Constantinescu, A. T., Schwager, A., Goehring, N. W., Kumar, P., & Hyman, A. A. (2010, Jul 27). LGL can partition the cortex of one-cell Caenorhabditis elegans embryos into two domains. *Curr Biol, 20*(14), 1296-1303. https://doi.org/10.1016/j.cub.2010.05.061

Hurov, J. B., Watkins, J. L., & Piwnica-Worms, H. (2004, Apr 20). Atypical PKC phosphorylates PAR-1 kinases to regulate localization and activity. *Curr Biol, 14*(8), 736-741. http://www.ncbi.nlm.nih.gov/entrez/query.fcgi?cmd=Retrieve&db=PubMed&dopt=Citation&list_uids=15084291

Kamath, R. S., Fraser, A. G., Dong, Y., Poulin, G., Durbin, R., Gotta, M., Kanapin, A., Le Bot, N., Moreno, S., Sohrmann, M., Welchman, D. P., Zipperlen, P., & Ahringer, J. (2003, Jan 16). Systematic functional analysis of the Caenorhabditis elegans genome using RNAi. *Nature, 421*(6920), 231-237. http://www.ncbi.nlm.nih.gov/entrez/query.fcgi?cmd=Retrieve&db=PubMed&dopt=Citation&list_uids=12529635

Kemphues, K. J., Priess, J. R., Morton, D. G., & Cheng, N. S. (1988, Feb 12). Identification of genes required for cytoplasmic localization in early *C. elegans* embryos. *Cell, 52*(3), 311-320. http://www.ncbi.nlm.nih.gov/entrez/query.fcgi?cmd=Retrieve&db=PubMed&dopt=Citation&list_uids=3345562

Kim, A. J., & Griffin, E. E. (2020). PLK-1 Regulation of Asymmetric Cell Division in the Early C. elegans Embryo. *Front Cell Dev Biol, 8*, 632253. https://doi.org/10.3389/fcell.2020.632253

Klinkert, K., Levernier, N., Gross, P., Gentili, C., von Tobel, L., Pierron, M., Busso, C., Herrman, S., Grill, S. W., Kruse, K., & Gönczy, P. (2019, Feb 26). Aurora A depletion reveals centrosome-independent polarization mechanism in Caenorhabditis elegans. *Elife, 8*. https://doi.org/10.7554/eLife.44552

Knoblich, J. A. (2010, 2010/12/01). Asymmetric cell division: recent developments and their implications for tumour biology. *Nature Reviews Molecular Cell Biology, 11*(12), 849-860. https://doi.org/10.1038/nrm3010

Kotak, S. (2019, Feb 25). Mechanisms of Spindle Positioning: Lessons from Worms and Mammalian Cells. *Biomolecules, 9*(2). https://doi.org/10.3390/biom9020080

Krueger, L. E., Wu, J. C., Tsou, M. F., & Rose, L. S. (2010, May 3). LET-99 inhibits lateral posterior pulling forces during asymmetric spindle elongation in C. elegans embryos. *J Cell Biol, 189*(3), 481-495. https://doi.org/10.1083/jcb.201001115

Kyte, J., & Doolittle, R. F. (1982, May 5). A simple method for displaying the hydropathic character of a protein. *J Mol Biol, 157*(1), 105-132. https://doi.org/10.1016/0022-2836(82)90515-0

Longhini, K. M., & Glotzer, M. (2022, Dec 19). Aurora A and cortical flows promote polarization and cytokinesis by inducing asymmetric ECT-2 accumulation. *Elife, 11*. https://doi.org/10.7554/eLife.83992

Morrison, S. J., & Kimble, J. (2006, Jun 29). Asymmetric and symmetric stem-cell divisions in development and cancer. *Nature, 441*(7097), 1068-1074. http://www.ncbi.nlm.nih.gov/entrez/query.fcgi?cmd=Retrieve&db=PubMed&dopt=Citation&list_uids=16810241

Motegi, F., Zonies, S., Hao, Y., Cuenca, A. A., Griffin, E., & Seydoux, G. (2011, Oct 9). Microtubules induce self-organization of polarized PAR domains in Caenorhabditis elegans zygotes. *Nat Cell Biol, 13*(11), 1361-1367. https://doi.org/10.1038/ncb2354

Munro, E., Nance, J., & Priess, J. R. (2004, Sep). Cortical flows powered by asymmetrical contraction transport PAR proteins to establish and maintain anterior-posterior polarity in the early *C. elegans* embryo. *Dev Cell, 7*(3), 413-424. http://www.ncbi.nlm.nih.gov/entrez/query.fcgi?cmd=Retrieve&db=PubMed&dopt=Citation&list_uids=15363415

Park, D. H., & Rose, L. S. (2008, Mar 1). Dynamic localization of LIN-5 and GPR-1/2 to cortical force generation domains during spindle positioning. *Dev Biol, 315*(1), 42-54. http://www.ncbi.nlm.nih.gov/entrez/query.fcgi?cmd=Retrieve&db=PubMed&dopt=Citation&list_uids=18234174

Pichler, S., Gonczy, P., Schnabel, H., Pozniakowski, A., Ashford, A., Schnabel, R., & Hyman, A. A. (2000, May). OOC-3, a novel putative transmembrane protein required for establishment of cortical domains and spindle orientation in the P(1) blastomere of C. elegans embryos. *Development, 127*(10), 2063-2073. http://www.ncbi.nlm.nih.gov/entrez/query.fcgi?cmd=Retrieve&db=PubMed&dopt=Citation&list_uids=10769231

Pickett, M. A., Naturale, V. F., & Feldman, J. L. (2019, Oct 6). A Polarizing Issue: Diversity in the Mechanisms Underlying Apico-Basolateral Polarization In Vivo. *Annu Rev Cell Dev Biol, 35*, 285-308. https://doi.org/10.1146/annurev-cellbio-100818-125134

Price, K. L., & Rose, L. S. (2017, Sep 1). LET-99 functions in the astral furrowing pathway, where it is required for myosin enrichment in the contractile ring. *Mol Biol Cell, 28*(18), 2360-2373. https://doi.org/10.1091/mbc.E16-12-0874

Ramanujam, R., Han, Z., Zhang, Z., Kanchanawong, P., & Motegi, F. (2018, Oct). Establishment of the PAR-1 cortical gradient by the aPKC-PRBH circuit. *Nat Chem Biol, 14*(10), 917-927. https://doi.org/10.1038/s41589-018-0117-1

Rodriguez, J., Peglion, F., Martin, J., Hubatsch, L., Reich, J., Hirani, N., Gubieda, A. G., Roffey, J., Fernandes, A. R., St Johnston, D., Ahringer, J., & Goehring, N. W. (2017, Aug 21). aPKC Cycles between Functionally Distinct PAR Protein Assemblies to Drive Cell Polarity. *Dev Cell, 42*(4), 400-415.e409. https://doi.org/10.1016/j.devcel.2017.07.007

Rose, L., & Gonczy, P. (2014). Polarity establishment, asymmetric division and segregation of fate determinants in early C. elegans embryos. *WormBook*, 1-43. https://doi.org/10.1895/wormbook.1.30.2

Rose, L. S., & Kemphues, K. (1998, Apr). The let-99 gene is required for proper spindle orientation during cleavage of the C. elegans embryo. *Development, 125*(7), 1337-1346. http://www.ncbi.nlm.nih.gov/entrez/query.fcgi?cmd=Retrieve&db=PubMed&dopt=Citation&list_uids=9477332

Schetter, A., Askjaer, P., Piano, F., Mattaj, I., & Kemphues, K. (2006, Jan 15). Nucleoporins NPP-1, NPP-3, NPP-4, NPP-11 and NPP-13 are required for proper spindle orientation in C. elegans. *Dev Biol, 289*(2), 360-371. http://www.ncbi.nlm.nih.gov/entrez/query.fcgi?cmd=Retrieve&db=PubMed&dopt=Citation&list_uids=16325795

Schonegg, S., Hyman, A. A., & Wood, W. B. (2014, Jun). Timing and mechanism of the initial cue establishing handed left–right asymmetry in Caenorhabditis elegans embryos. *Genesis, 52*(6), 572-580. https://doi.org/10.1002/dvg.22749

Sunchu, B., & Cabernard, C. (2020, Jun 29). Principles and mechanisms of asymmetric cell division. *Development, 147*(13). https://doi.org/10.1242/dev.167650

Tabuse, Y., Izumi, Y., Piano, F., Kemphues, K. J., Miwa, J., & Ohno, S. (1998, Sep). Atypical protein kinase C cooperates with PAR-3 to establish embryonic polarity in Caenorhabditis elegans. *Development, 125*(18), 3607-3614. http://www.ncbi.nlm.nih.gov/entrez/query.fcgi?cmd=Retrieve&db=PubMed&dopt=Citation&list_uids=9716526

Timmons, L., & Fire, A. (1998, Oct 29). Specific interference by ingested dsRNA. *Nature, 395*(6705), 854. https://doi.org/10.1038/27579

Tsou, M. F., Hayashi, A., DeBella, L. R., McGrath, G., & Rose, L. S. (2002, Oct). LET-99 determines spindle position and is asymmetrically enriched in response to PAR polarity cues in C. elegans embryos. *Development, 129*(19), 4469-4481. http://www.ncbi.nlm.nih.gov/entrez/query.fcgi?cmd=Retrieve&db=PubMed&dopt=Citation&list_uids=12223405

Venkei, Z. G., & Yamashita, Y. M. (2018, Nov 5). Emerging mechanisms of asymmetric stem cell division. *J Cell Biol, 217*(11), 3785-3795. https://doi.org/10.1083/jcb.201807037

Wang, C., Shang, Y., Yu, J., & Zhang, M. (2012, May 9). Substrate recognition mechanism of atypical protein kinase Cs revealed by the structure of PKCι in complex with a substrate peptide from Par-3. *Structure, 20*(5), 791-801. https://doi.org/10.1016/j.str.2012.02.022

Watts, J. L., Etemad-Moghadam, B., Guo, S., Boyd, L., Draper, B. W., Mello, C. C., Priess, J. R., & Kemphues, K. J. (1996, Oct). par-6, a gene involved in the establishment of asymmetry in early C. elegans embryos, mediates the asymmetric localization of PAR-3. *Development, 122*(10), 3133-3140. http://www.ncbi.nlm.nih.gov/entrez/query.fcgi?cmd=Retrieve&db=PubMed&dopt=Citation&list_uids=8898226

Wu, J. C., Espiritu, E. B., & Rose, L. S. (2016, Apr 15). The 14-3-3 protein PAR-5 regulates the asymmetric localization of the LET-99 spindle positioning protein. *Dev Biol, 412*(2), 288-297. https://doi.org/10.1016/j.ydbio.2016.02.020

Wu, J. C., & Rose, L. S. (2007, Nov). PAR-3 and PAR-1 inhibit LET-99 localization to generate a cortical band important for spindle positioning in Caenorhabditis elegans embryos. *Mol Biol Cell, 18*(11), 4470-4482. https://doi.org/10.1091/mbc.e07-02-0105

Zhao, P., Teng, X., Tantirimudalige, S. N., Nishikawa, M., Wohland, T., Toyama, Y., & Motegi, F. (2019, Mar 11). Aurora-A Breaks Symmetry in Contractile Actomyosin Networks Independently of Its Role in Centrosome Maturation. *Dev Cell, 48*(5), 631-645.e636. https://doi.org/10.1016/j.devcel.2019.02.012

Zonies, S., Motegi, F., Hao, Y., & Seydoux, G. (2010, May). Symmetry breaking and polarization of the C. elegans zygote by the polarity protein PAR-2 [Research Support, N.I.H., Extramural
Research Support, Non-U.S. Gov't]. *Development, 137*(10), 1669-1677. https://doi.org/10.1242/dev.045823